REMOVAL OF ALUMINIUM FROM FILTER BACKWASH WATER

USING ADSORBENTS AND A GEOTEXTILE

by

Iffat Jahan

Submitted in partial fulfilment of the requirements

for the degree of Master of Applied Science

at

Dalhousie University

Halifax, Nova Scotia

October 2016

Dedicated to My Parents

Md Fakhruddin

&

Mrs. Kamrun Nahar

TABLE OF CONTENTS

List of Tables

List of Figures

Abstract

Aluminium present in filter backwash water (FBWW) at the J. Douglas Kline Water Treatment Plant (JDKWTP), located in Halifax, Nova Scotia, represents a challenge for environmental compliance. The aluminum (Al) concentration in the FBWW sometimes exceeds the provincial regulation of guidelines of 184 (µg/L). The utilization of alum ($Al_2(SO_4)_3 14H_2O$) coagulation during treatment operations is the predominant source of this aluminum. The aim of this study is to investigate utilizing adsorbents and geotextiles to reduce total and dissolved Al concentration and total suspended solids (TSS) in the FBWW. Three adsorbents; calcium oxide (CaO), magnesium oxide (Mg0) and ferric oxide (Fe_3O_4) and several combinations of these adsorbents were investigated in the study. In addition, Tencate GT500 woven geotextiles were chosen as filter media to remove Al as well as to minimize TSS from the adsorbent-treated FBWW. An optimal dosage of cationic polymer was also considered to assist with the acceleration of floc formation to achieve better removal efficiency. For the testing, 1 mg/L of cationic polymer was utilized considering both pH adjustment (approx. 6.5) and without pH adjustment conditions. Adsorbent dosage was increased stepwise with an addition of 0.1~5.0 gm per liter in the FBWW resulting in removal of total Al between 95% to 98% using MgO and CaO and around 83~89% using ferric oxide. Reduction of TSS was also achieved in these trials. Geotextiles were also used to efficiently remove TSS and removal of total Al concentration was found around 95% from these treated FBWWs. An optimal (i.e. 1 g/L) dosage of a combination of 50/50 mix of CaO and iron oxide adsorbents was found to be an effective dosage resulting from the analysis which can be useful for further recommendations in future.

List of Abbreviations and Symbols Used

Abbreviations:

JDKWTP	J.D. Kline Water Treatment Plant
FBWW	Filter Backwash Water
TSS	Total Suspended Solids
Al	Aluminium
WHO	World Health Organization
EPA	Environmental Protection Agency
SMCLs	Secondary Maximum Contaminant Levels
NSE	Nova Scotia Environment
DSI	Dewatering Solution Inc.
HBT	Hanging Bag Test
FHT	Falling Head Test
PFT	Pressure Filtration Test
RDT	Rapid Dewatering Test
GRT	Gradient Ratio Test
OPWA	Ontario Public Works Association
APWA	American Public Works Association
ZP	Zeta Potential
ECD	Equivalent Circular Diameter
MFI	Micro Flow Imaging
CaO	Calcium Oxide
MgO	Magnesium Oxide
Fe_3O_4	Ferric Oxide
SEM	Scanning Electron Microscope
MFI	Micro Flow Imaging
AOS	Apparent Opening Size

Acknowledgments

At the very outset, with all the impulse of my heart, I would like to express gratitude and praise the universal owner, almighty Allah the most beneficent and merciful creator who has enabled me to accomplish the project thesis for the fulfillment of the degree of Master of Applied Science in Civil Engineering.

I wish to express my indebtedness to Dr. Craig Lake, Professor, Dalhousie University, Department of Civil and Resource Engineering for his constant supervision, continuous guidance, helpful criticism, valuable suggestions and great encouragement given throughout the course of this research. I would definitely say without him my research work would not be accomplished. I would also like to extend my heartfelt gratitude to Dr. Graham Gagnon, professor, department of Civil and Resource Engineering for his continuous guidance and support for sharing his valuable ideas and thoughts throughout my research work.

My special gratitude to the students and staffs of the water lab, especially Elliott Wright and Yuri Park, for their cordial support and encouragement during these experiments.

Finally, I wish to thank to my beloved parents and other family members as they always inspired me to accomplish my research work during my miserable times. I would like to express my deep sense of gratitude to my husband, Md Nur Hossain, for his affectionate advice, enthusiasm and undying support during starting of this course to till complete of this research.

Chapter 1 Introduction

1.1 **Background**

The J.D. Kline Water Supply Plant (JDKWSP) in Halifax, Nova Scotia was commissioned in 1977 and is operated by Halifax Water. It produces potable drinking water with an average discharge of 90 ML/day (Clark 2010). The plant is typically operated as a direct or a conventional filtration plant, as shown in Figure 1-1, that supplies treated water to the greater urban core of Halifax, Bedford, Sackville, Fall River, Waverly and Timberlea (HMC 2009). As summarized by Wood (2014), water from Pockwock Lake is used as the source water. This water is characterized by water quality parameters such as low pH, low alkalinity, and low turbidity. After screening, the water is sent through three pre-mix tanks for pH adjustment up to approximately 10; oxidation ($KMnO_4$) to assist in removal of iron and manganese, and then subsequent addition of CO_2 to reduce the pH back down to about 5.5. Aluminum sulphate (alum $Al_2(SO_4)_314H_2O$) is then added as a coagulant. At cold temperatures, a polymer (Magnafloc LT20) is also added during this process to improve the floc strength. After flocculation, the water and suspended materials are then filtered through eight dual media filters consisting of sand and anthracite. Final polishing of the filtered water consists of chlorine addition for disinfection, zinc/ortho phosphate addition for corrosion control, sodium hydroxide addition for pH adjustment (approximately 7.4) and hydrofluosilic acid addition for prevention of tooth decay (Wood, 2014). As discussed by Wood (2014), backwashing of the dual media filters requires approximately 700,000 L of water which is used to fluidize the filter media and this water containing in the filter bed media is called filter backwash water (FBWW).
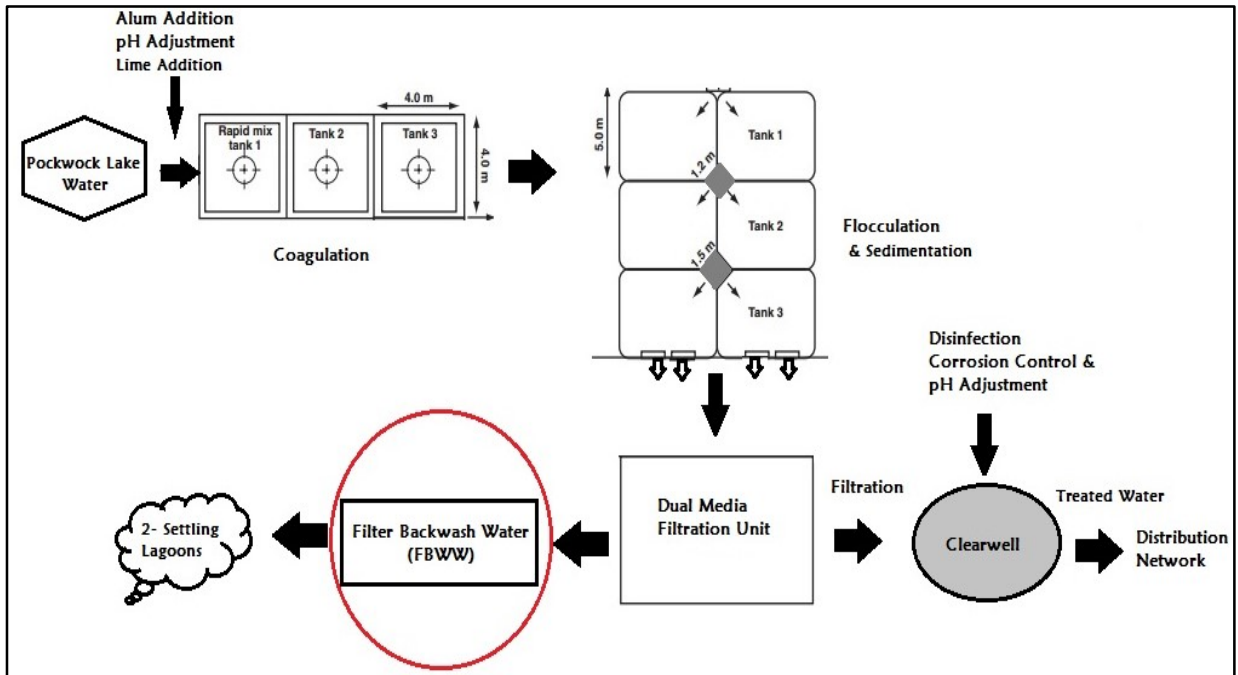
Figure 1-1   Generation of FBWW in Conventional and Direct Filtration Water Treatment Plant (Vadasarukkai et al. 2011)

The alum added in the treatment process tends to result in elevated levels of aluminum in the filter backwash water (FBWW). As a result of this, filter backwash water in the treatment plant sometimes contains total aluminium concentrations in excess of the provincial regulations, as well as large number of suspended particles (Fanous 2014).

Previous work by Wood (2014) has studied the distribution of Al in the filter backwash treatment system and examined the used of polymers for providing treatment of Al. No follow up work has been performed since Wood's study with respect to Al removal from FBWW. A literature review of Al treatment in water, to be presented in the next chapter, reveals the potential for metal oxides to be used as adsorbents for Al. Adsorbents

such as magnesium oxide, ferric oxide and aluminium oxide (either individual or in combination) offer the potential to remove metals such as Al in wastewater treatment operations (Ikari et al. 1979). Once removed, conventional usage of cationic polymer in treatment operations can assist as a flocculation aide in particle destabilization and promote agglomeration (Stoddart & Gagnon, 2015). Once agglomeration occurs, some form of particle/water separation stage (i.e. clarification) would have to be performed.

Geotubes represent a potential novel way of providing this solid/particle separation. Tencate (2011) describes the usage of geotextile tubes, commonly known as geotubes, in many engineering applications, in assisting to separate solids during wastewater treatment. The geotextile material serves the function of removal of solids by trapping the solids inside the geotube and promoting water to escape. According to Tencate (2011), approximately 99% of suspended solids are trapped inside the geotube during the process of water recirculation. Geotube dewatering technology is simple and cost effective. Most of the publications on geotubes have focused on engineering applications to dewater high water content materials including marine sediments, water and wastewater treatment sludges, agricultural waste, mine tailings, and chemical and industrial discharges (Moo-Young, Gaffney, & Mo 2002). To the author's knowledge, there are few current publications related to low concentration Al removal from FBWW using geotubes.

1.2 Research Objectives

The goal of this research is to examine if same form of combination of adsorbent, polymer and geotube solid removal technique can provide a practical solution to removing Al from the FBWW at JDKWTP. The secondary objective of this work is to better understand the removal mechanisms responsible for these reductions in Al levels in the FBWW. To achieve these goals, a bench scale laboratory testing program is performed where three adsorbents (CaO, MgO and Fe_3O_4) have been considered to remove aluminium from

FBWW. Geotextiles have been chosen as filter media for FBWW treatment and a cationic polymer for the flocculation aide. The experiments were conducted to observe the performance of the geotube filtration in a small scale laboratory environment, accompanied with the usage of the adsorbents and polymer to remove total aluminium and total suspended solids (TSS). Various materials engineering techniques were introduced throughout this work to further examine the Al removal mechanisms.

1.3 **Organization of the Thesis**

Organization of this thesis includes five individual chapters which are as follows:

Chapter 2 contains a literature review for the research. Aluminium (Al) chemistry and fate in the water distribution system is reviewed. The chemical processes of Al involved in water and wastewater systems are described. The guidelines for regulating Al in the wastewater distribution system are reviewed. Also discussed the problems associated with the presence of aluminium in water distribution systems.

The second focus of this chapter is to discuss geotube applications for wastewater treatment. The chapter provides a brief background on geotubes, technical specifications, their applications, working mechanisms and fundamental principles, feasibility testing and case histories for wastewater applications.

Chapter 3 provides a description of the materials and methods used in the laboratory experiments. This chapter is structured with the general methods and methodologies and analytical approaches of each experiment.

Chapter 4 provides results and discussion of the experiments.

Chapter 5 focuses an overall summary and conclusions of the research work as some overall recommendations for future research.

Chapter 2 Literature Review

2.1 Introduction

This chapter presents a literature review related to the research presented in this thesis. The focus relates to two main topics; aluminium in water and geotubes use in water and wastewater applications. With respect to aluminium (Al), there is a brief review of aluminium chemistry, toxicity of Al, guidelines for regulating Al in water environment, and various treatment strategies in wastewater treatment operations to remove Al. With respect to geotubes, the review highlights theoretical aspects of geotubes, technical specifications of geotubes and applications in a variety of fields, working principles of geotubes, fundamental principles of geotube operation, feasibility testing of geotubes, and case histories involved in recently practiced geotube in dewatering applications.

2.2 Aluminium Chemistry

Aluminium as a solid is an abundant compound that can be found in nature in different forms of minerals. Sometimes it is found as a more complex form of silicate (Kadlec and Wallace, 2009), however, usually it can be found in minerals as a combination of elements such as silicon, oxygen, phosphates, fluorine, and hydroxides (Lide 1991, as cited in WHO 1997; Frank *et al*. 1985; Hudson *et al*. 1985). Most of the aluminium sources in nature are found in soil and rock. The cationic exchange of the metals in the soil can trigger release of Al in water environments. Most of the Al compounds in water come from surface water due to wind and water erosion in the agricultural lands (WHO 1997) and mineral weathering of feldspars (e.g. anorthite, albite, micas and bauxite etc., Lenntech 2015). It can also be

present in either oxide or hydroxide forms, which are insoluble in water. Al can be naturally found as Al^{+3} (aq) under acidic conditions and $Al(OH)_4$ (aq) under neutral to alkaline conditions, as shown in Figure 2-1.

Aluminium salt (Alum) is extensively used in various industries, in different applications. In water treatment plant processes, when Alum is added to water, it causes a number of sequential reactions and dissociates into Al^{3+} (John et al. 2005). When this Al^{+3} come in contact with water, it reacts and hydrolyzes to form a hydroxide of Al. The hydrolysis reaction is shown below in equation 2.1 (Lenntech 2015) as:

$$Al^{+3} (aq) + 6H_2O (l) \rightarrow [Al (H_2O)_6]^{+3}(aq)\dots\dots\dots\dots\dots\dots\dots\dots\dots\dots\dots\dots2.1$$
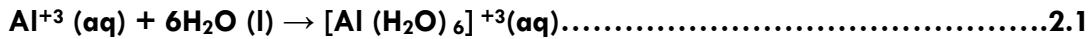
These trivalent ions of $2Al^{3+}$ hydrate to form the aquometal complexes $Al (H_2O)_6^{3+}$. During the coagulation process in the treatment plant operations, alum is added for precipitation reactions (Lenntech 2015). This alum reacts with $Ca(OH)_2$ or lime and finally a series of hydrolysis reactions cause to form finally $Al(OH)_3$ (s) as an amorphous precipitate as shown in equation 2.2 (Droste 1997):

$$Al_2 (SO4)_3 14H_2O + 3Ca (OH)_2 \rightarrow 2Al (OH)_3 (s)\downarrow + CaSO_4 + 14H_2O\dots\dots\dots\dots2.2$$

(Alum)   **precipitate   Salt**
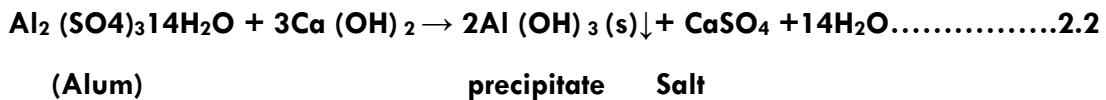
The solubility is largely dependant on the variation of pH. Figure 2-1 shows the speciation diagram for aluminium in aqueous solutions is as a function of pH. A variety of hydroxol complexes are formed, including aluminium hydroxide $Al(OH)_3(s)$, which is essentially insoluble at pH~6.5 and precipitates near this pH. To remove aluminium from water treatment operations, it is essential to maintain the pH adjusted in the water to achieve more floc formations as shown in Figure 2-1.
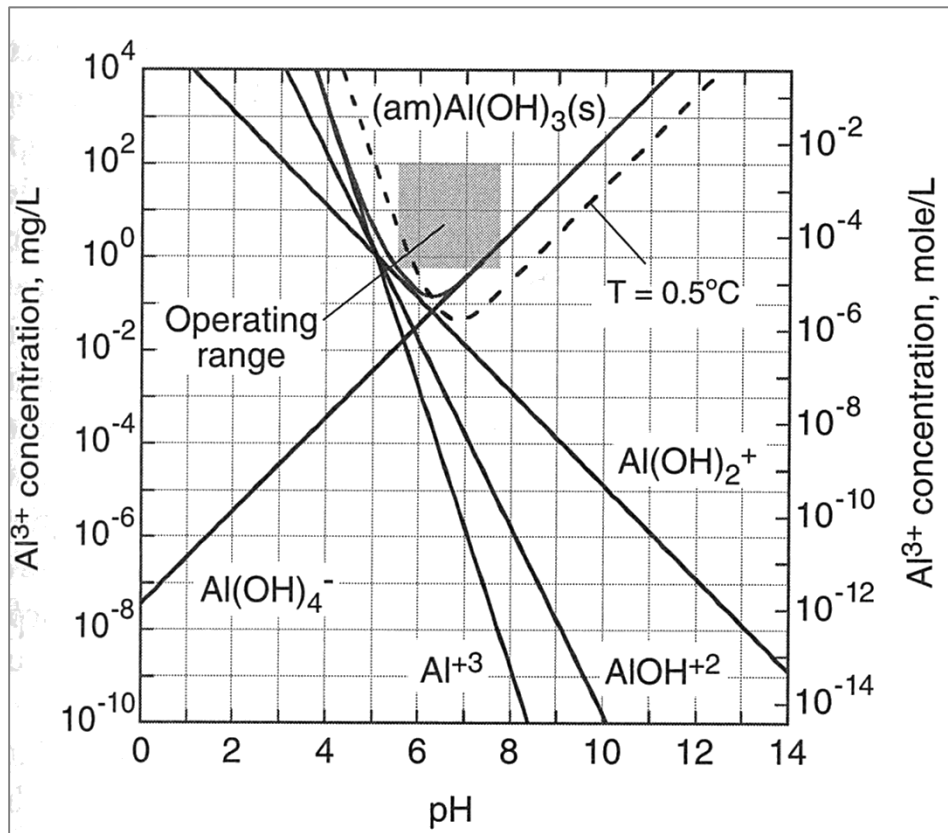
Figure 2-1   Speciation Diagram for Aluminium (John et al. 2005).

2.3 Aluminium Toxicity

2.3.1   Effects on Aquatic Plants and Fishes

Elevated level of aluminium present in the fresh water e.g (lake, pond, river, streams, etc.) can cause a number of detrimental effects in aquatic environments. Al ions in lower pH water are toxic to aquatic species and phytoplankton. Excessive amount of aluminium existing in the lake water and other sources at lower pH levels might cause harmful effects to aquatic life (Lenntech 2015). It may cause abnormalities in plants and phosphorus deficiencies in

vegetation (Kaggwa et al. 2001). Aluminium ions that migrate into the ground water through acidified soil might also damage roots and trees (Health Canada 2007). Elevated Al can be very harmful to fish in water bodies. Positively charged Al ions can bind to the gulls of fish and can cause suffocation, clogging and even cause death (Exley et al. 1991). Particularly, Al shows toxicity in the aquatic media for fish in the pH range 5.0 to 5.5 (Lenntech 2015). This pH range and Al concentration jointly increase the possibility of larvae mortality. Al toxicity triggers the severity for Atlantic salmon in the freshwaters at low pH between (5.0- 6.0) and the threshold limit for toxicity is 15 μg/L (Howells et al. 1990).

2.3.2 Human Health Risks Due to Aluminium Consumption

Health risk of aluminium toxicity may be triggered due to uptake of food consumption and skin contact. On an average, healthy people can tolerate aluminum consumption up to 7 g/day without experiencing any health effects. However, the progressive uptake of food containing Al, might pose various negative impacts of health hazards (e.g. it can affect the nervous system of humans). The intake of excessive aluminium also can cause anemia, glucose intolerance, and cardiac arrest in humans (Health Canada 2007).

Several studies have recognized that Alzheimer's disease or related dementia has been found in the communities of the drinking water source that contains excess aluminium (Health Canada 2007). This may also lead to health hazards in humans (e.g. loss of memory, listlessness, severe trembling and neurodegenerative diseases). It can lead to the risk of allergies and might cause deficiencies of vitamin D and calcium named osteomalacia (Lenntech 2015). It can also cause Lou Gehrig's and Parkinson's diseases (Health Canada 2007). Excessive Al in water can also cause death to human due to ingestion of high Al concentration (Frecker 1991).

2.4 Guidelines for Regulating Al in Water Environment

The drinking water standards for Al, according to World Health Organization (WHO), is a maximum acceptable aluminium concentration in water of 100 to 200 µg/L (Water Quality Association 2013). According to the US Environmental Protection Agency (EPA) in the USA considering Secondary Maximum Contaminant Levels (SMCLs), this value would be 50 to 200 µg/L (Water Quality Association 2013). Whereas, according to CCME, the allowable limit of Aluminium for fresh water aquatic life is restricted to 100 µg/L at pH>6.5 and 5 µg/L at pH<6.5. The recommended Canadian water quality guideline for livestock drinking water is 5000 µg/L (CCME 1999). The guidelines for Aluminium according to Canadian drinking water quality in Nova Scotia Environment for health related parameter is 100 to 200 µg/L (Terms of Reference 2002). Also, the maximum acceptable concentration for aluminium for monitoring public drinking water supplies is 100 to 200 µg/L.

Filter Backwash Water Discharge Value: The discharge criteria in Nova Scotia Environment (NSE) for Aluminium containing water is based on CCME on site specific limits. The discharge criteria of the backwash effluent water depend on the following parameters: TSS should not exceed 25 mg/L, pH range in between 6.5 to 9, total Al must be below 184 µg/L and the effluent water should be nontoxic prior to discharge (CCME 2004).

2.5 Various Treatment Strategies to Remove Aluminium from Water and Wastewater Systems

The literature contains few studies that have been devoted to that removing aluminium in waste water treatment. In India, an excellent source of bio-sorbents was discovered to

remove aluminium (+3) species from polluted wastewater (industrial effluents and polluted lakes) which is the thermally activated powder of leaves, stems and their ashes of Moryngea millingtonia and Cygium arjunum plants (Kumari & Ravindhranath, 2012). They investigated that such plants mentioned above have excellent sorption capacities to remove about 100% of aluminium; having 150 minutes of detention time and optimal pH near to 6-8 using adsorption processes. Another study of water treatment process showed that aluminium removal was achieved significantly using low cost adsorbents such as rice husk char and activated rice husk char (Singh & Parikh, 2006). Furthermore, utilizing humic acid as a coagulant aid in associated with water-soluble polymers by the process of precipitation of metals successfully was able to remove Al from wastewater (Humintech 2014).

Different studies were found using coal mining waste to remove Al (III) ions to near 100% in acid mine drainage using in an increase of pH around 7.8. The metal oxides of the coal mining waste acted as adsorbents of H_3O^+ to remove Al (III) ions by increasing the pH in the presence of the surface charge through precipitation and adsorption mechanism (Geremias et al. 2008).

Several investigations were conducted to study the usefulness of adsorbents for contaminant removal. These investigations used metal oxides (alumina, iron oxide and magnesia) adsorbents either in combination or individually showed excellent adsorption capacities in the wastewater treatment strategies (Ikari et al. 1979). A recent study shows the usage of calcium oxide or lime for the removal of Al from freshwater Al sampling operations (Macleod 2015).

According to alum coagulation theory, there are two mechanisms by which a coagulant can remove particulates through the treatment of water and wastewater operations. The first theory postulates neutralization of the surface charge to form particles and settle due to

gravitational force in reasonable time period. The other one involves sweep flocculation theory which implies the mechanism of particle aggregation due to sweep coagulation as shown in the solubility diagram of Aluminium in Figure 2-2. In this mechanism, particles tend to adhere to each other and form a bigger particle in size in a reasonable time. Finally, these particles precipitate, removing most of the particles with them due to the gravitational force. When an adsorbent (i.e CaO or MgO) is added in wastewater treatment, they attempt to increase the pH which might help to perform sweep flocculation and adsorption mechanism to form precipitates of metal hydroxides. Also, adsorption of a cation such as Al^{3+} is easier at an alkaline pH than at acidic pH. In addition, when ferric oxide adsorbents (cationic) are mixed with water in presence of an alum coagulant; they may aid in the adsorption process in the pH range between 6.0 to 8.0. They help to remove particulates through particle entrapment or sweep floc via charge neutralization as an amorphous precipitation of metal hydroxides (John et al. 2005). Higher dosage of adsorbents is beneficial to particle precipitation during alum coagulation to form insoluble precipitates.
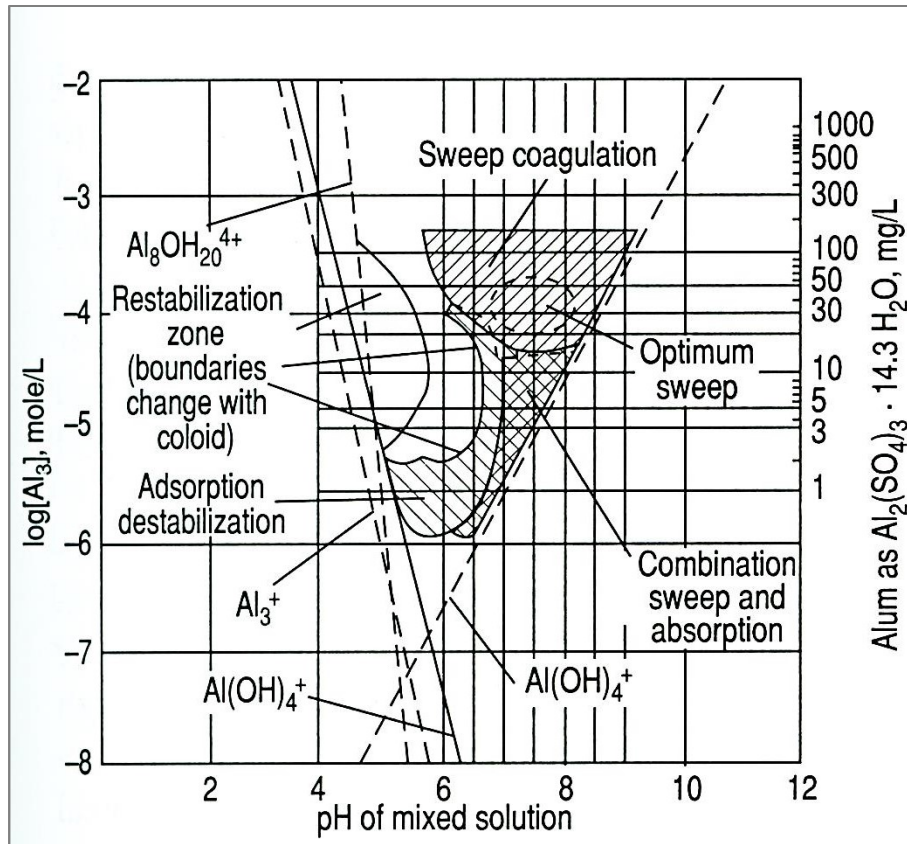
Figure 2-2   Aluminium Solubility Diagram (John et al. 2005).

The usage of geotubes were also found in the application of water treatment facilities and municipal wastewater applications. In Vicksburg, MS and Baton Rougue, LA, geotextile tubes have been used to dewater alum (Aluminium sulphate) sludge lagoons to remove alum wastes successfully (Fowler et al. 1995). In Jekyll Island, GA, geotubes were used to remove 400,000 gallons of anaerobically digested sludge from digesters that helped to dry its alum sludge to 28% through dewatering process in a simple and fast way (Tencate Geotube 2006). The details of the geotubes are outlined in the next sections.

2.6 Previous Research on Filter Backwash Water (FBWW)

In recent years, few studies have been conducted with FBWW. A study on FBWW obtained from Giza water plant, Egypt shows on the possibility of reusing FBWW with raw water for treatment. This investigation was conducted by (Hanan et al. 2016) reveals that with a mixing ratio of 40% FBWW to 60% RW can be reused and is economically acceptable. If this raw water can be reused, it can be beneficial either for drinking or for irrigation purposes. Wood (2014) has studied the distribution of Al in the filter backwash treatment system and examined the used of polymers for providing treatment of Al.

The effects of reusing Filter Backwash Water and its water quality was examined by EDZWALD (2003) in six full-scale surface water treatment plants in Connecticut. This investigation evaluated treatment strategies and recommended better improvement of the treatment operation for recycle practices of FBWW in the treatment facilities.

A pilot studies have been conducted on Spent Filter Backwash water at the Utah Valley Water Purification Plant located in Utah. This study was investigated on the innovative applications of treatment processes for Spent Filter Backwash. However, a bench scale test set up was run to evaluate membrane treatment alternatives for Spent Filter Backwash including low pressure microfiltration/ultrafiltration (MF/UF) types, such as hollow fiber membranes, tubular membranes, and ceramic membranes. (EPA, David A. Cornwell, John Tobiason, and Richard Brown, 2010).

Another research was found analyzing the impacts of recycling FBWW and membrane backwash water (MBWW) for the removal of organic contaminants from raw water in coagulation–sedimentation processes. This research highlights that the FBWW blended with 5 and 10% by its volume having a specific UV absorbance (SUVA) value within the range

of 2–4 mg/L m provides higher DOC removal from the raw water (*Gottfried, A., Shepard, A. D., Hardiman, K., & Walsh, M. E., 2008*).

.

2.7 Geotextile Tubes (i.e. Geotubes)

Geotubes represent an innovative and emerging technology which can assist with space limitations, cost, personnel, operational difficulty and efficiency to successfully rapid dewater and contain contaminated wastewater in the field of wastewater treatment technologies, marine applications etc. Geotextile tubes, or geotubes as they are commonly referred to, are factory assembled geotextiles tubes or closed end cylinders, which are manufactured from high strength, permeable, specially woven or non-woven engineered dewatering geotextiles (i.e polypropylene or polyester), designed for containment and dewatering of sludges. Geotextiles consist of polymers of varying composition but are typical made from polymers such as polyethylene, polypropylene, polyester and polyamide (Koerner 1998). They are usually continuous sheets of woven or non-woven geotextiles formed from knitted or stitch-bonded fibers, filaments or yarns using conventional textile manufacturing facilities (see Figure 2-3). Geotube dewatering containers are formed from the sewing of woven geotextiles to the circumference and length required (Geofabrics NZ 2015). Geotubes are designed with the adequate strength seam capacity to meet the expected pumping pressure.
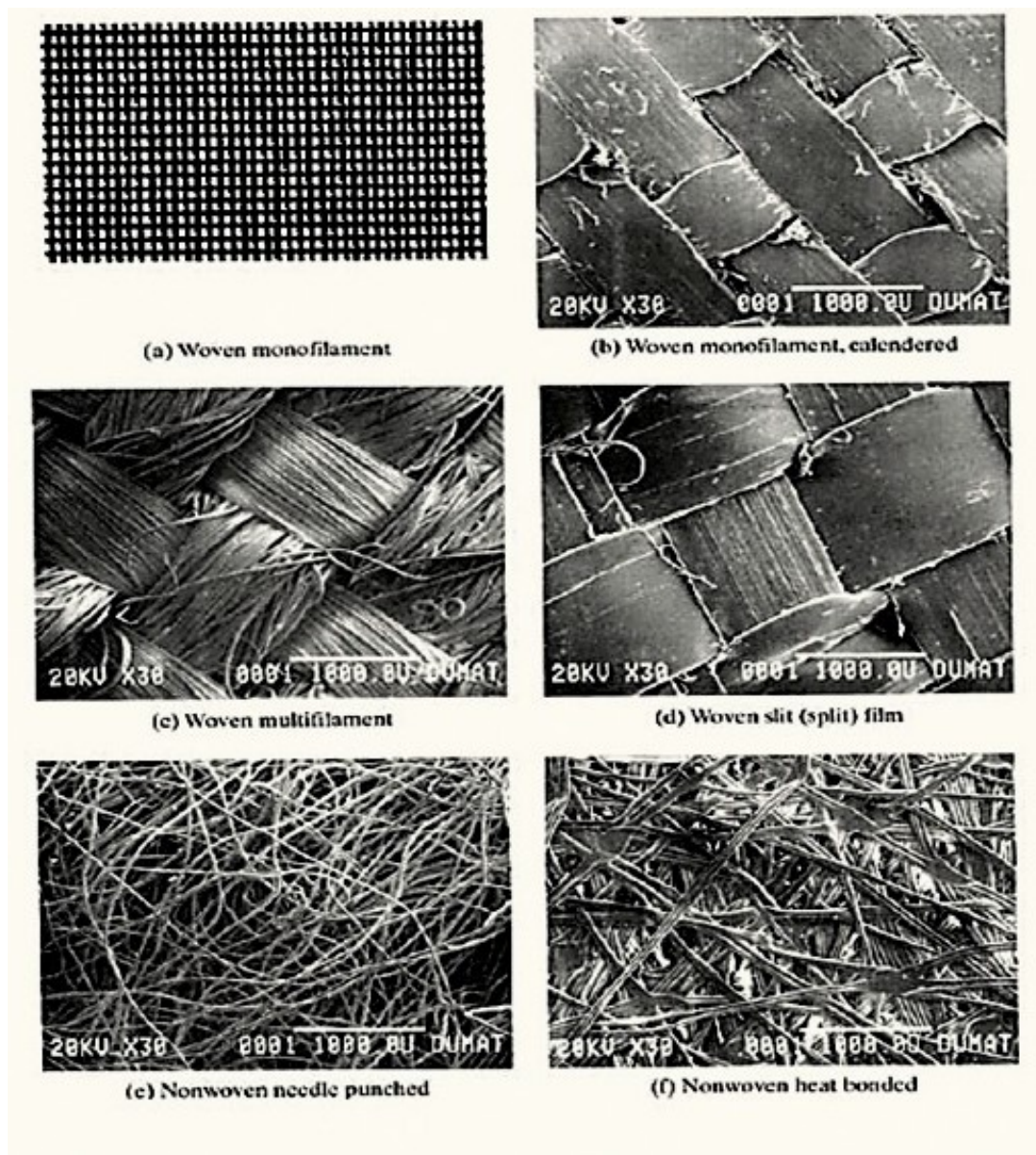
Figure 2-3   Photomicrographs of Various Fabrics Used as Geotextiles (From Koerner 1998).

Geotubes are custom fabricated (using seaming techniques) that can resist pressures during pumping operations (Dewatering Solution Inc. (DSI) 2007). They are theoretically

manufactured within 1 to 10 m in diameter, with a circumference up to 14 m and length varying up to 100m; lengths of 20 to 30m are most common (Smith 2008). The tubes are pumped full of the liquids with solids to capture solids inside the tube; liquid is then expelled through the pores of the geotubes via hydraulic gradient differences, as the dewatering process progresses, as shown in Figure 2-4.

Geotubes provide efficient, affordable, and cost effective dewatering processes. Approximately, 400 million of cubic yards of sediments are dredged in the United States using geotubes each year (Palermo and Wilson, 1997). They can also create volume reduction up to 90% and offer facilities lower equipment cost, low maintenance, low labor cost with no requirement for special equipment (Tencate 2007).

Figure 2-4   Typical Geotextile Tube (Bishop Water Technologies Inc. 2013)

2.8 Technical Specifications of Geotextile Tubes

Geotextile tubes are used in wastewater treatment in a large scale for the dewatering of sludge in the field of industrial lagoons, agricultural ponds and so on. They are

available in different configurations and require proper technical specification depending on the surface area for dewatering purposes. The Typical Technical specifications, size and capacity of the tubes and fabric properties are shown in Table 2-1 below.

Table 2-1   Typical   Range   of   Specifications   for   Geotextile   Tubes   (Granite Environmental, 2016).

Geotextile Filter Tubes Technical Specifications		
Length	50', 100', 150', 200'	Other lengths by special order
Width (laying flat)	7.5', 15', 22.5', 30', 37.5', 45'	
Circumference	15', 30', 45', 60', 75', 90'	
Filling Port Spacing	1, 2, or 3 Ports	Equally spaced depending on tube length and volume
Bracing Loop	Every 20' OC	

Size & Estimated Capacity per Tube		
Circumference	**Tube Height**	**Tube Volume**
15' (4.6 m)	3.5' (1.0 m)	0.6 cy/ft
30' (9.1 m)	5' (1.5 m)	2 cy/ft
45' (13.7m)	5.5' (1.7 m)	3.5 cy/ft
60' (18.3 m)	6' (1.5 m)	5.4 cy/ft

Fabric	Woven Geotextile	UV Stable	Weight/Unit Area	Color
Polypropylene	Yes	Yes	16.6 oz/sqyd. (560 g/sq m)	Black
Polyester	Yes	Yes	17.7 oz/sqyd. (600 g/sq m)	White
Polyester	Yes	Yes	24 oz/sqyd (810 g/sq m)	White

2.9 Applications of Geotubes

Geotubes are widely used due their simple construction, minimal environmental impact and lower operational cost. However, most geotube applications can be classified into two categories. The first being semi-permanent structures in shoreline and watercourse environments and the second one dewatering of sludges and dredged materials (Gaffney 2001). Geotubes have emerged as an innovative technology that have been used to dewater high water content materials including marine dredge material, water and wastewater treatment sludges, agricultural waste, mine tailings, and chemical and industrial discharges (Moo-Young et al. 2002). Furthermore, geotextile tubes have been used in a variety of structural applications including dike construction in wetlands, underwater stability berms, shoreline protection and island construction (Fowler and Sprague, 1993). Geotextile tubes in a larger diameter have been used to contain and dewater dredge materials from river channels and harbors for decades (Fowler et al. 1995). Geotubes offer a wide range of dewatering options for various environmental dredging projects providing facilities including cost effectiveness, solids and contaminant retention and solids handling time (Mastin et al. 1999). They provide applications in a variety of fields in dewatering, drainage runoff, structural, erosion and scour protection, containment, etc. Various applications of geotextile tubes are shown in Table 2-2.

Table 2-2   Potential Applications for Geotextile Tubes (After Moo-Young et al. 2002).

Application	Category
Dewatering	Dredged materials, sewage sludge, municipal sewage sludge, water treatment sludge, animal waste, paper mill sludge, fly ash, mine tailings.
Drainage Runoff	Airfield, highways, oil spills, farming.
Structural	Dikes, coastal areas, rivers, wetlands, berms, silt fences.
Erosion and Scour Protection	Bridge piers, tunnels, walls, abutmnets, wind erosion.
Containment	Fine grained dredged material, placement of contaminated dredged material, cappings of contaminated material.

2.10 Working Principles of Geotubes

Geotubes, as shown in Figure 2-5, are manufactured by sewing of one or more layer of high strength permeable geotextile fabric sheets together to form tubes. These also contain number of ports located at the top of the geotube cylinder at discrete intervals. The numbers of ports on the geotubes depend on its length; the longer the tube, the more ports required. These ports receive the liquid via pumping. Geotubes can be transported to various sites as a mobile operation. Once pumping begins, the effluent of interest passes through the pipes, through the ports and into the geotube containers. At the same time, the liquid drains from the geotube through the small openings in the permeable geotextile fabric while trapping the solid particles inside the geotube. The whole process continues until the tube becomes full of solids. The pore size of the geotextile tube in relation to the size of the solids is a key factor for a successful dewatering process. If the openings are too small, it is difficult to trap the solid materials inside the container. Also, if the openings are too narrow, excessive pressure might exceed the fabric or seam strength of the geotextiles cause failure (Koerner

and Koerner, 2006). During pumping, the elevation or height of the tube is usually monitored to prevent rupture (i.e, to control overfilling).
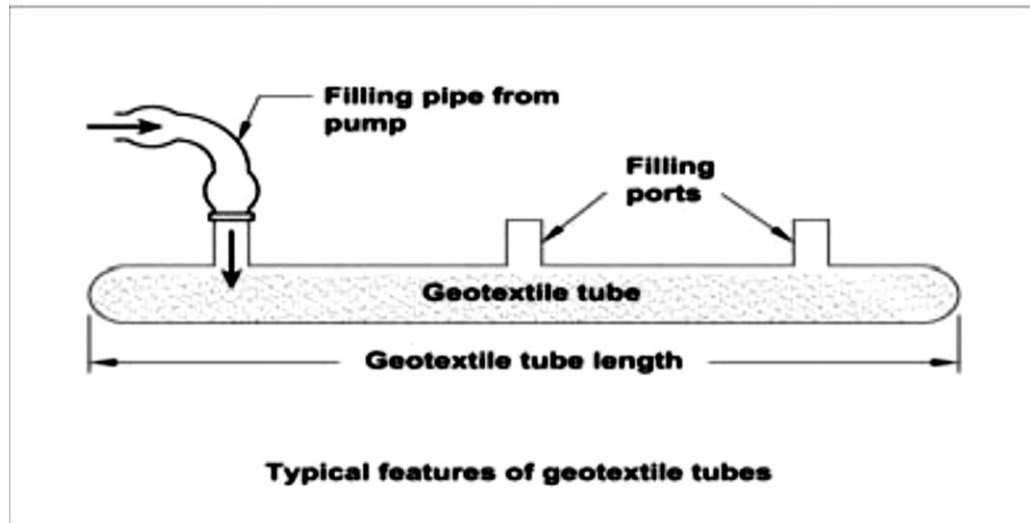
Figure 2-5   Typical Geotextile Tube (Smith 2008)

It is possible to fill a geotube to a height of about 70 to 80% of the theoretical maximum circular diameter. It depends upon the fill of materials and pumping conditions (Liao 2008). When geotubes are filled with granular sands or gravels, (i.e in the case of shoreline protection), the drainage capability of the geotube is rapid. However, in the process of dewatering of any fine sediments or sludges, the drainage capability becomes slower as the fine grained soil builds a filter cake and blocks the pores of the fabric inside the geotube.

2.11 **Fundamental Principles of Geotube Operation**

Geotube dewatering technology fundamentally consists of a three-step process. These steps include (1) filling or containment, (2) dewatering, and, (3) consolidation (see Figure 2-6).

Figure 2-6   Fundamental Principles of Geotubes (From Tencate 2007)

In the containment stage, polymers are usually mixed with the liquids and the solids to improve the solids content and aid in clarifying water for more effective dewatering. High water content materials such as fine grained sludge, hazardous contaminated soils, or dredged waste materials are hydraulically and mechanically pumped into the geotube container under an imposed pressure. As previously discussed, it is essential to maintain the pumping rate at a level so as to not exert excessive pressure on the geotube container which can cause failure or rupture of the geotextile or seam properties.

In the dewatering phase, excess water drains through the pores of the geotextile tube. The fabric properties of the geotextile acts as a filter medium and confines the fine grained particles. The dewatering process results in volume reduction of the contained materials that

allows the container to be refilled with additional slurry. This process is repeated until the tube becomes full with solids. The clear water filtered through the container usually can be recycled and reused without additional treatment or for further processing.

Consolidation is the final stage of the geotube process and occurs predominantly after filling. In this stage, consolidation of the particles occurs due to self-weight and consolidation water seeps out of the geotube while maintaining the solid particles inside. About 99% of the solids are captured in the geotube container. When the entire dewatering process is completed and the geotube container is full, the entrapped solid can be deposited at a landfill site, used as construction materials or remain on-site depending on the quality and composition of the sludge. Familiarity with sludges, pumping operations and hydraulic properties of solids is important for a successful dewatering process of geotubes (Tencate 2007).

2.12 Feasibility Testing for Geotubes

There are numerous test methods commonly used to assess the performance of geotubes. The performance tests are associated with the evaluation of the common factors comprising of dewatering efficiency and dewatering time (Gaffney et al. 2001; Liao 2008; Huang and Koerner, 2005). There are some common and efficient feasibility tests of geotubes comprising of the hanging bag test (HBT), the falling head test (FHT), the pressure filtration test (PFT), the rapid dewatering test (RDT) and the gradient ratio test (GRT). Rapid dewatering test (RDT) is the most common of these tests to assess potential solids removal and will be outlined below.

Rapid Dewatering Test

One of the quickest and efficient test in the dewatering technique is a rapid dewatering test (RDT) illustrated in Figure 2-7. The rapid dewatering test on a small scale is employed in order to evaluate some of the important parameters such as sludge filtration rates, suspended solids, efficiency of the candidate polymer, and selection of filter media, dewatering time, and quality of effluent water (Tencate 2007).

The materials of RDT test include a bucket, a funnel, a disk of geotube fabric (GT 500 fabric), a centimeter scale, a graduated cylinder, a syringe, and a stop watch.

At first, the RDT Test apparatus is assembled with the test kits. A funnel is placed on the top of a bucket with a geotextile filter medium inserted in the bottom of the funnel. The wastewater is then treated with polymer by using a syringe at pre-selected dosage using jar test apparatus. Variation of the polymer dosage can be examined to figure out the suitable dosage required for the test solution to form flocs. Vigorous shaking or mechanical mixing is essential to invert the neat polymer into solution. Then, the conditioned sludge solution is poured through the geotextile GT500 fabric to pass over the funnel and finally stored in the bucket while the solids in the solution are trapped on the top of the geotextile fabric.

Observations are performed to identify the parameters i.e. filtration rate, dewatering capacity and the amount of captured solids at specific time intervals periodically. Initial and final total suspended solid, turbidity and contaminant before and after passing the sludge through the geotextile are measured to evaluate the performance of dewatering fabric. The RDT test is applied and analysed further in the experimental section in this report.

Figure 2-7   Rapid Dewatering Test Unit (Tencate 2007)

2.13   Case Histories of Geotubes in Practice

The geotube dewatering technique has a lot of applications which has been practiced in a numerous field of case studies. The case study as described below is taken from an article from the website of Bishop Water Technologies Incorporation (Bishop Water Technologies Inc. 2013). The case study mainly focuses on a problem, its challenges, solution, construction and the result as a performance of the study which are described and analyzed belows:

The Green Way Pollution control plant in the city of London, Ontario collects sludge from five different wastewater treatment plants, produce ashes through the incineration process, store in the lagoon and transport them to the disposal sites periodically as shown in Figure 2-8(a). But management of excessive ash and the capacity of the disposal sites are major challenges with limited options in a cost effective manner.

In 2010, Bishop Water Technologies took an initiative to overcome the overall situation by introducing Geotube dewatering technology in a small scale project in the city of London. They started working to assess the effective of the geotube technology while maintaining ashes through the dewatering process in terms of ease of operation, construction friendly, cost effectiveness, less handing time and finally to produce a larger scale of retaining solids. Later in late 2010, they started a pilot project using of 30' in circumference and 50' in length Geotube unit was chosen to transfer the ash slurry from the lagoon cells to the geotube unit which was laying around the existing lagoon cells to dewater the ash. After achieving significant success from the pilot project, a large scale test with an advanced methodology and the design of installation was performed.

The installation of the geotube unit was accomplished by choosing a new dimension of the geotube unit of 80' in circumference and 55' in length, which was constructed with concrete cells and jersey barriers, were in use to accommodate the cell segregation as shown in Figure 2-8(b). The performance of the geotube unit not only satisfied the desired level but also exceeded the desired expectations to some extent.

Figure 2-8   **(a) Prior to Implementation of Geotube Units (b) Working in Operation after Geotube Installation (Bishop Water Technologies Inc. 2013)**

Chapter 3 Materials and Methods

This chapter provides an overview of the materials and methods that have been undertaken in this research. The overall experimental framework of this project is structured in terms of the sample water collection and preparation, experimental set up, general methodologies and technical approaches for the analysis of the samples.

3.1　Generation of FBWW from JDKWTP

The source water of the research work is FBWW which was collected from the J. D. Kline water treatment plant (JDKWTP), that treats water from Pockwock Lake situated in a protected watershed in Halifax, Nova Scotia. The FBWW at this plant is generated from the regular backwashing of the filter bed media of the treatment plant operations with the purpose to remove solids in the filter media. At the beginning of the water treatment process at JDKWTP, the source water is pumped into the treatment facility at a constant flow rate through a 1.2 m (48-in.) inlet pipe with a design capacity of about 220ML/day (Vadasarukkai et al. 2011). Thereafter, the flow of water is sent into the three rapid mixing tanks, in series, for further treatment processes as shown in the process diagram of the JDKWTP in Figure 3-1. The water in the treatment facility is treated via screening, coagulation, flocculation, dual media filtration and chlorination where alum is added as a coagulant aid and polymer (Megnafloc LT20) is added at some point of the winter season to increase the floc strength (Wood 2014). The water is then passed into the four identical flocculation chambers that include two parallel sets of three stage tanks where the tapered hydraulic flocculation process runs. In the next step, the water is then allowed to be filtered into the eight dual media filtration units. In this unit, regular backwashing is required to remove suspended solids in the filter bed media. The backwashing of the filter bed media

is accompanied releasing approximately about of 700,000 L of water in the opposite direction of the process flow of water to dislodge the particulate materials from the filter pores (Wood 2014). This backwashing water is referred as FBWW.
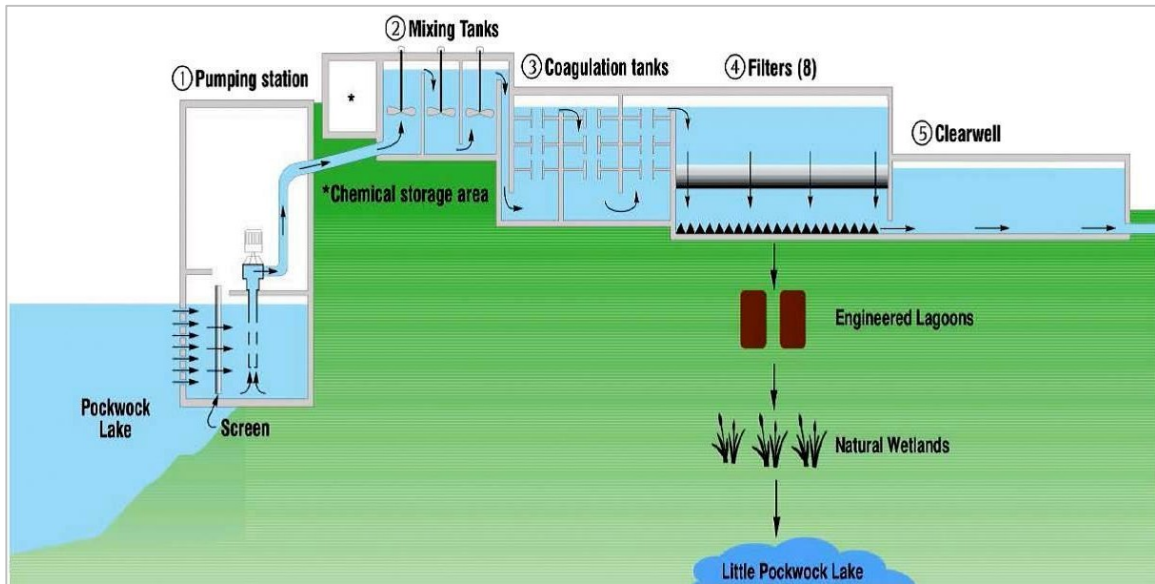
Figure 3-1   Process Diagram For the JDKWTP (Adapted from Halifax Water, 2005)

This backwash water is then gravity fed to the filter backwash treatment area at JDKWTP. The treatment area consists of two lagoons (14000 m³) in parallel followed by a natural wetland as shown in Figure 3-1. Overflow weirs are used for both lagoons prior to discharge at an outlet chamber. At this point the filter backwash wastewater (FBWW) is then released into a natural wetland via a pipe of 3 ft (1m) downstream to a little Pockwock Lake to the southwest of the plant which is separated by a controlled dam from Pockwock Lake as shown in Figure 3-2 (Wood 2014).

The engineered lagoons are cleared of solid material via transfer to the two drying beds. The alum added in the treatment process tends to result in elevated levels of aluminum in the filter backwash water (FBWW). Predominantly total suspended solids (TSS) and aluminium are of major concern. The FBWW that is eventually discharged into the Pockwock Lake, may attain levels of aluminium in excess of the provincial guidelines of 184 µg/L (Wood 2014). According to CCME 2004, for aluminium in the FBWW, discharged water quality must meet the following criteria: pH must be between 6.5 and 9, Total Al should be below 184 µg/L, TSS should be below 25 mg/L and chorine residual must be below 0.002 mg/L and the discharge should not be toxic to aquatic life.

In this chapter, several treatment strategies and approaches were trialed for the removal of aluminium from FBWW. A description of the materials and methods used in this thesis are described below:

Figure 3-2   Discharge Of FBWW from the Settling Lagoon (Wood 2014)

3.2 Materials

3.2.1   Filter Backwash Wastewater (FBWW)

Samples of filter backwash wastewater (FBWW) effluent used in this research were collected from J. D. Kline Water Supply Plant, operated by Halifax Water. Hereafter, this FBWW effluent will simply be referred to as FBWW. Samples were collected from the top of the filter at the beginning of a backwash using a 10-gallon bucket. The samples from the J. D. Kline water supply plant were collected bi-monthly in sterile 40 L plastic containers/jars, and were labeled and stored at room temperature (21°C $\pm$ 1°C). The samples were collected during the fall and winter seasons. In fall season, the total aluminium concentration was found to be more (3104 µg/L) compared to winter season (2250 µg/L) as summarized as shown in the next chapter.

To prepare the FBWW samples for the experimental program described subsequently, the plastic storage containers were homogenized by shaking to ensure that any suspended solids in the FBWW were not residing on the bottom of the container. Subsamples from these plastic containers were then poured into 1 L jars and passed through a digitally controlled ultrasonic cleaner for at least five minutes. This ultrasonic procedure was performed to promote the breakdown of larger suspended solid particles when analyzing total and dissolved Al concentration of the samples. The FBWW was characterized for the following selected parameters: pH, total Al, dissolved Al, total suspended solids (TSS), zeta potential (ZP) and particle size in ECD (Equivalent Circular diameter). The methods used to perform this testing are summarized below.

3.2.1.1 *Water Quality Methods Used to Characterize FBWW*

(a) Total Al and Dissolved Al Concentrations

For total and dissolved aluminium concentrations presented in this thesis, testing was performed at room temperature ranging from (21 ° ± 1°C). For total Al testing, the nonfiltered samples were taken into account for the experiments. Both total and dissolved Al samples were diluted with 900 Milli-Q water (dilution factor of 10). Testing for dissolved Al involved passing the samples through a Micron-PES, polysulphone 0.45 micron (47 mm diameter) filter paper prior to analysis. Unfiltered samples were used for total Al concentrations prior to analysis. Total Al and dissolved Al concentrations were analyzed with HACH DR5000/2010 Spectrophotometer (HACH Company, Loveland, CO) using Eriochrome Cyanine R Method (method 8326) having a range of 0.002 mg/L to 0.250 mg/L Al^{+3}. In this procedure, the pH of the samples was adjusted to between 2.9-4.9 or 7.5-11.5 as the range between pH of 4.9 to 7.5 may accelerate dissolved aluminum to partially convert to colloidal and insoluble forms. All the experiments were repeated as duplicate for three individual trials for accuracy of the results and the average results were obtained.

(b) Total Suspended Solids (TSS)

Prior to Total Suspended Solid (TSS) testing, 934-AHTM Whatman glass microfiber filter papers (diameter 47 mm) were placed in an aluminium dish and placed in the oven at 100 °C to dry for at least an hour. A 100 ml sample is placed in a prewashed glass beaker for each test. Mili Q water is used for the TSS test. The samples are agitated to ensure mixing and then poured into the filter apparatus. A vacuum is used to draw the sample through the filter. When all the sample passes through the filter paper, a few drops of mili Q water

was sprayed to wash away the remainder of the samples that may have adhered to the inner wall of the beaker. The total volume of sample (initial plus water used to clean beaker) was recorded. The filter paper with the solids were then placed on the aluminium dishes, labelled for each dosage and kept in the oven for a temperature of (104~105) °C for 24 hours. After the samples were dried in the oven, the filter papers were placed in the desiccator for at least half an hour. The blank weight of the filter paper and oven dried residue were measured using measuring balance up to four decimal values. TSS was calculated as shown in equation 3.1 below:

$$\text{TSS (mg/L)} = \frac{(\text{Final Weight of filter and Residue-Initial weight of filter}) \text{in mg} \times 1000}{\text{Amount of samples taken in mL}} \quad \ldots\ldots\ldots\ldots\ldots\ldots.3.1$$

(c) Zeta Potential Analysis

Zeta potential analyses of the samples were performed using a Melvern Zeta Sizer to obtain the electrophoretic mobility of the particles at 25°C having a detection limit of 5.54 mV (Follett 2012). The unfiltered samples were collected from the beakers just after the rapid mixing and completion of the detention period of 1.5 hours immediately. Next, a disposable folded capillary cell was filled with unfiltered samples by syringes that were placed inside the zeta sizer. Then, each of the samples was analyzed taking five measurements and an average value was taken. Before using the syringe was cleaned properly using deionized water and the two electrodes of capillary cell were rigorously cleaned with the ethanol solution. Care was taken while placing the capillary cell so that it becomes free from air bubbles to avoid poor or wrong results and also to avoid spillage inside the cell area (Malvern Zeta Sizer 2008).

(d) Particle Size Analysis

Particle size analysis of the FBWW was performed using Micro Flow Imaging (MFI) software that was incorporated with DPA 4100/4200 flow microscope for obtaining the particle size (Brightwell Technologies Inc. 2009). The measurements were performed for a range of particle sizes between 2μm and 400 μm. For analyzing the samples, 1 mL of unfiltered samples were taken using a pipette and a syringe that was filled with the samples and then mounted properly in the designated places inside the cell holder. The syringe was placed with care without any splitting of water so that it cannot obstruct the sensing zone of the flow cell. Each sample was analyzed with triplicate measurements and an average value was taken for the particle size measurements. Finally, particle size distribution was created using MFI images as a distribution chart showing particle concentration as expressed in numbers/mL versus ECD (Equivalent circular diameter) in μm. During the preparation of the size analysis of the samples, the flow cell was cleaned properly using ethanol solution. The micrometer position was set properly before the analysis according to the flow cell configuration. The narrow tube which fits with the flow cell was set properly to be free form air bubbles and make sure no contaminants can obstruct inside the tube while flowing the samples.

The raw filter backwash water quality consisted of the characteristics as shown in Table 3-1. Each sample was performed in three consecutive trials and the average value was taken to characterize the FBWW. The raw data for this Table 3-1 is in Appendix B.

Table 3-1   Characteristics of Filter Backwash Water (FBWW)

Raw Water Quality Parameters	Average Values (3 trials)
pH	7.5 (Winter and Fall season)
Total Al	2250 µg/L (Winter season) 3104 µg/L (Fall season)
Dissolved Al	140 µg/L (Winter season)
Zeta Potential (ZP)	+33 mV by 10 times dilutions (Winter season)
Size (Equivalent Circular Diameter range)	2-39 µm by 100 times dilutions (Winter season)
TSS	1 mg/L (Winter and Fall Season)

3.2.2 Adsorbents

In this research, three types of adsorbents were used in an attempt to remove Al from the FBWW; calcium oxide (CaO), magnesium oxide (MgO), and iron oxide (Fe_3O_4). All three adsorbents were obtained from Thermo Fisher Scientific, Fredericton, New Brunswick.

3.2.3 Polymer

A cationic polymer (NOVUS CE 2667) was used in this research to assist in particle removal and was obtained from the Lake Major Water treatment plant in Dartmouth, NS. The polymer is composed of isoparaffinic petroleum distillate (15- 40 % by weight), poly (oxy-1, 2-ethanediyl (1-5) %, and (1-5) % by wt.) of ammonium chloride. Its specific gravity is 1.034, is white to off-white color in emulsion stage liquid and pH is 5.0. In the experiments,

1 mg/L of cationic polymer was chosen for each of the adsorbent dosage with varying parameters. 1 mg/L polymer dosage was observed to be as an effective dosage, based on the previous studies of Fanous's M. Eng report (Fanous 2013).

3.2.4   Geotextile

To filter out the solids generated during the proposed treatment of FBWW, a GT500 Engineered polypropylene woven geotextile manufactured by Tencate (see Figure 3-3) was obtained in a 0.3 m wide by 5 m long strip from Bishop Water Technologies in Ontario, Canada. The typical properties of the geotextiles used as provided by the manufacturer are given in the Table 3-2.

Figure 3-3   GT500 Engineered Geotextiles

Table 3-2   Properties of GT500 Engineered Geotextile (Tencate 2011)

Mechanical Properties	Test Method	Unit	Minimum Average Roll Value	
			MD	**CD**
Wide Width Tensile Strength (at ultimate)	ASTM D4595	lbs/in (kN/m)	470 (78.8)	625 (109.4)
Wide Width Tensile Elongation	ASTM D4595	%	20 (max)	20 (max)
Factory Seam Strength	ASTM D4884	lbs/in (kN/m)	400(70)	
CBR Puncture Strength	ASTM D6241	lbs (N)	2000 (8900)	
Apparent Opening Size (AOS)	ASTM D4751	U. S. Sieve (mm)	40 (0.43)	
Water Flow Rate	ASTM D4491	Gpm/ft^2 (l/min/m^2)	20(813)	
UV Resistance % strength retained after 500 hours)	ASTM D4355	%	80	

Filtration Properties	Test Method	Unit	Typical Value
Pore Size Distribution (O_{50})	ASTM D6767	Micron	80
Pore Size Distribution (O_{95})	ASTM D6767	Micron	195

Physical Properties	Test Method	Unit	Typical Value
Mass/Unit Area	ASTM D5261	Oz/yd^2(g/m^2)	17.3 (585)
Thickness	ASTM D5199	mils (mm)	70 (1.8)

3.3 Experimental Testing Program

In an attempt to remove aluminum (total and dissolved) as well as total suspended solids from the FBWW effluent, a combination of adsorbents (CaO, MgO, and Fe_3O_4), pH adjustment and polymer dosage were used in this research. Essentially the research consisted of two distinct phases: 1) Preliminary jar testing with the adsorbents, pH adjustment to 6.5 and polymer addition for flocculation, and, 2) geotextile filtration tests with some of the resulting water from some of the more successful treatments. Below is a more detailed description of each of the two phases.

3.3.1 Phase 1 Testing: Jar Testing

The jar testing used in this research was selected to perform relatively quick and easy determinations of removal of Al and TSS from the FBWW effluent using the treatment techniques explained in this section. In general, each of the jar testing treatment evaluations involved taking 1 L of the FBWW and transferring it to the testing apparatus. Then without addition of polymer and adsorbent powder, total Al and TSS were identified for the characterization of FBWW and the results were recorded.

Then, 1 mg/L of the cationic polymer was added to the FBWW into the jars using a pipette. The selected adsorbent powder was then applied immediately to the jar at the desired dosage, as shown in Table 3-3. The mixture was then stirred using a glass rod at a constant rate (ie about 80 rpm) until the mixture was dissolved in the solution. A glass rod was used instead of magnetic stirrer for the Fe_3O_4 adsorbent powder due to the attraction of magnetic stirrer to the Fe_3O_4 particles. As noted in Table 3-3, the CaO, MgO, and Fe_3O_4 adsorbent was applied at four different dosages with the polymer. In addition, a 50/50

mix of the CaO and Fe_3O_4 adsorbents were used at three different dosages, as shown in Table 3-3.

After a given polymer/adsorbent dosage was added, the pH of the mixture was monitored for 1.5 hours. The resulting pH is provided in Table 3-3. To investigate the role of pH on removal of Al and TSS, experiments were repeated as described above but with the pH initially adjusted to 6.5 using 3M of H_2SO_4 or a base of 1N NaOH. For mixing, each jar was covered using plastic parafilm to minimize CO_2 ingress from the atmosphere. The mixing process continued until the pH adjusted to 6.5. After the pH was adjusted to 6.5, the flocs were allowed to settle down for a detention period of one and a half (1.5) hours. Finally, pH was recorded again and the influent water collected. The influent water was characterized for the parameters of total aluminum (with and without PH adjustment conditions), dissolved Al, TSS, zeta potential, and particle size (with PH adjustment conditions) were performed for the samples using the following Table 3-3.

Table 3-3   Testing Program for Phase 1 Testing

Adsorbent Used	Polymer Dosage (mg/L)	Adsorbent dosage (g/L)	pH Measurement (after 1.5 hrs Without pH adjustment)	pH Measurement (after 1.5 hrs with pH adjustment to 6.5)
CaO	1	0.1 g/L	9.0	6.5
		1.0 g/L	11.3	7.5
		2.5 g/L	12.2	7.5
		5.0 g/L	12.7	6.9
MgO	1	0.1 g/L	9.1	8.7
		1.0 g/L	10.3	8.9
		2.5 g/L	10.4	9.4
		5.0 g/L	10.4	8.6

Adsorbent Used	Polymer Dosage (mg/L)	Adsorbent dosage (g/L)	pH Measurement (after 1.5 hrs Without pH adjustment)	pH Measurement (after 1.5 hrs with pH adjustment to 6.5)
Fe_3O_4	1	0.1 g/L	6.2	6.2
		1.0 g/L	6.3	6.3
		2.5 g/L	6.4	6.4
		5.0 g/L	6.7	6.7
CaO and Fe_3O_4	1	1.0 g/L	N/A	10.5
		2.5 g/L		11.2
		5.0 g/L		11.3

3.3.2   Phase 2 Testing: Geotextile Filtration Testing

As shown in Table 3-3, phase 2 of the testing involved repeating the jar testing described above for only the 6.5 pH adjustments but examining the ability of the geotextile to separate the solids created in the treatment process from the FBWW. The results of Phase 2 Testing is summarized in Table 3-4. The pH 6.5 adjustment was only performed in Phase II because of better removal results in the Phase I testing (to be discussed in Chapter 4). Aluminum (with PH adjustment conditions) and TSS were measured for effluent water samples. To assess the ability of the geotextile material to remove solids from the treated FBWW, a modification of the Rapid Dewatering Test was used. The geotextile fabric was cut in a 0.15m diameter circle from the larger roll, and situated in a funnel, over a clean plastic bucket, as shown in Figure 3-4.

Table 3-4   Testing Program for Phase 2 Testing

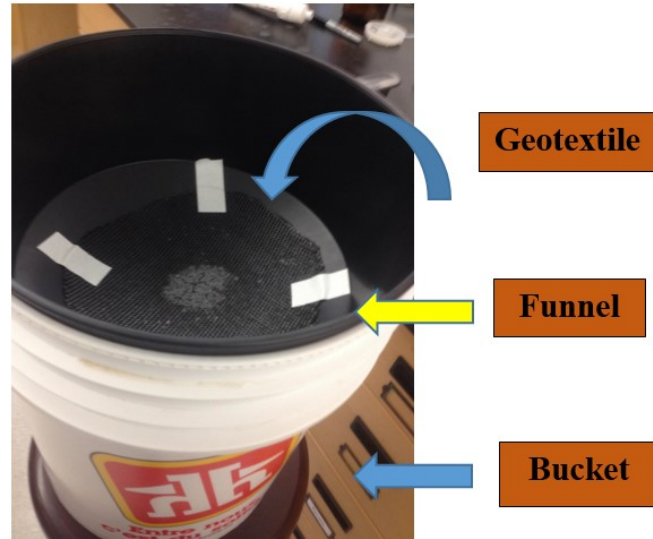| Adsorbent Used	Polymer Dosage (mg/L)	Adsorbent dosage (g/L)	pH Measurement (after 1.5 hrs with pH adjustment to 6.5)
CaO	1	0.1 g/L	6.5
		1.0 g/L	7.5
		2.5 g/L	7.5
		5.0 g/L	6.9
MgO	1	0.1 g/L	8.7
		1.0 g/L	8.9
		2.5 g/L	9.4
		5.0 g/L	8.6
Fe_3O_4	1	0.1 g/L	6.2
		1.0 g/L	6.3
		2.5 g/L	6.4
		5.0 g/L	6.7
CaO and Fe_3O_4	1	1.0 g/L	10.5
		2.5 g/L	11.2
		5.0 g/L	11.3

Figure 3-4   Geotextile, Bucket and Funnel Used For the Geotube Dewatering Process

After the 1.5-hour retention period required for jar testing, the entire treated FBWW samples were mixed homogeneously and poured through the geotextile fabric. Any flocs formed in the treated FBWW samples which were larger than the pore openings of the geotextile filter media, would be trapped on the top surface of the geotextile. An additional 100 ml of mili Q water was used to wash the jars completely of treated FBWW and ensure all flocs were removed from the jar. This additional mili Q water was accounted for when determining effluent concentration. The effluent water that passed through the geotextile fabric was analyzed for total Al and TSS.

In addition, Scanning Electron Microscope (SEM) was performed to examine the floc material on the geotextile after passing the influent water. To do this, the flocs trapped on the geotextile sample for each individual adsorbent dosage was diluted with mili Q water, mixed properly to make a slurry and placed on the small carbon plate (diameter around 10-15 mm) using pipette and then let them dry in room temperature. The samples were labelled, covered and placed them in the desiccator. After 1-2 days, the carbon plates

were collected and subjected to SEM analysis. SEM analysis was performed to assess the elemental composition of the flocs as well as to view the image of the flocs trapped on the top of the geotextiles. The entire process of phase-2 is summarized in Figure 3-5 below.
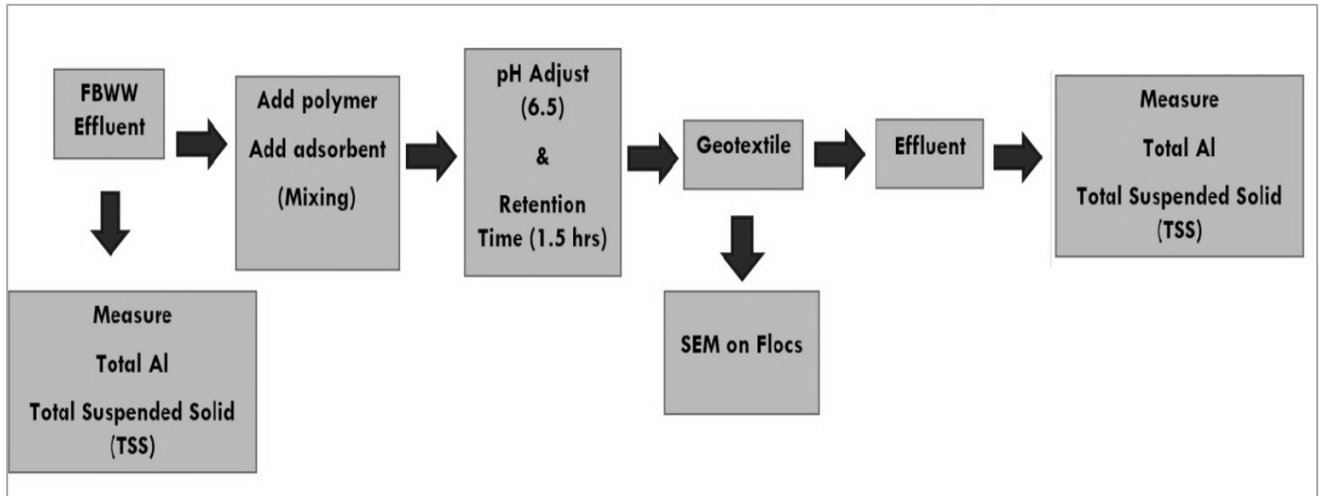

Figure 3-5   Flow Diagram Phase-2

3.4   Preliminary Testing to Confirm Methods

3.4.1   Variation of pH Due to Sample Storage Conditions

Phase-1 of the experimental work investigated potential pH variations due to length of time the experiments as well as the method of covering the samples during the testing. During these preliminary experiments, 1 L of FBWW samples having capacities of 1 L jar is taken and the pH of the FBWW water was adjusted to 6.5 using the techniques. The glass jars were then either left exposed to the atmosphere (i.e. CO_2) in the lab or covered with paraffin wax film. The pH was measured at 0, 0.75, 1.0, and 24 hours. As shown in Figure

3-6 below, the initial pH of 6.5 remained relatively unchanged at 0.75 hrs, 1.5 hours and even after 24 hours for both covered and non-covered samples.
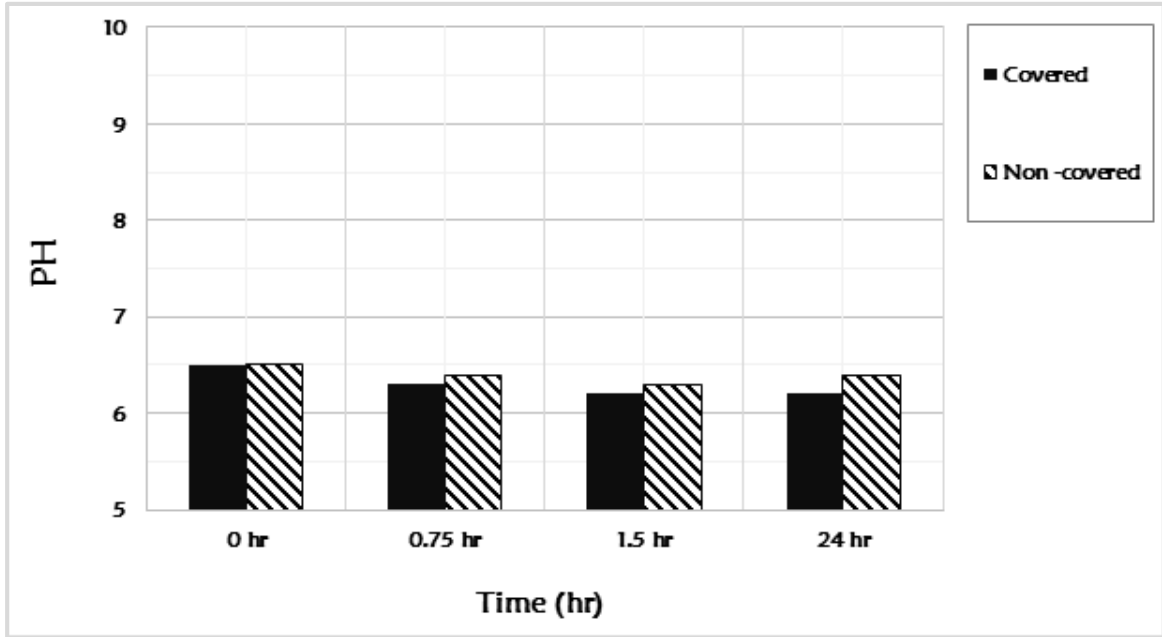
Figure 3-6   Observation of pH Changes with Time for FBWW (No Adsorbent)

As discussed in section 3.4.1, to investigate potential pH changes due to adsorbent addition, the pH was monitored for different times, after adding adsorbent dosage ranging from 0 hours to 24 hours. As shown in Figure 3-7, for CaO adsorbent dosage at 0.1 g/L, the pH was unchanged after 24 hours. After further addition of adsorbent dosage at 1 g/L, 2.5 g/L, and 5 g/L, the pH increased as time elapsed. This pH change was likely due to the CaO becoming dissolved in the water as time elapsed.

	0.1 g/L	1 g/L	2.5 g/L	5 g/L
(O hr)	6.5	6.5	6.5	6.5
(0.75 hrs)	6.5	7.1	6.9	6.7
(1.5hrs)	6.5	7.5	7.5	6.9
(24 hrs)	6.5	7.6	7.8	7.3

Adsorbent Dosage (g/L)

(O hr)   (0.75 hrs)   (1.5hrs)   (24 hrs)
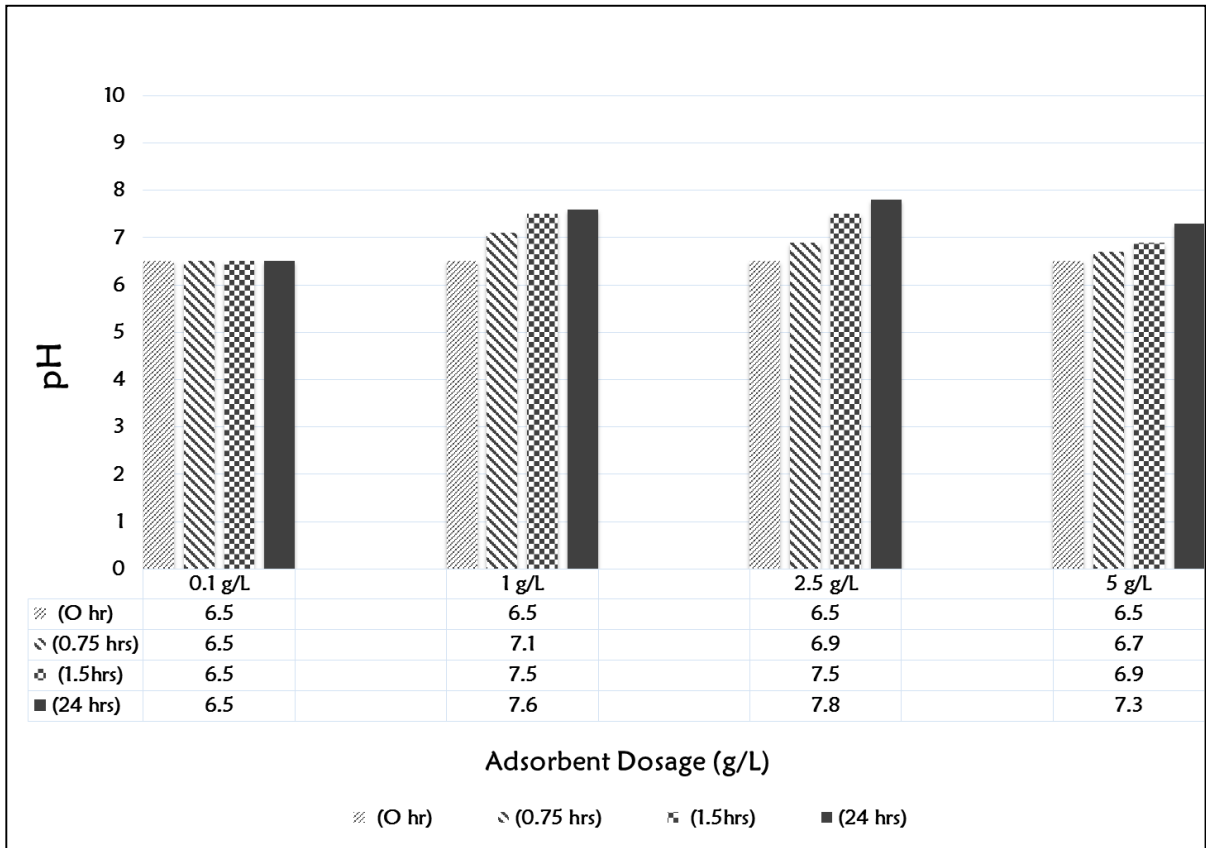
Figure 3-7   Observation of pH Changes with Time for FBWW after Addition of CaO Dosage

Similarly, pH observation for Fe_3O_4 and MgO with time is shown in Figures 3.8 and 3.9. For Fe_3O_4, there were some minor changes in pH at same of the adsorbent dosages shown in Figure 3-8. The most variation was observed for the 5 g/L dosage.

	0.1 g/L	1 g/L	2.5 g/L	5 g/L
O hr	6.5	6.5	6.5	6.5
0.75 hrs	6.3	6.4	6.5	7.2
1.5hrs	6.2	6.3	6.4	6.7
24 hrs	6.2	6.3	6.5	7.1

Adsorbent Dosage gm/L

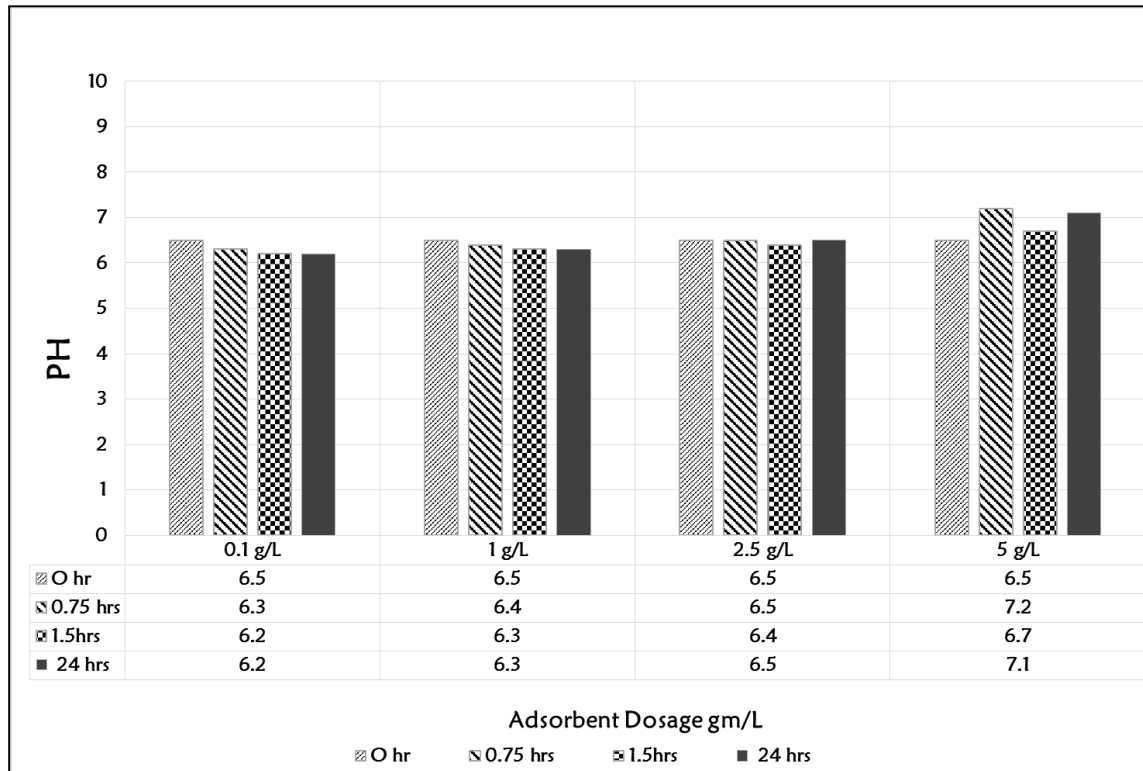**Figure 3-8   Observation of pH Changes with Time for FBWW after Addition of Fe₃O₄ Dosage vs. Time**

MgO exhibited the largest change in pH with the time as shown in Figure 3-9. After adding higher dosage of adsorbents to 2.5g/L and 5 g/L, pH increases after time at 1.5hrs and 24 hrs. It is apparent that longer test times (>1.5 hrs) are causing higher concentrations of MgO to dissolve in the FBWW.
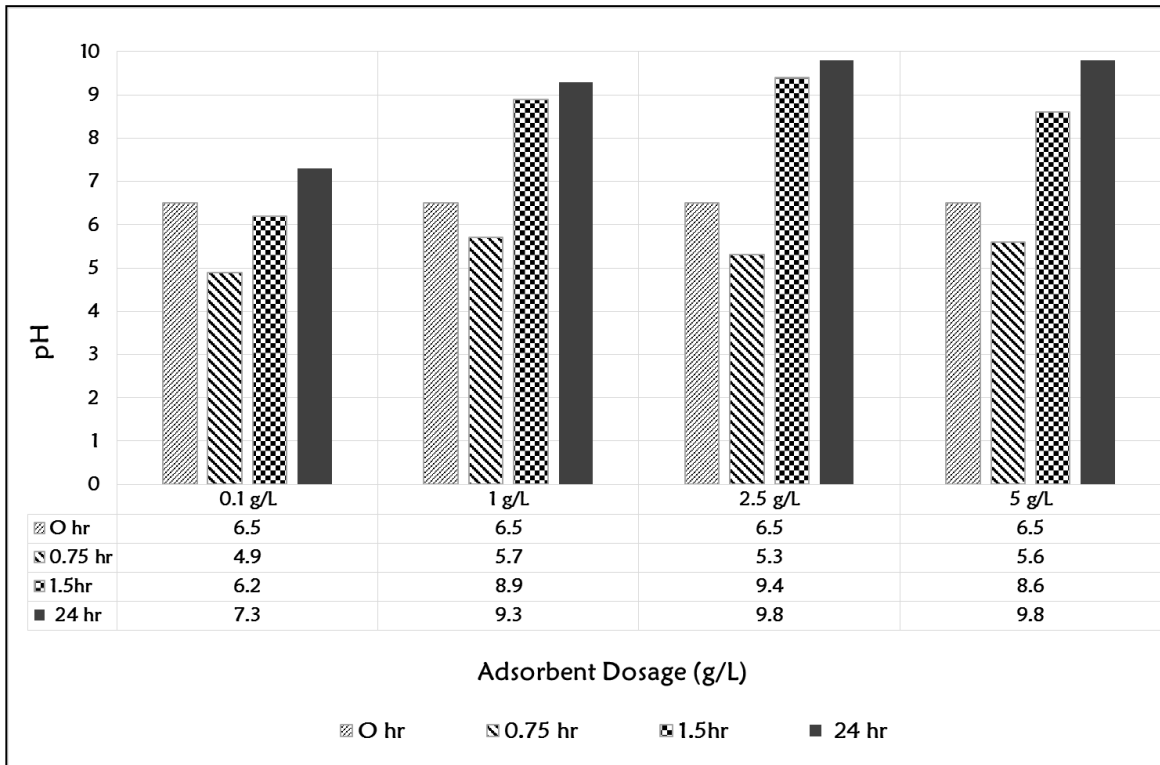
	0.1 g/L	1 g/L	2.5 g/L	5 g/L
⊞ O hr	6.5	6.5	6.5	6.5
⊠ 0.75 hr	4.9	5.7	5.3	5.6
⊞ 1.5hr	6.2	8.9	9.4	8.6
■ 24 hr	7.3	9.3	9.8	9.8

Adsorbent Dosage (g/L)

⊞ O hr   ⊠ 0.75 hr   ⊞ 1.5hr   ■ 24 hr

Figure 3-9   Observation of pH after Addition of MgO Dosage vs. Time

The objective of the above study was to observe the effect of time on pH with various adsorbents which ultimately allowed an assessment on the testing time. From the observation of pH study, it is clear that MgO is causing a large pH change at 24 hours. From the observations of the above graphs, it is found that adding higher dosage of the adsorbent greatly impact to change in pH from 1.5 hours to 24 hours; a slight change for CaO, not much change for Fe_3O_4 and a large change for MgO at higher concentrations. A testing time was chosen to be 1.5 hours as it is a reasonable testing and likely reflective of a practical contact time for field treatment.

Chapter 4 Results and Discussion

This chapter provides the results to the testing described earlier and provides some discussion of these results in the context of the objectives of the thesis. As previously described, the efficacy of the adsorbents utilized for the removal of Al from FBWW and the performance of GT500 Engineered geotextiles were investigated.

4.1 Aluminium Removal from FBWW Via Adsorbents Without pH Adjustment and Polymer Addition: Phase 1

As discussed in Chapter 3, the first phase of the research involved jar testing with the FBWW and different concentrations of adsorbents (CaO, Fe_3O_4, and MgO) and letting the pH stabilize to its equilibrium pH in the 1.5 hours of the test. The total aluminium concentrations were recorded before and after the addition of the adsorbents. As shown in Figure 4-1, the highest levels of total Al removal were achieved using the 5 g/L dosage of adsorbents, with the best removal rates at this dosage level being achieved with CaO and MgO. These results are recorded in Table 4-1and summarized graphically in Figure 4-1.

Table 4-1   FBWW Water Treatment Using Without pH Adjustment and No Polymer

Adsorbent Dosage (g/L)	Adsorbent	Measured pH (After 1.5 hrs)	FBWW Al Conc. (Before) (µg/L)	FBWW Al Conc. (After) (µg/L)	% Removal of Al
0.1		9.0	3104	2229	28%
1.0		11.3	3104	2145	31%
2.5	CaO	12.2	3104	2242	28%
5.0		12.7	3104	688	78%
0.1		9.1	3104	1654	47%
1.0		10.3	3104	940	70%
2.5	MgO	10.4	3104	383	88%
5.0		10.4	3104	142	95%
0.1		6.2	3104	2306	26%
1.0		6.3	3104	2697	13%
2.5	Fe_3O_4	6.4	3104	2825	9%
5.0		6.7	3104	1301	58%

Using MgO adsorbent dosage, relative to each other, provided the best removal of Al with the 0.1g/L dosage removing 47% Al, 1 g/L removing 70%, 2.5 g/L removing 88% and 5g/L removing 95%, as shown in Figure 4-1. After 1.5 hours with the treatment of adsorbent dosage, pH was increased from 9.1 to 10.4. The results reveal that maximum Al removal was obtained at the highest dosage of MgO adsorbent at 5 g/L. As it is obvious from the Figure 4-1 that there is no impact of pH on MgO dosage as no change in pH is observed due to higher dosage. So higher removal of Al might be because of the reason of higher dosage of MgO adsorbent causes sweep flocculation and adsorption mechanism to absorb particles and accelerate the attraction of floc formation.
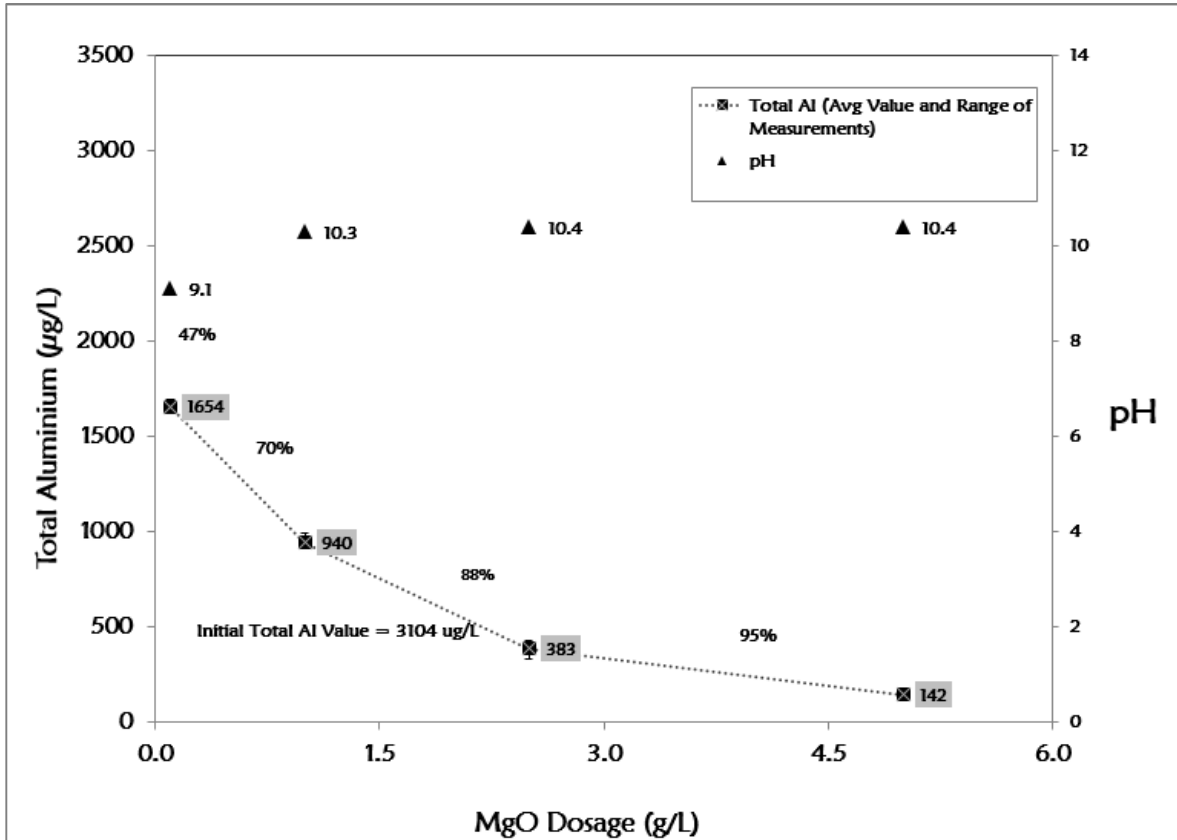
Figure 4-1   Total Al of Influent Water after Treating with MgO Adsorbent Without pH Adjustment and No Polymer Addition Condition

CaO provided the next best removal rates illustrated in Figure 4-2. The removal of Al as follows: at 0.1g/L dosage 28% removal, at 1 g/L 31% removal, at 2.5 g/L 28% removal and at 5g/L 78% removal as shown in Figure 4-2. After 1.5 hours with the treatment of adsorbent dosage, the pH increase ranged from 9.0 to 12.7. Similarly, higher Al removal results were found as MgO adsorbent dosage and the results reveal that maximum Al removal was attained at higher pH and at a higher dosage of CaO (i.e 5 g/L).
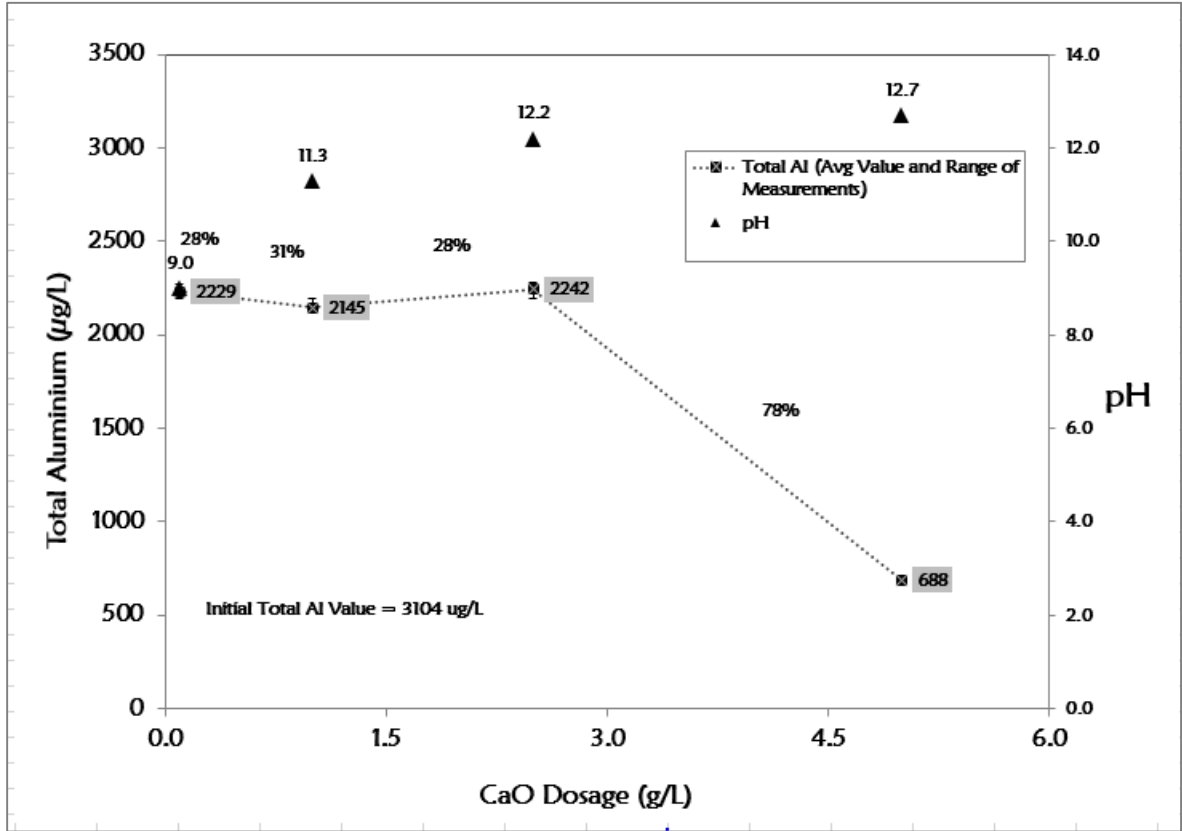
Figure 4-2   Total Al of Influent Water after Treating with CaO Adsorbent Without pH Adjustment and No Polymer Addition Condition

Compared to MgO and CaO, lower Al removal rates were found for Fe_3O_4 adsorbent as shown in Figure 4-3. In case of Fe_3O_4, the 5 g/L dosage provided the maximum Al removal of 58%. Whereas, the lower dosage could remove Al at 26% for 0.1 g/L dosage, 13% for 1 g/L dosage and 9% for 2.5 g/L dosage. pH remained constant throughout the treatment process even with increased dosage of the adsorbents around 6.2 to 6.7.
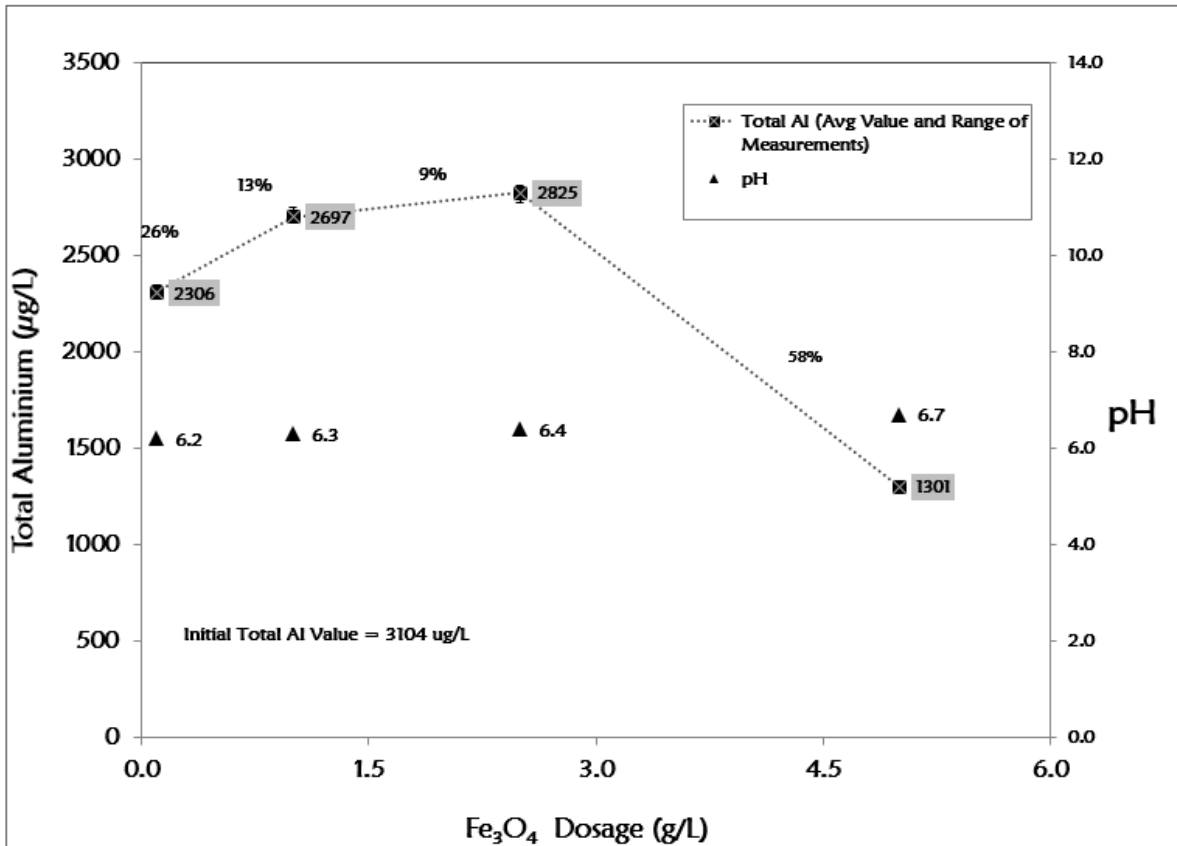
Figure 4-3   Total Al of Influent Water after Treating with Fe₃O₄ Adsorbent Without pH Adjustment and No Polymer Addition Condition

4.2 FBWW Treatment Via Adsorbents With pH Adjustment and 1 mg/L Polymer Addition: Phase 1

As discussed in Chapter 3, the second stage of phase 1 of the research involved jar testing with the FBWW and different concentrations of adsorbents (CaO, Fe₃O₄, MgO and a 50/50 mix of CaO and Fe₃O₄). In these tests, 1 mg/L of polymer was added and the initial pH adjusted to 6.5, letting it stabilize to its equilibrium pH during the 1.5-hour duration of the test. These tests only sampled the supernatant and hence water quality results shown in

subsequent sections do not reflect the solid portion of the FBWW removed from this treatment.

4.2.1 Measurement of the Amount of Total Al Concentration in FBWW after Treatment with Adsorbents, pH Adjustment and 1 mg/L Polymer Addition

The total aluminium concentrations were measured and recorded after 1.5 hours of pH adjustment and addition of the adsorbent and polymer. The results are illustrated in Table 4-2. The highest levels of total Al removal were achieved using the 5 g/L dosage of adsorbents as shown in Figure 4-4, Figure 4-5, Figure 4-6 and Figure 4-7, with the best Al removal rates at this dosage level being achieved with a 50/50 mix of CaO and Fe_3O_4 adsorbent in a combination. The results were revealed as found in Table 4-2.

Table 4-2   **Al Removal from FBWW via Adsorbents with pH Adjustment and 1 mg/L Polymer Addition**

Adsorbent Dosage (g/L)	Adsorbent	Measured pH (After 1.5 hrs)	FBWW Al Conc. (Before) ($\mu g/L$)	FBWW Al Conc. (After) ($\mu g/L$)	% Removal of Al
0.1		6.5	2250	1400	38%
1.0		7.5	2250	900	60%
2.5	**CaO**	7.5	2250	520	77%
5.0		6.9	2250	70	97%
0.1		8.7	2250	1630	28%
1.0		8.9	2250	940	58%
2.5	**MgO**	9.4	2250	670	70%
5.0		8.6	2250	50	98%
0.1		6.2	2250	630	72%

Adsorbent Dosage (g/L)	Adsorbent	Measured pH (After 1.5 hrs)	FBWW Al Conc. (Before) (µg/L)	FBWW Al Conc. (After) (µg/L)	% Removal of Al
1.0		6.3	2250	570	75%
2.5	Fe_3O_4	6.4	2250	380	83%
5.0		6.7	2250	240	89%
1.0		10.5	2250	151	93%
2.5	CaO	11.2	2250	102	95%
5.0	and Fe_3O_4	11.3	2250	61	97%

The results showed that using Magnesia (MgO) adsorbent, with a lower dosage of 0.1 gm/L was able to remove 28%, 1 g/L removed 58%, 2.5 g/L removed 70% and higher dosage of 5 g/L was able to remove aluminium to 98%. The pH changed from 6.2 to 9.4 as shown in Figure 4-4. Compared to without pH adjustment, these results summarized that higher dosage of MgO with increased pH at 8.6 were producing more Al flocs of Al $(OH)_3$(s) as precipitates due to adsorption. Thereby, higher dosage increased more Al removal using various adsorbents.
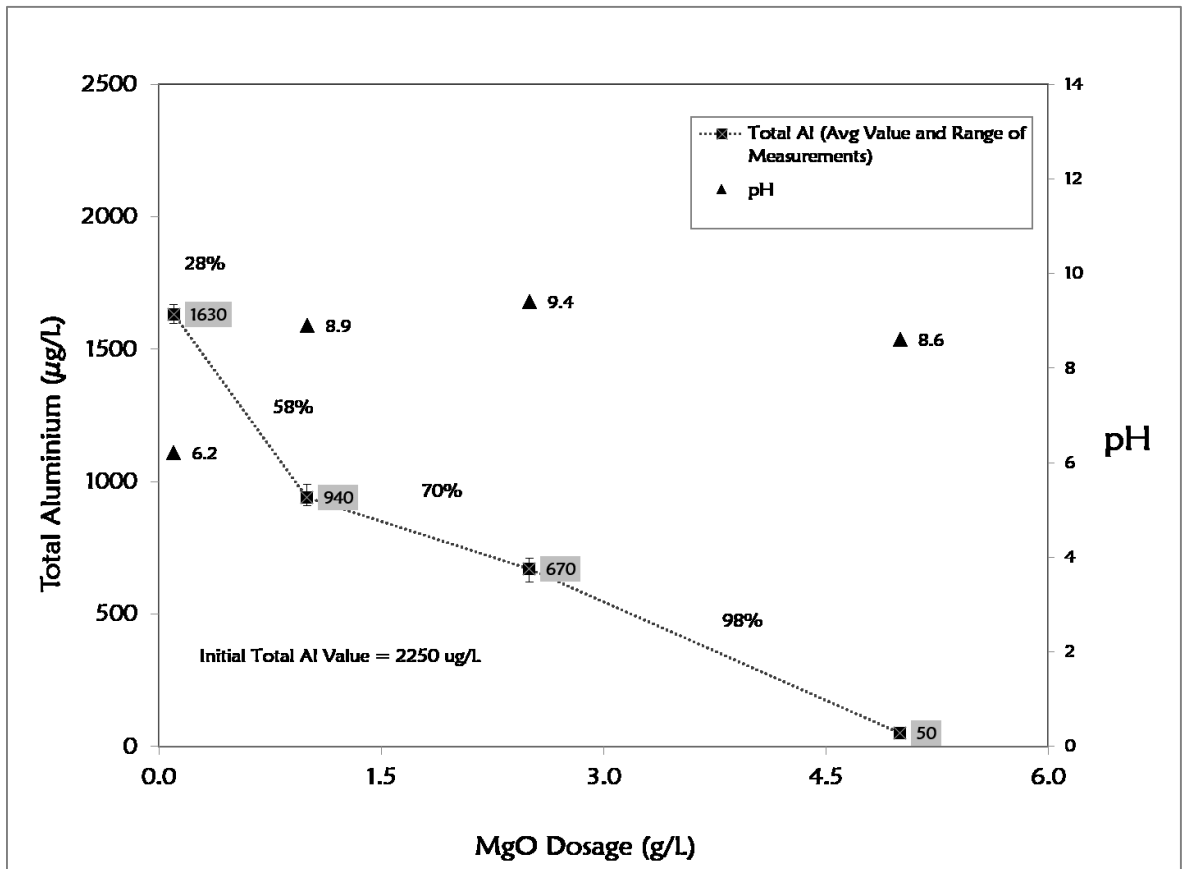
Figure 4-4 Total Aluminium Conc. Vs Different Dosage of MgO Adsorbent (1 mg/L Polymer & pH Adjust)

In the case of calcium oxide, removal was achieved at 38%, 60%, 77% and 97% respectively when using 0.1 g/L, 1g/L, 2.5 g/L and 5 g/L of the adsorbent as shown in Figure 4-5 which was more compared to the without PH adjustment results. As with the results found from CaO, it was obvious that higher dosage of adsorbent was contributing to the higher removal of aluminium at adjusted pH conditions. This might be due to the higher dosage of the adsorbents were taking part into more adsorption processes in the solution while acting with the adsorbents.
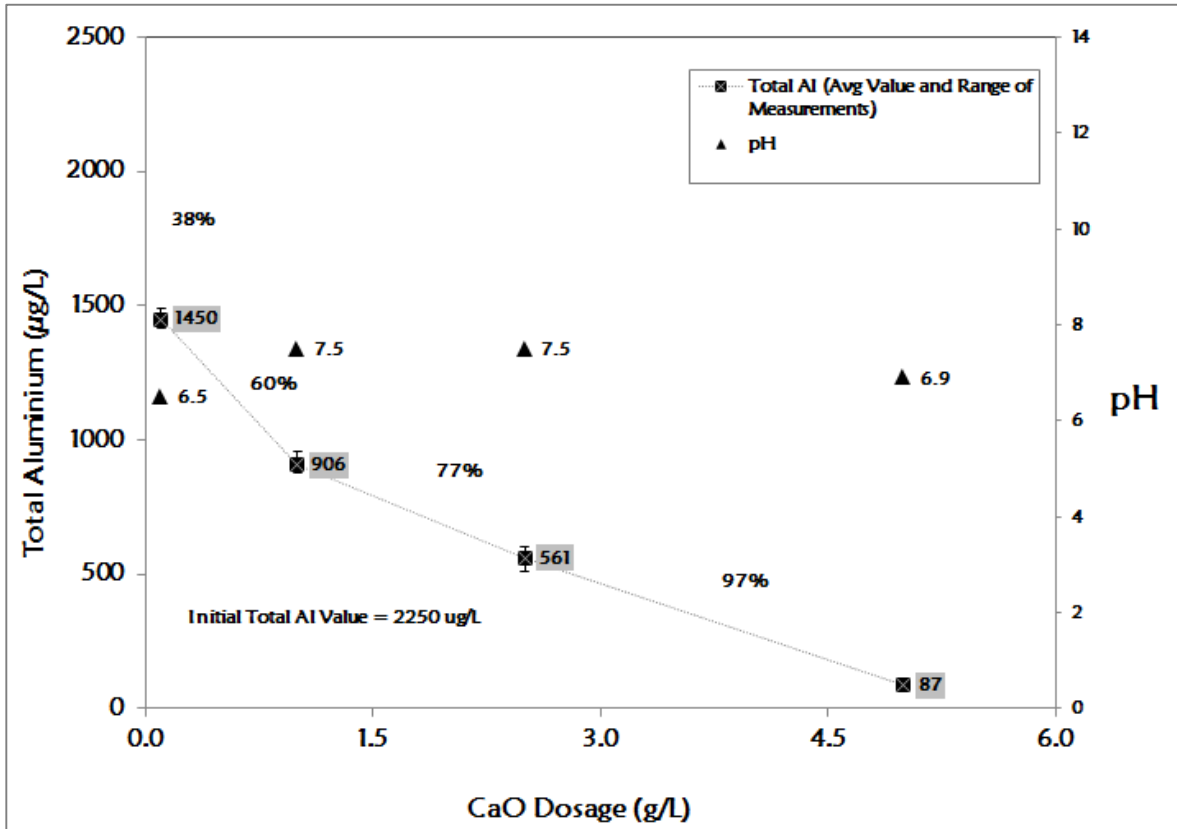
Figure 4-5   Total Aluminium Conc. Vs Different Dosage of CaO Adsorbent (1 mg/L Polymer & pH Adjust)

When using Fe_3O_4 adsorbents compared to without pH adjustment condition, more removal efficiency was achieved increasing from lower to higher dosage of adsorbents. At 72%, 75%, 83% and 89% of total Al removal were achieved for the dosage of the adsorbents using 0.1g/L, 1g/L, 2.5 g/L and 5 g/L respectively as shown in Figure 4-6. It is also apparent that the pH was remained constant with each increasing amount of adsorbent dosage. This time Al removal was more achieved using pH adjustment condition compared to the without pH adjustment.
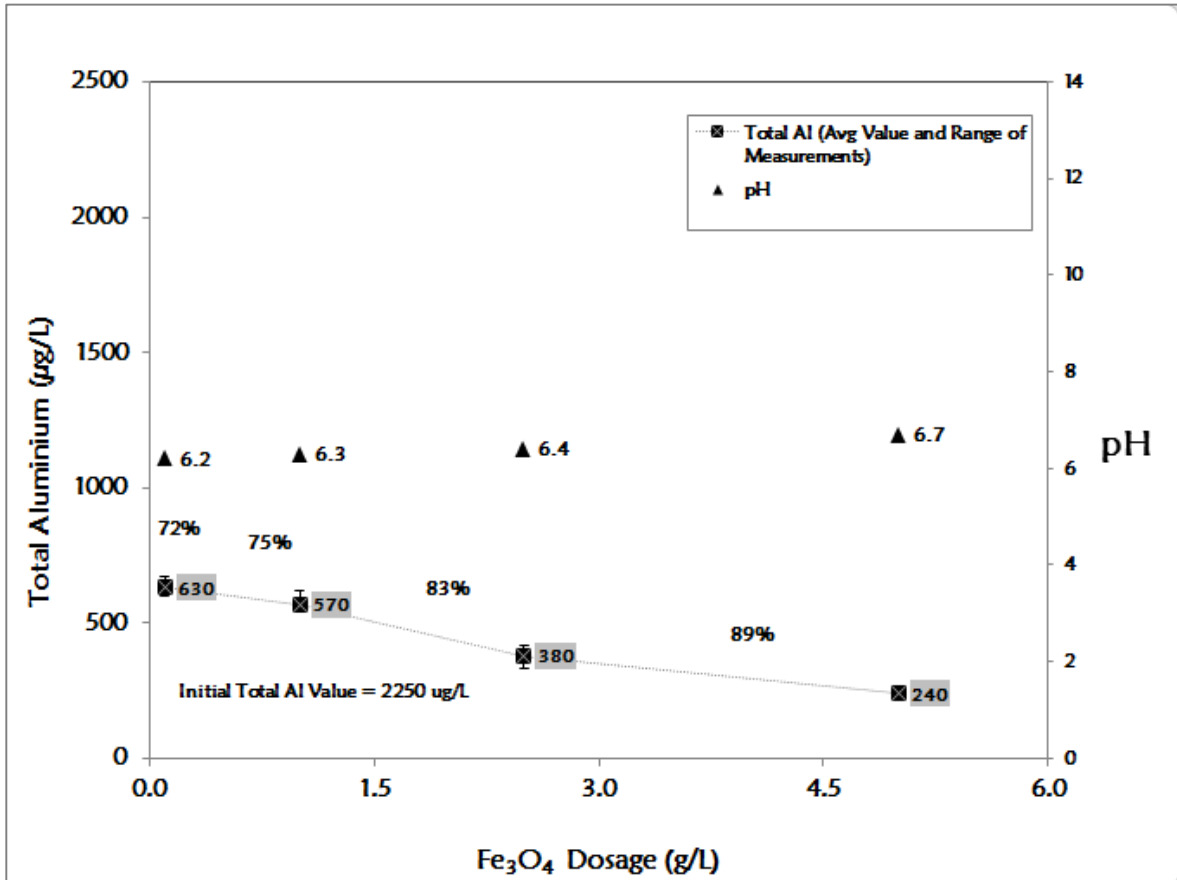
Figure 4-6   Total Aluminium Conc. Vs Different Dosage of Fe₃O₄ Adsorbent (1 mg/L Polymer & pH Adjust)

In addition, a trial combination of two metal oxides (CaO & Fe₃O₄) adsorbents was considered to mix with the FBWW with the polymer dosage to see the synergetic effects of the adsorbents. The result found that using lower dosage of adsorbents, 93% removal was achieved using lower at 1g/L adsorbent dosage. With an increased higher dosage of adsorbents, around 95% to 97% removal efficiency was attained using 2.5g/L and 5 g/L respectively as more adsorption took place in the mixture of the final solution and better removal was attained as shown in Figure 4-7 below.
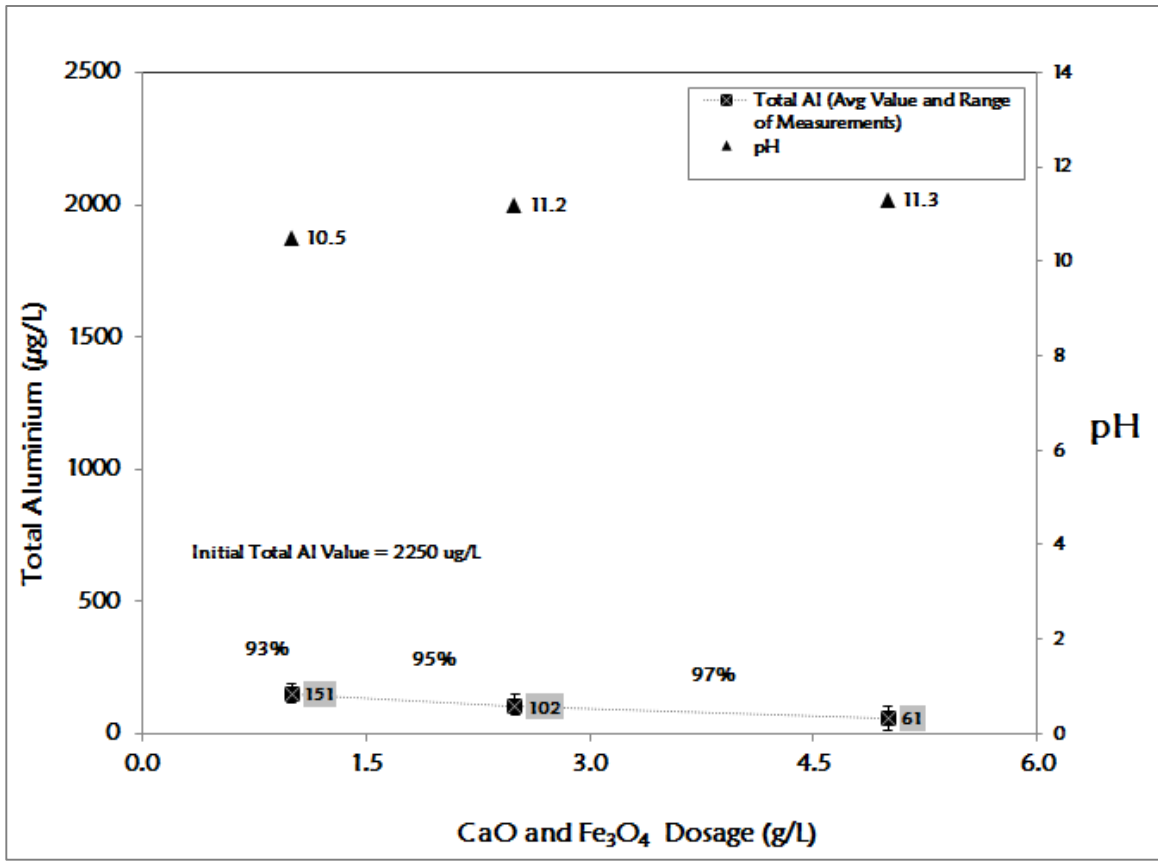
Figure 4-7   Total Aluminium Conc. Vs 50/50 Mix of CaO & Fe₃O₄ Adsorbent Dosage (1 mg/L Polymer & Adjusted pH)

4.2.2 Measurement of the Amount of Dissolved Al in FBWW after Treatment with Adsorbents, pH Adjustment and 1 mg/L Polymer Addition

Testing for dissolved Al was performed to establish the nature of Aluminium (dissolved versus particulate) from the treatments. The results revealed that as Iron oxide adsorbents from increased in dosage from (0.1g/L) to (5g/L), dissolved Al increased sequentially after adding higher dosages. This might be the reason of the increased dosage of adsorbents also increase the pH of the solution that contributed to the Al to dissolve more in water. As

found from Figure 4-8, the value varies at 10μg/L, 10μg/L, 60μg/L and 115 μg/L using different adsorbent dosage for Fe_3O_4 adsorbent dosage from (0.1~5) g/L respectively.
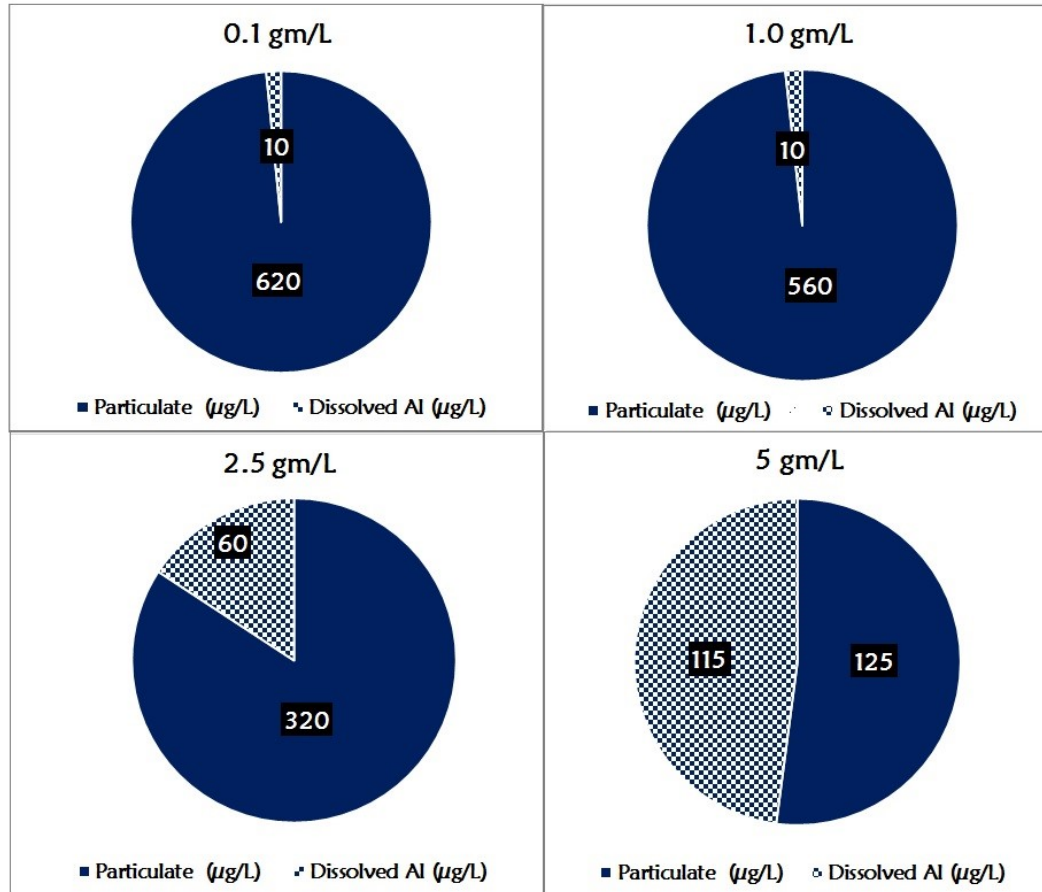

Figure 4-8   Particulate and Dissolved Al using Fe_3O_4

When using CaO samples, from lower dosage (0.1g/L) to higher dosage (5g/L), dissolved Al decreases sequentially after adding higher dosages. As found from Figure 4-9, the value varies from 300 μg/L, 200 μg/L, 80 μg/L and 50 μg/L using different adsorbent dosage as 0.1 g/L, 1 g/L, 2.5 g/L and 5 g/L respectively. It is obvious from the Figure 4-9 that CaO adsorbent at higher dosage is helping to remove dissolved Al conc. as it increases pH in the solution to form precipitates.
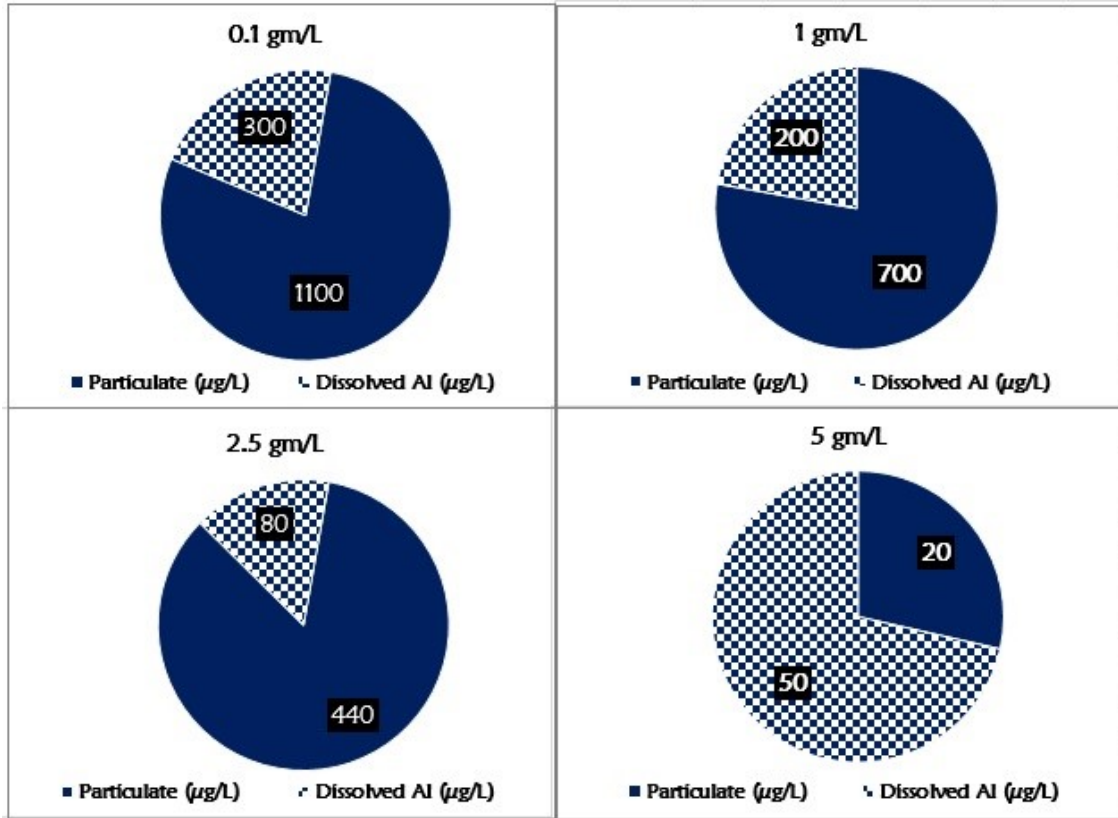
Figure 4-9   Particulate and Dissolved Al using CaO

Similarly, as CaO adsorbent, using MgO samples, from lower dosage (0.1g/L) to higher dosage (5g/L), dissolved Al decreases sequentially after adding higher dosages. As found from Figure 4-10, the value varied from 80 µg/L, 110 µg/L, 300 µg/L and 30 µg/L using different adsorbent dosages of 0.1 g/L, 1 g/L, 2.5 g/L and 5 g/L respectively. Higher dosage of MgO adsorbent (5 g/L) is removing more dissolved Al from the solution after treatment.
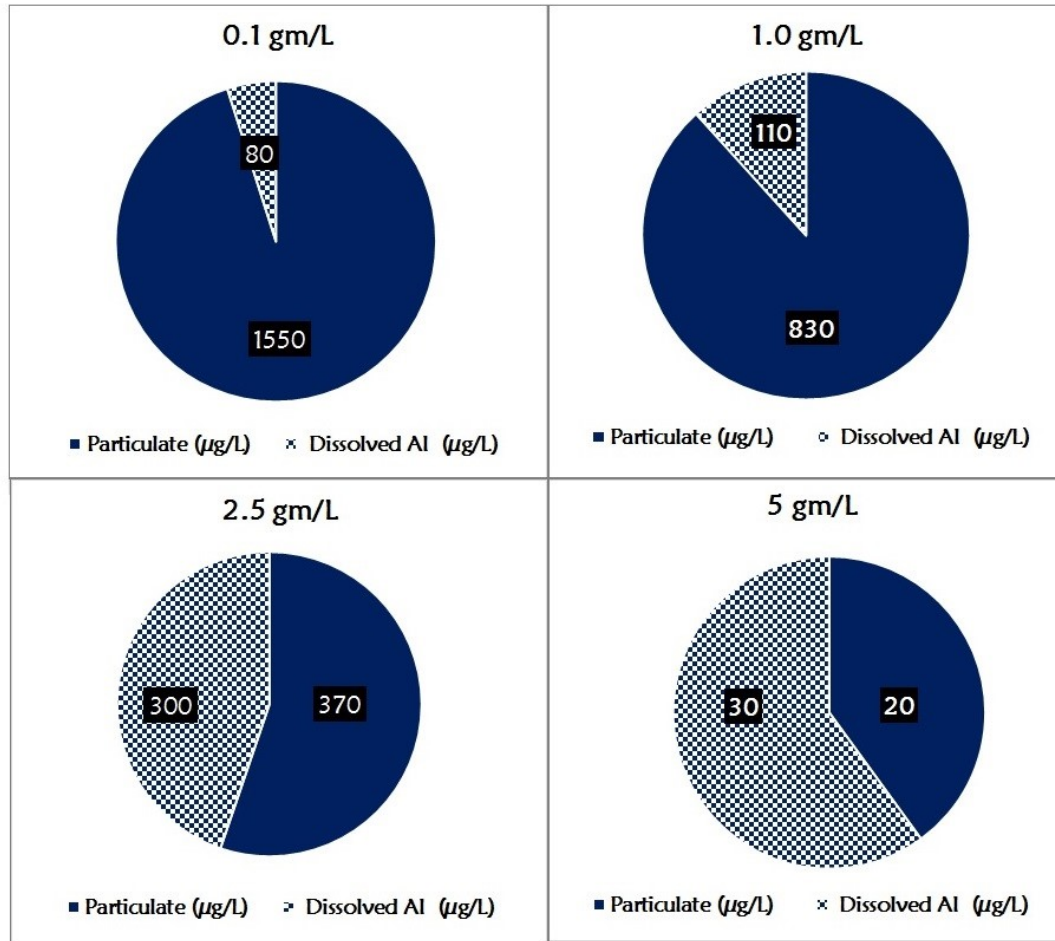
Figure 4-10   Particulate and Dissolved Al using MgO

Using 50/50 mix of CaO & Fe_3O_4 samples, three adsorbent dosages (1 g/L, 2.5 g/L and 5.0 g/L) were selected to observe the results due to 0.1 g/L dosage of adsorbent shows negligible impact on dissolved Al conc. From lower dosage (1g/L) to higher dosage (5g/L), dissolved Al decreases sequentially due to addition of higher dosages of the adsorbents. As found from Figure 4-11, the value varies from 102μg/L, 38.5 μg/L, and 37 μg/L increasing at different adsorbent dosage as 1 g/L, 2.5 g/L and 5 g/L respectively.
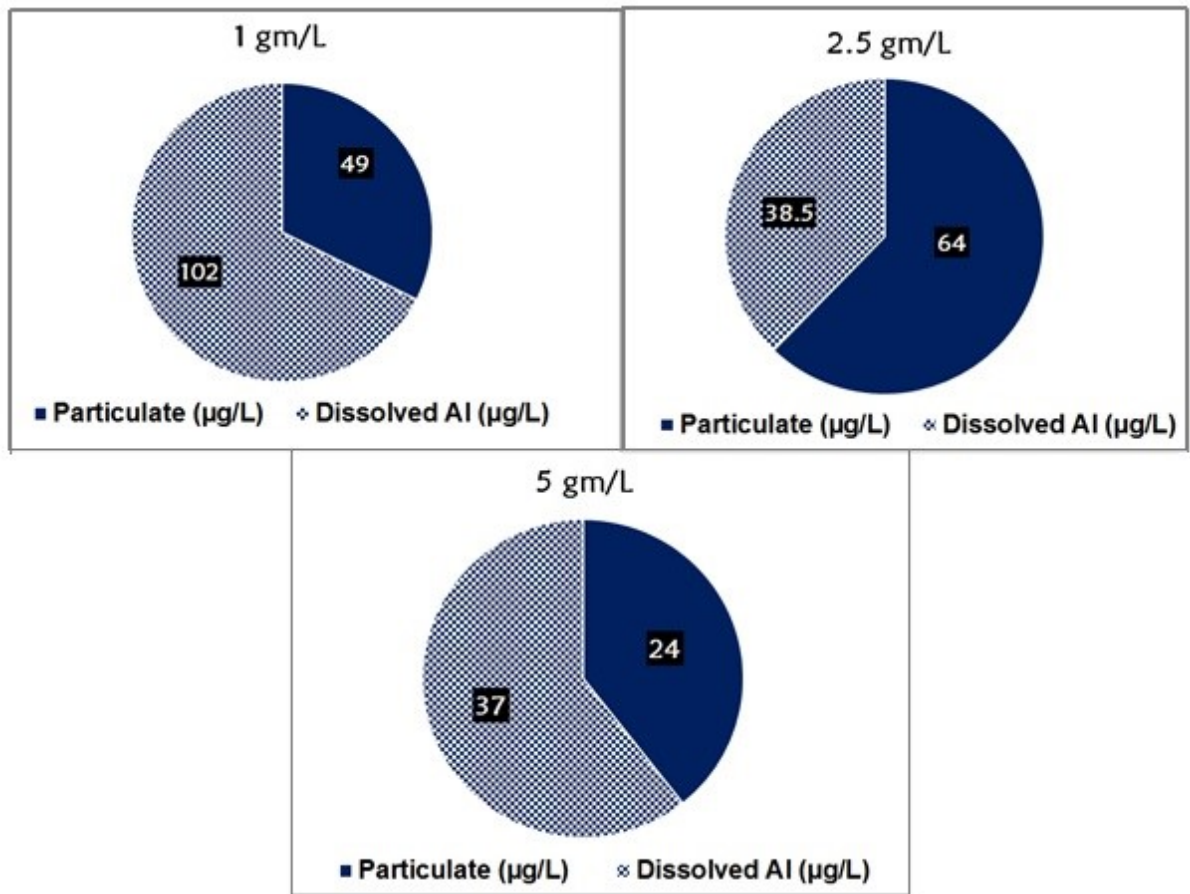
Figure 4-11   Particulate and Dissolved Al using CaO & Fe$_3$O$_4$

4.2.3 TSS

TSS testing was conducted in three phases using FBWW, influent water and effluent water. The test results were found consistent in each trial of the different adsorbent dosage. The results obtained from the TSS test reflect that the TSS concentration in FBWW was as low as 1 mg/L. When CaO adsorbent was mixed in association with an optimum lower dosage of 1 mg/L of polymer, TSS found from the influent water was increased from 1 mg/L to 50 mg/L due to 0.1 g/L addition of adsorbent. Further addition of higher dosage of the adsorbents up to 5 g/L, TSS conc. also increased to 144 mg/L as shown in Figure 4-12.

The reason behind that the polymer dosage was constant for all of the treatment while increasing additional adsorbent dosage, noticeable amount of TSS concentration was formed due to the higher dosage of adsorbents. Particularly, at higher dosage of adsorbent, they reacted with the polymer and then pass through the mechanism of coagulation and flocculation finally particles settle at the bottom due to the gravitational force. This occurrence suggested that more flocs were formed due to the addition of higher adsorbent dosage, thus creating more TSS concentration. This trend was also found similar using with the other adsorbent dosage e.g. Fe_3O_4, MgO and combination of CaO and Fe_3O_4 adsorbent dosage as shown in Figure 4-13, Figure 4-14 and Figure 4-15 respectively.
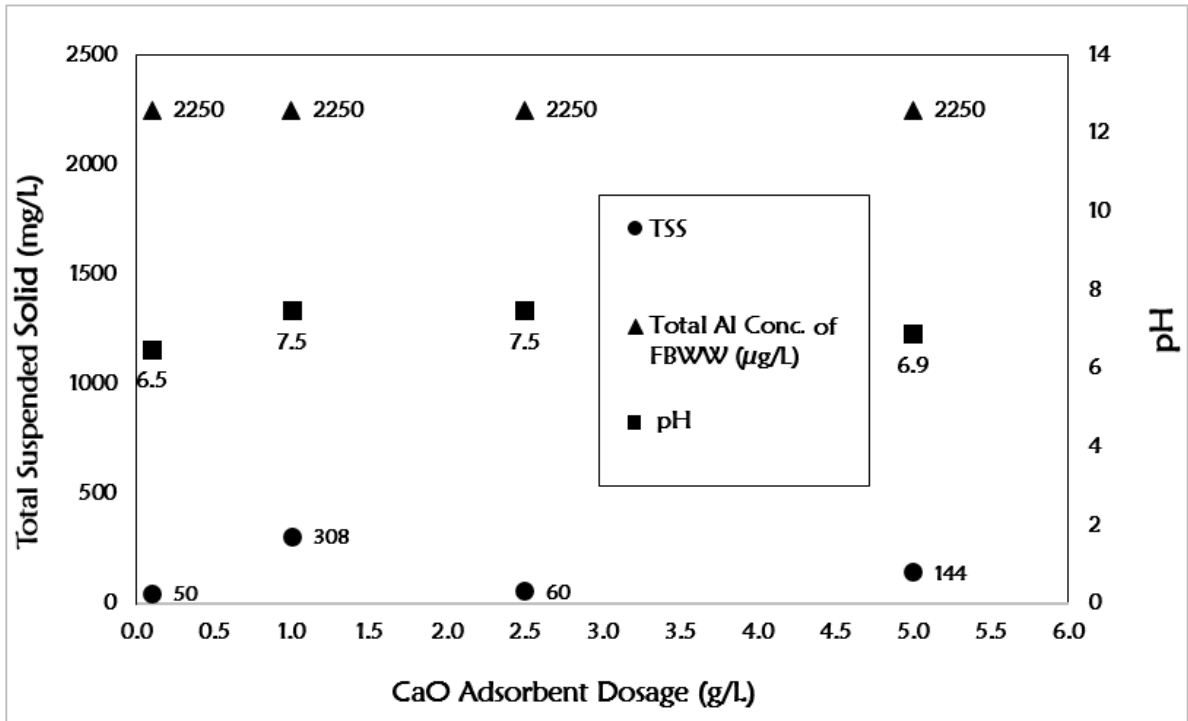
Figure 4-12   Total Suspended Solid (TSS) Using CaO Adsorbent
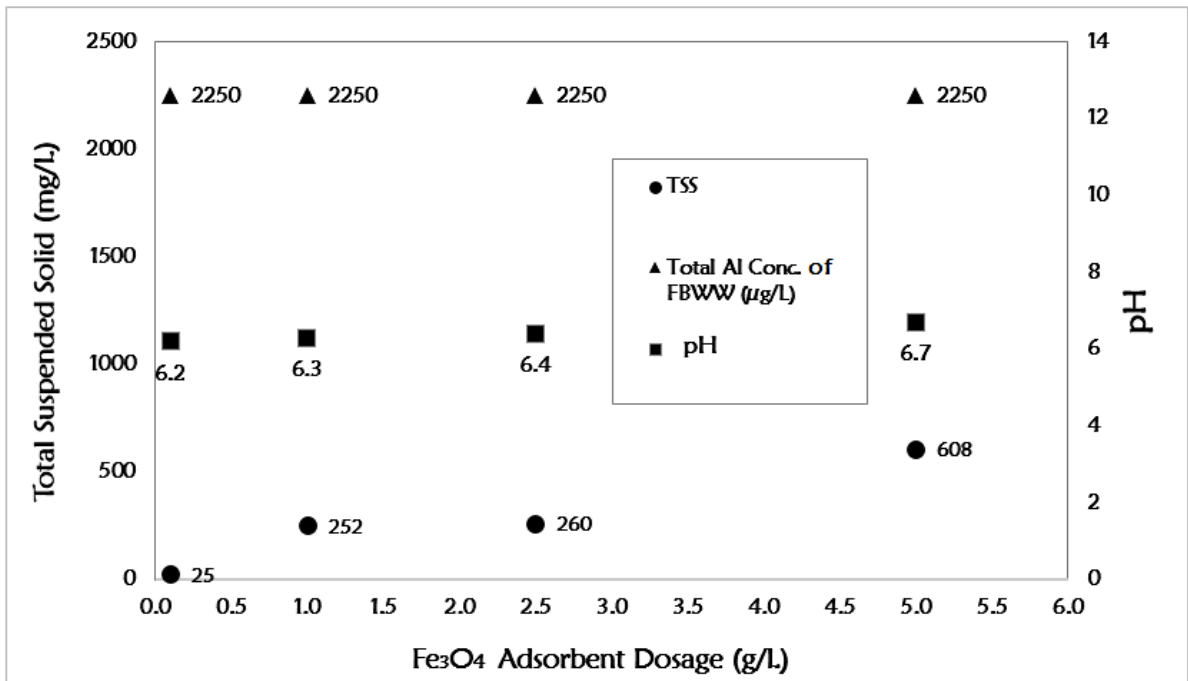

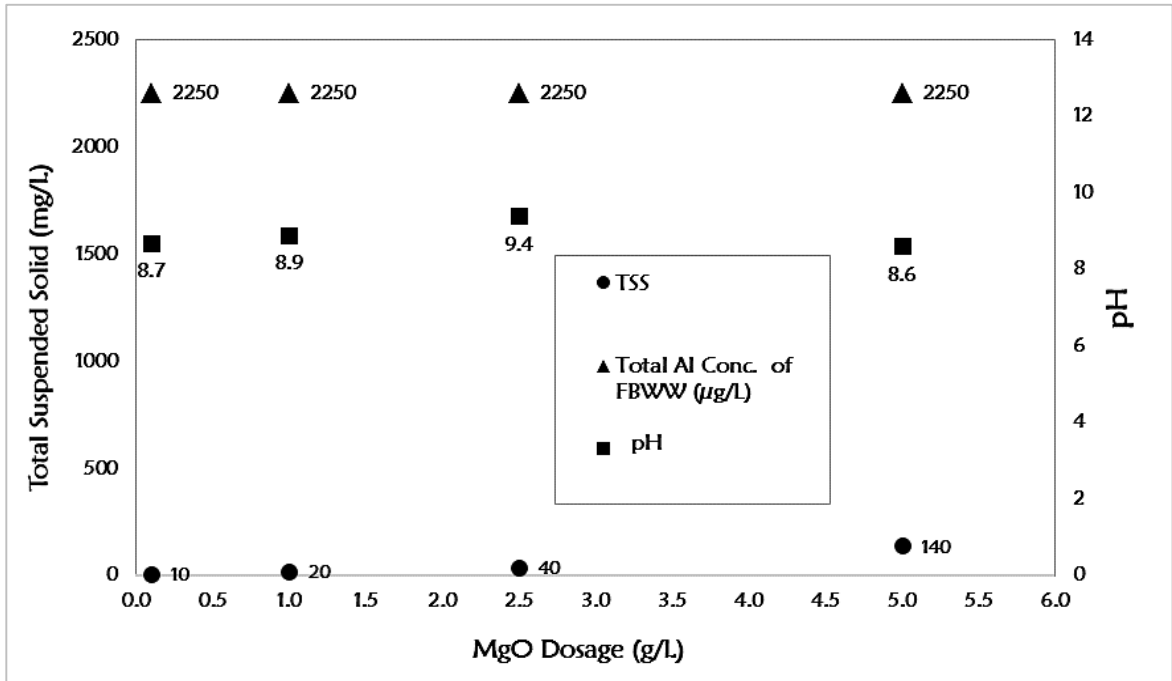**Figure 4-13   Total Suspended Solid (TSS) Using Fe₃O₄ Adsorbent**

Figure 4-14   Total Suspended Solid (TSS) Using MgO Adsorbent
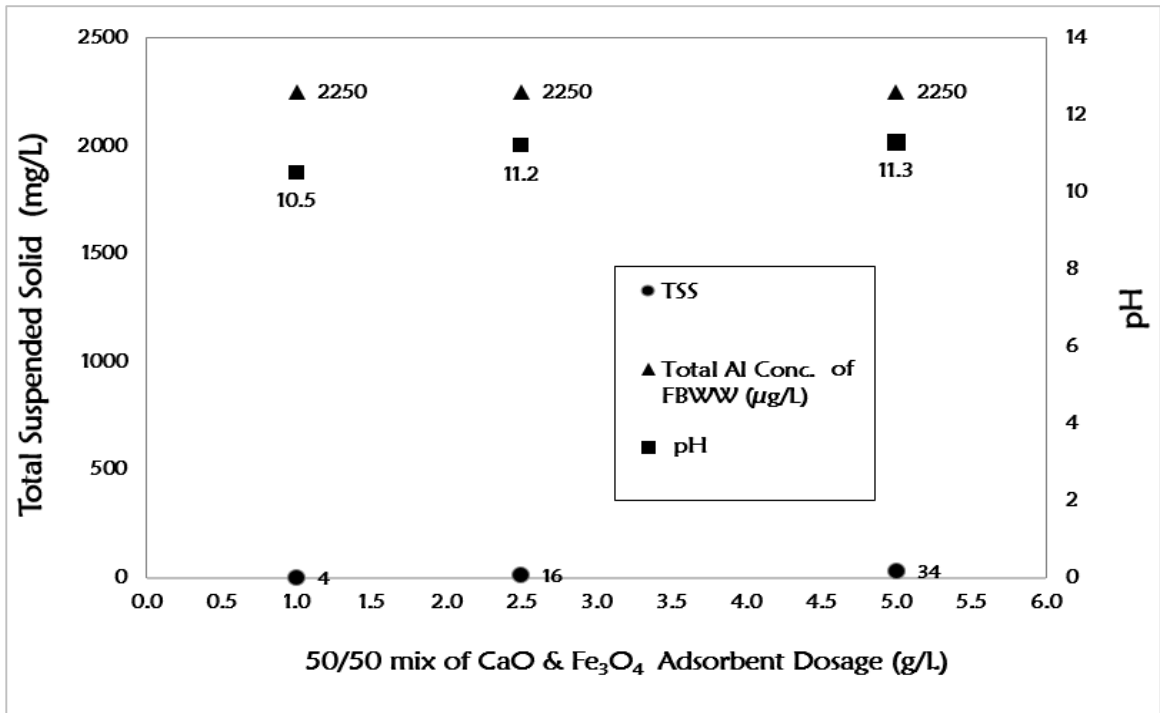

Figure 4-15   Total Suspended Solid (TSS) Using CaO & Fe₃O₄ Adsorbent

4.2.4 Size Analysis

The particle size distribution is illustrated in Figure 4-16 representing different dosage of adsorbent in x direction vs. particle size range (μm) in y direction for influent water found after treatment of FBWW taking 100 times dilution factor. The particle sizes were taken as the maximum values of three individual trials. The Figure 4-16 displayed that particle size increases due to the higher dosage of the adsorbents at 5 g/L. The primary particle size of the FBWW was measured 51 μm using 100 times dilution. All other experiments were similarly accomplished using the same dilution factor.

The Figure 4-16 reflects using CaO adsorbent, as easily seen for the influent water, particle size was lower initially which progressed later due to the gradual movement of the particle size to a larger size; that was observed at higher adsorbent dosage is 231 μm at 5 g/L. At higher dosage, small particles seemed to be trapped inside the gel like flocs of Al hydroxides as it grows larger in size dragging out most of the colloids and settle out due to gravitational force, leading to sweep floc mechanism (John et al. 2005).
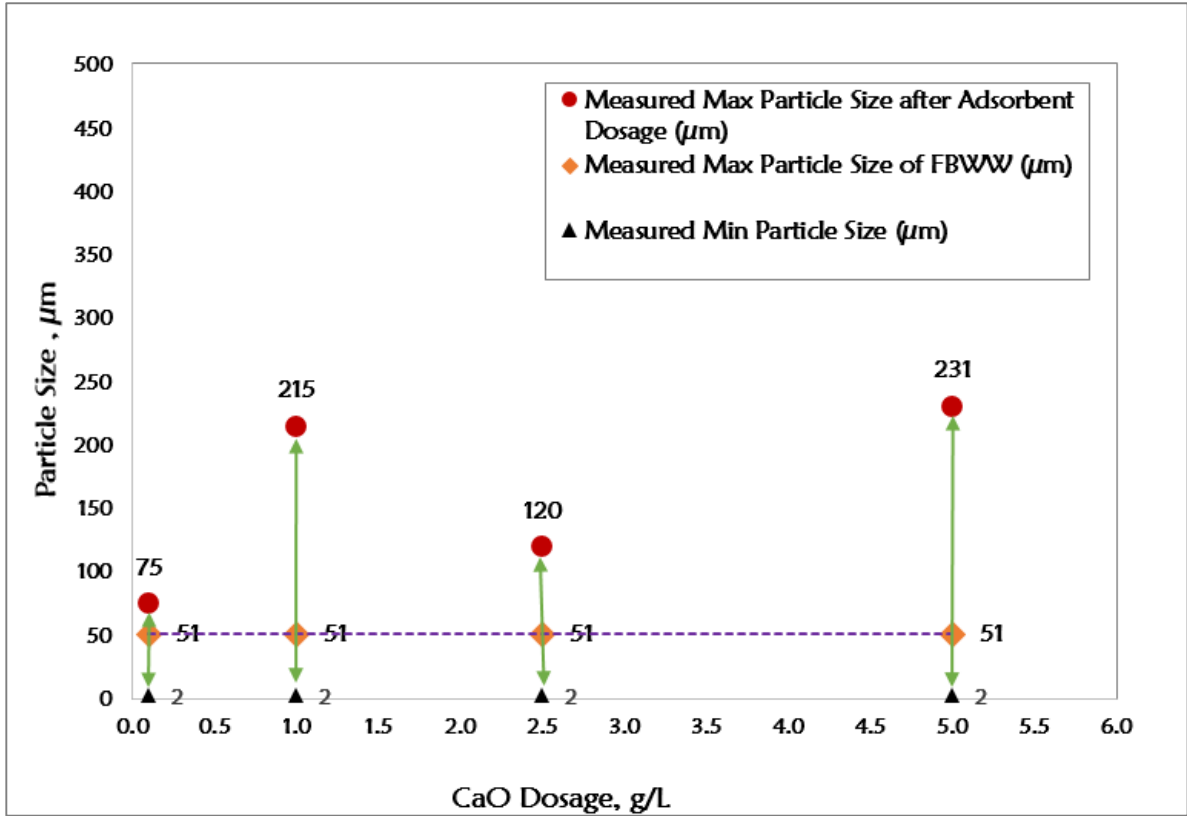
Figure 4-16   Particle Size of CaO Dosage (1 mg/L Polymer & Adjusted PH)

Again using MgO adsorbent, the particle size was found 215 μm using 1 gm/L adsorbent. But further addition of adsorbent dosage, the particle size increases to 282 μm as shown in Figure 4-17. This similar progression was also observed with other adsorbent dosage using Fe_3O_4 and combination of (CaO and Fe_3O_4) as illustrated in Figure 4-18 and Figure 4-19 respectively. The maximum particle size was found using the combination of two adsorbents as (CaO and Fe_3O_4). The maximum particle size was found 495 μm using 2.5 gm/L of this combination. Later, for using 5 gm/L adsorbent dosage, the particle size was not found appropriate as it was predicted to be much higher and could not be measured using Brightwell micro Flow Imaging (MFI) software as the detection limit was out of range > 400 μm.
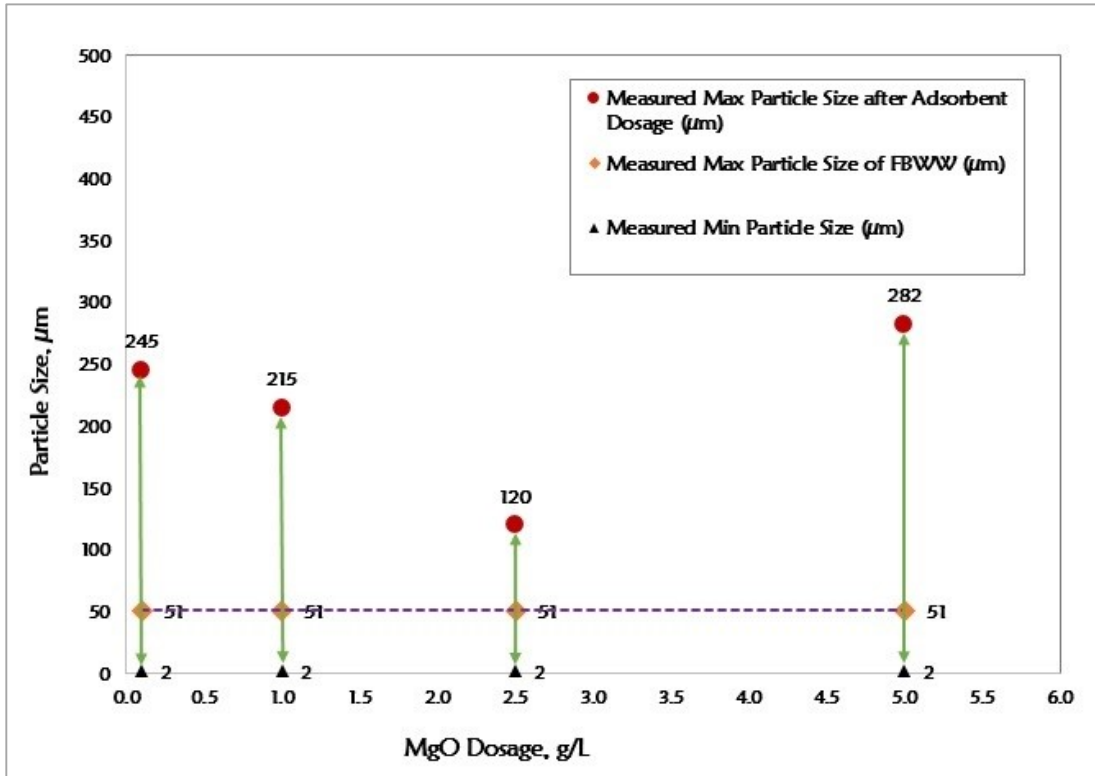
Figure 4-17   Particle Size of MgO Dosage (1 mg/L Polymer & Adjusted pH)
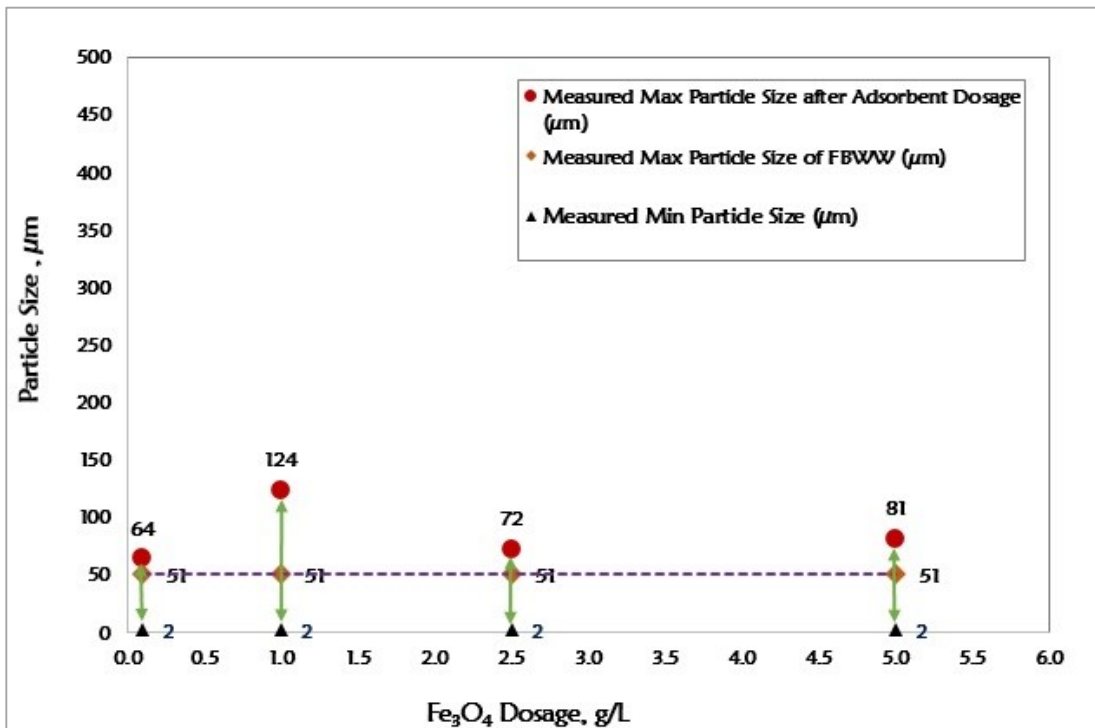
Figure 4-18   Particle Size of Fe₃O₄ Dosage (1 mg/L Polymer & Adjusted PH)
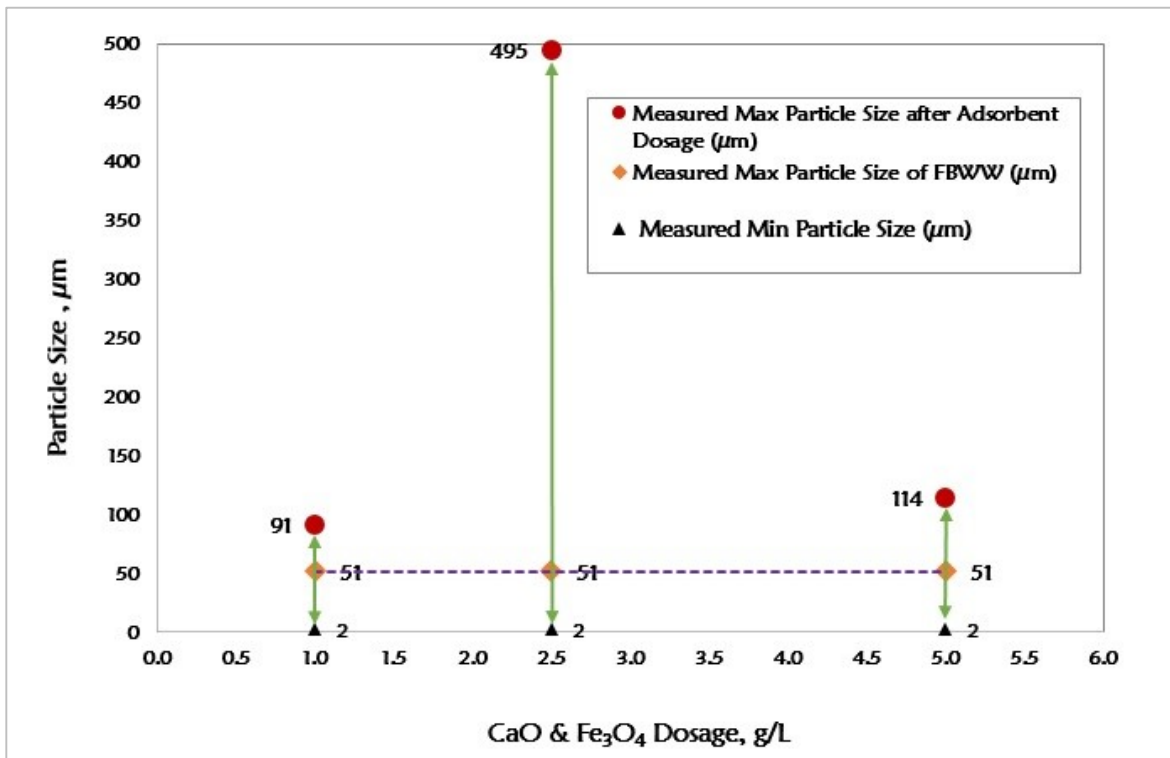
Figure 4-19   Particle Size of CaO and Fe$_3$O$_4$ Dosage (1 mg/L Polymer & Adjusted pH)

4.2.5 Zeta Potential Analysis

The magnitude of zeta potential of a particle in suspension indicates the degree of electrostatic repulsion of the charged particles in a dispersion media; which is a key indicator of the stability of the colloidal suspensions. The value of the zeta potential was characterized in the experiment using the influent water with a 10 times dilution factor. An image of the zeta potential distribution was created representing apparent zeta potential value against total counts of the particles in the solution. Each of the image was created calculating an average value among the four consecutive zeta potential values.

The zeta potential value of the influent water using MgO adsorbent was illustrated in the Figure 4-20 as (-2.18) at lower dosage of 0.1 gm/L. This value is near to the zero potential values or simply referred as isoelectric point. At this stage, the particle in suspension becomes more unstable as the attractive forces at this point may exceed the repulsion that results in breaking into particles to coagulate or flocculate in the dispersion media.

Later, further addition of MgO adsorbent in the solution, altered the dispersion media more (-) anionic. The Figure 4-20 shows that the negative zeta potential values are increasing at higher dosage of adsorbent from -2.18 to -20.9 from 0.1 gm/L to 5 gm/L adsorbent dosage. At the range in between $\pm$ (10 to 30) of the zeta potential value, the particles show incipient instability. As more anions were added in the solution, the pH was changed to increase from 6.2 to 8.6 and as a result of this; more aluminium removal was attained with increasing higher dosage as more adsorption process was expected to happen. In this unstable suspension, the particles may adhere to one another to make the aggregate grow in size which finally settles as precipitate due to the influence of gravity.
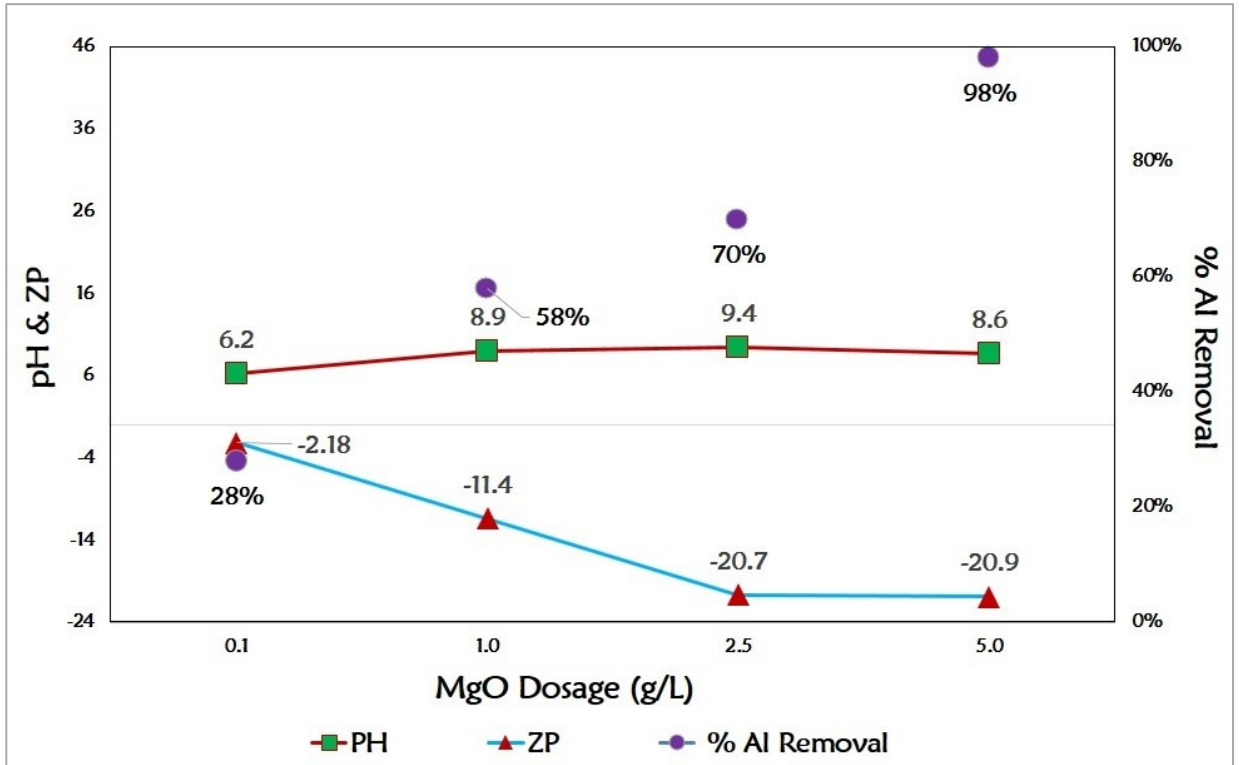
Figure 4-20   Zeta Potential of MgO Dosage

In case of CaO adsorbent and combination of (CaO and Fe_3O_4), the mechanism of Aluminium chemistry is pretty similar that is described earlier using MgO adsorbent. These mechanisms are illustrated in Figure 4-21and Figure 4-22 respectively.
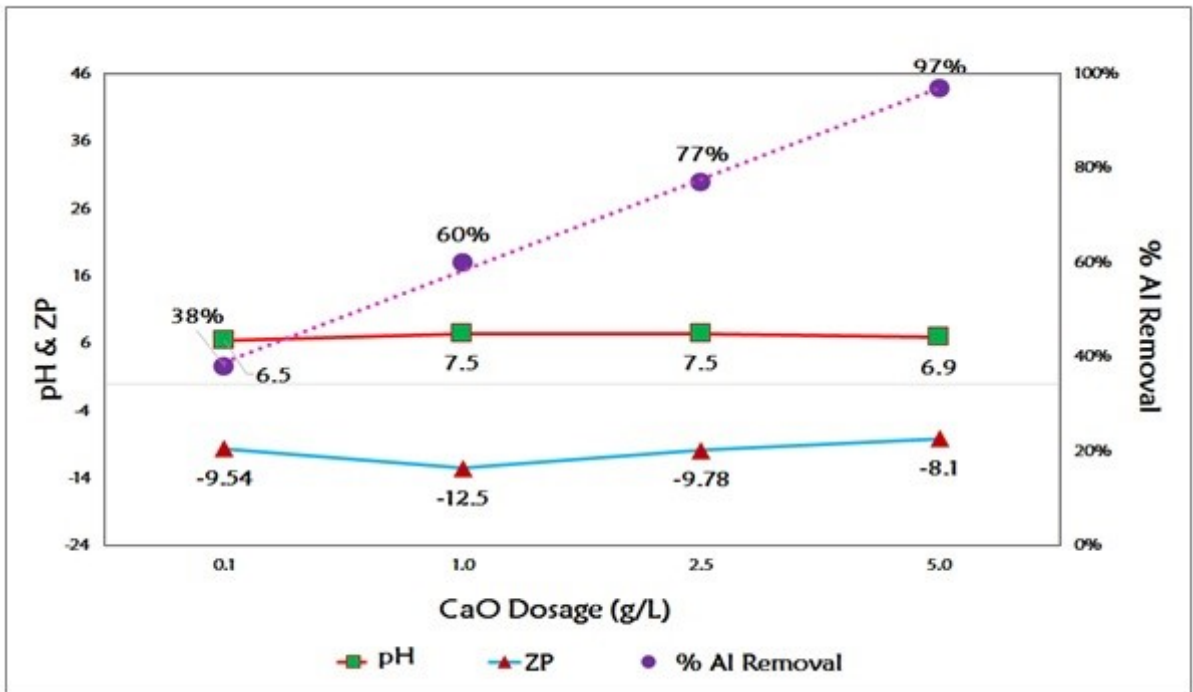
Figure 4-21   Zeta Potential of CaO Dosage
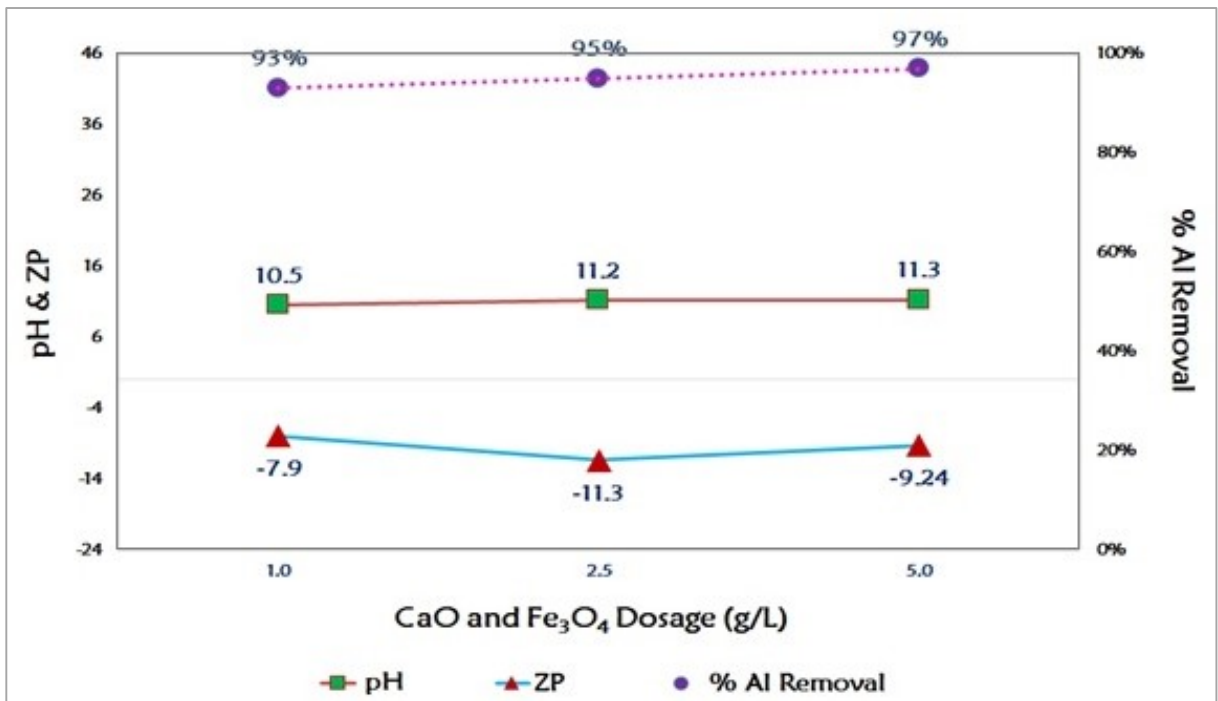
Figure 4-22   Zeta Potential of CaO and Fe₃O₄ Dosage

But in case of iron oxide adsorbent, the particles in suspension showed the maximum zeta potential value reached at 41.2. At this point, the particles reach at the stable condition as all the ZP values at different adsorbent dosage showed the range above 30 mV at constant pH. So when additional adsorbent was added in the solution, a slight variation of zeta potential value was noticed as well as no change of pH was observed. As previously noted, a small fraction of aluminium removal was attained using higher dosage of the adsorbent dosage as shown in Figure 4-23.
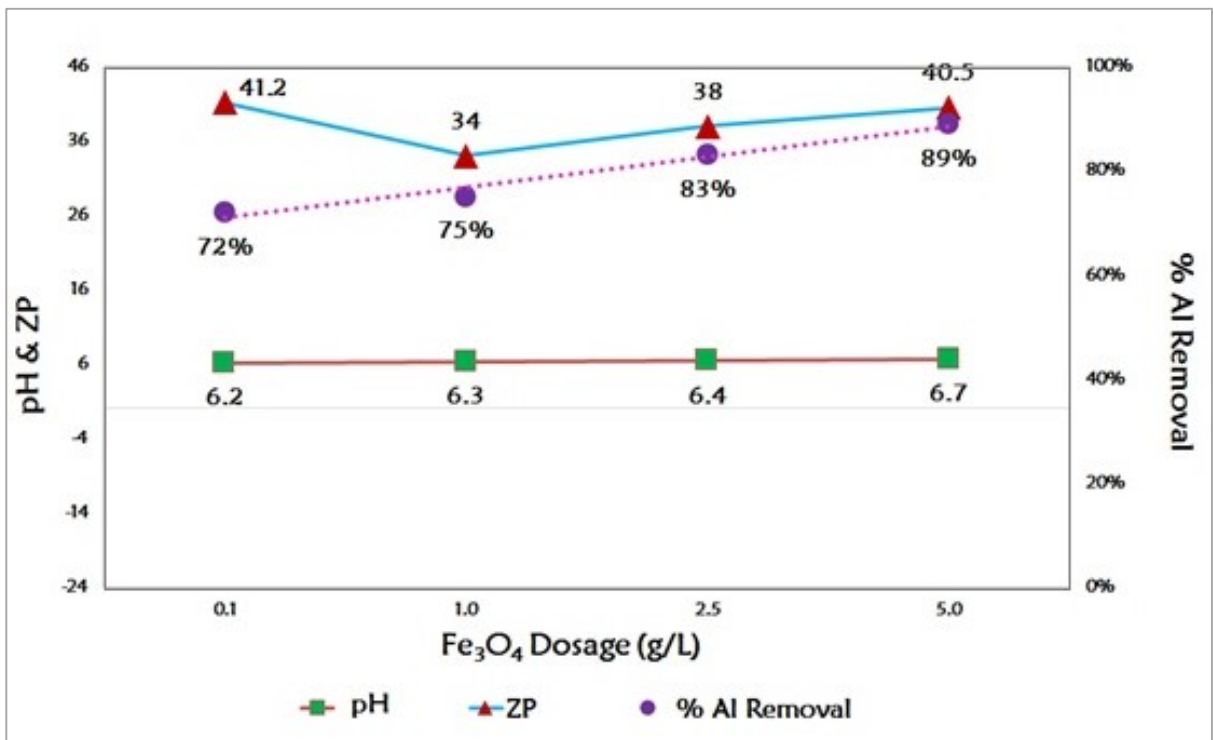
Figure 4-23   Zeta Potential of Fe$_3$O$_4$ Dosage

4.3 Geotube Dewatering

Geotube dewatering represented phase-2 of the experiments that was performed to separate the solid particles after wastewater treatment using geotextile filter media. This was done to compare the results of the influent and effluent water qualities. After geotube dewatering, the effluent water was analyzed for the parameters of total Al, TSS and SEM analysis as described in the sections below.

4.3.1 Total Al and TSS

From the results found for total Al of the effluent water quality was that it was observed to be capable to remove total Al significantly using filtering media of the geotube even using lower adsorbent dosage. From the effluent water test result revealed that Fe_3O_4 adsorbent using geotube, additional 20% removal was improved at 0.1 g/L, 15% using 1 g/L, 16% using 2.5 g/L and 10% using 5 g/L respectively. Similarly using MgO adsorbent additional 20% removal was achieved at 0.1 g/L, 15 % at 1 g/L, 14% using at 2.5 g/L, and 0% using 5 g/L. In addition, using CaO adsorbent 14% additional removal was achieved at 0.1 g/L, 18% at 1 g/L, 18% using 2.5 g/L, and 0 % using 5 g/L. All the results are shown in the Table 4-3 below. It was for the reason that the filtering media was helping to remove more Al while passing the influent water through the geotubes, by trapping larger particle of the flocs on the geotube. But in case of the combination of CaO and Fe_3O_4, additional Al removal was not achieved significantly using effluent water compared to influent water quality. It might be the reason of the small particles of this combination contributed more to increase Al solubility that already passed through the geotextile openings. Another potential reason might be due to the change of the zeta potentiality in the dispersion media and the change of pH due to the experimental error. But still Al removal was improved using higher dosage of the adsorbents while using this combination of effluent water sample as shown in

Figure 4-24. Besides, TSS was also observed to remove Al using geotextile filter media compared to the influent water treatment before as illustrated in Figure 4-25 below. For clear understanding to make the mechanism simpler, only the combination of CaO and Fe_3O_4 adsorbent dosage was described in the section below. The similar results of the other adsorbents are shown in the appendix section.

Table 4-3   Comparison of % Al Removal for Influent and Effluent Water Quality

| Name of Adsorbent	Adsorbent dosage (g/L)	% Influent Al removal from Raw Water (A)	% Effluent Al Removal Relative to Raw Water (B)	% Increase in Al Removal (B-A)/A
Fe_3O_4	0.1	72	80	11%
	1.0	75	90	20%
	2.5	83	99	19%
	5.0	89	99	11%
MgO	0.1	28	48	71%
	1.0	58	73	26%
	2.5	70	84	20%
	5.0	98	87	No more removal
CaO	0.1	38	52	37%
	1.0	60	78	30%
	2.5	77	95	23%
	5.0	97	96	No more removal
CaO & Fe_3O_4	1.0	93	79	No more removal
	2.5	95	75	No more removal
	5.0	97	95	No more removal
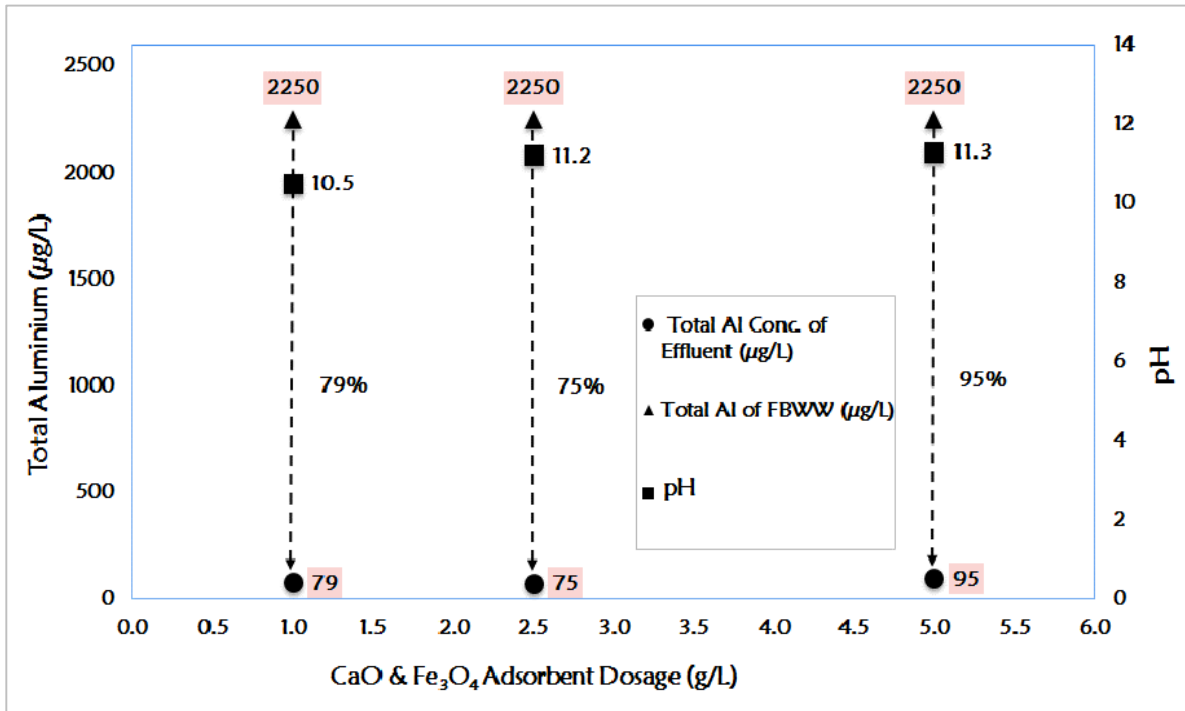
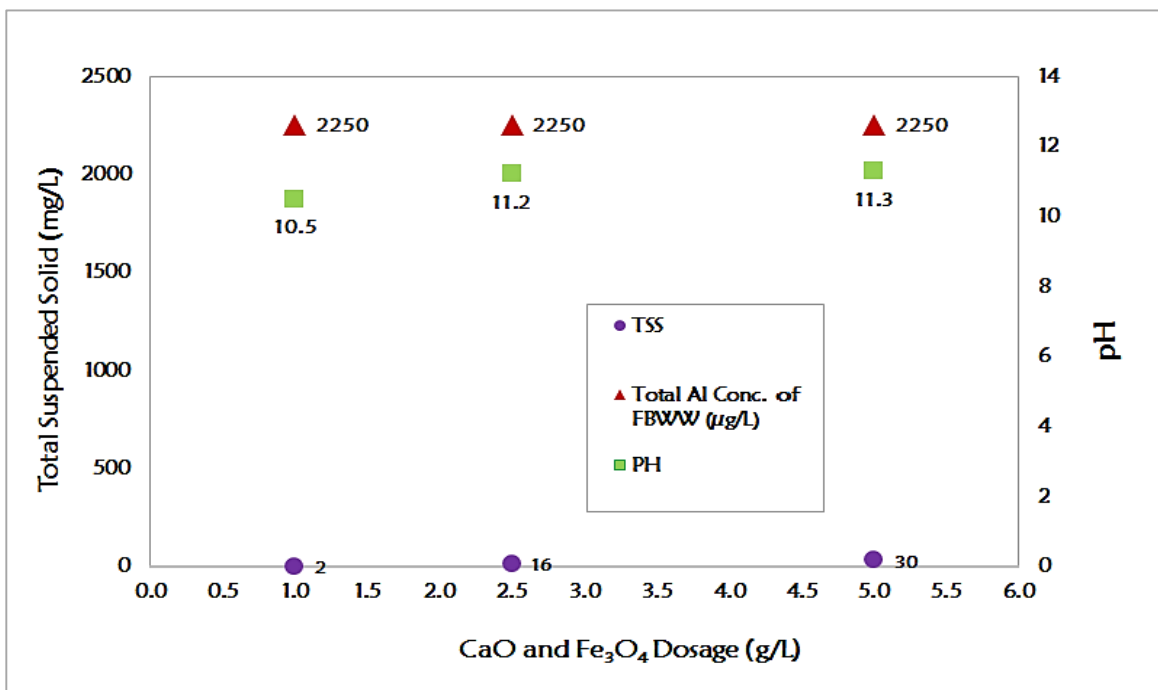**Figure 4-24   Total Aluminium Using CaO and Fe₃O₄ Adsorbent**

Figure 4-25   TSS Using CaO and Fe₃O₄ Adsorbent

4.3.2 SEM Analysis

In this research, scanning electron microscopy (SEM) technology was used to observe the flocs through the microscope at different magnification range which was settled in the bottom of the jars. Particularly, the flocs were observed that passed through the geotextile filter media as shown in Figure 4-26. In this experiment, three magnification ranges of 50, 150 and 500 SEM were taken into consideration to view the images. Elemental composition of the particles was considered to detect the metals formed that are illustrated in the Table 4-4. SEM results confirmed that Al is present in the flocs that were our main goal to eliminate from the FBWW. Table 4-4 shows some significant results highlighted that Al was identified in each of the adsorbent dosage of the FBWW treatment. The Al concentration (by weight) has been illustrated in the Table 4-4 below whereas using CaO & Fe_3O_4 (5 g) was able to detect more Al removal; which was pretty similar to be found from the previous analysis of the results. For better understanding, the SEM image of CaO & Fe_3O_4 (5 g) was shown in this section. Figure 4-26 shows the SEM images of CaO & Fe_3O_4 (5 g) Adsorbent in different magnification range at 50 SEM, 150 SEM and 500 SEM. It is observed from the Figure 4-26 that the flocs formed were stacked with each other and attached to the surface by the attraction of surface charge to form a bigger floc at higher dosage of the adsorbent. The other SEM images using other categories of adsorbents have been outlined in the appendices.

Table 4-4   Elemental Composition of Flocs (By Weight)

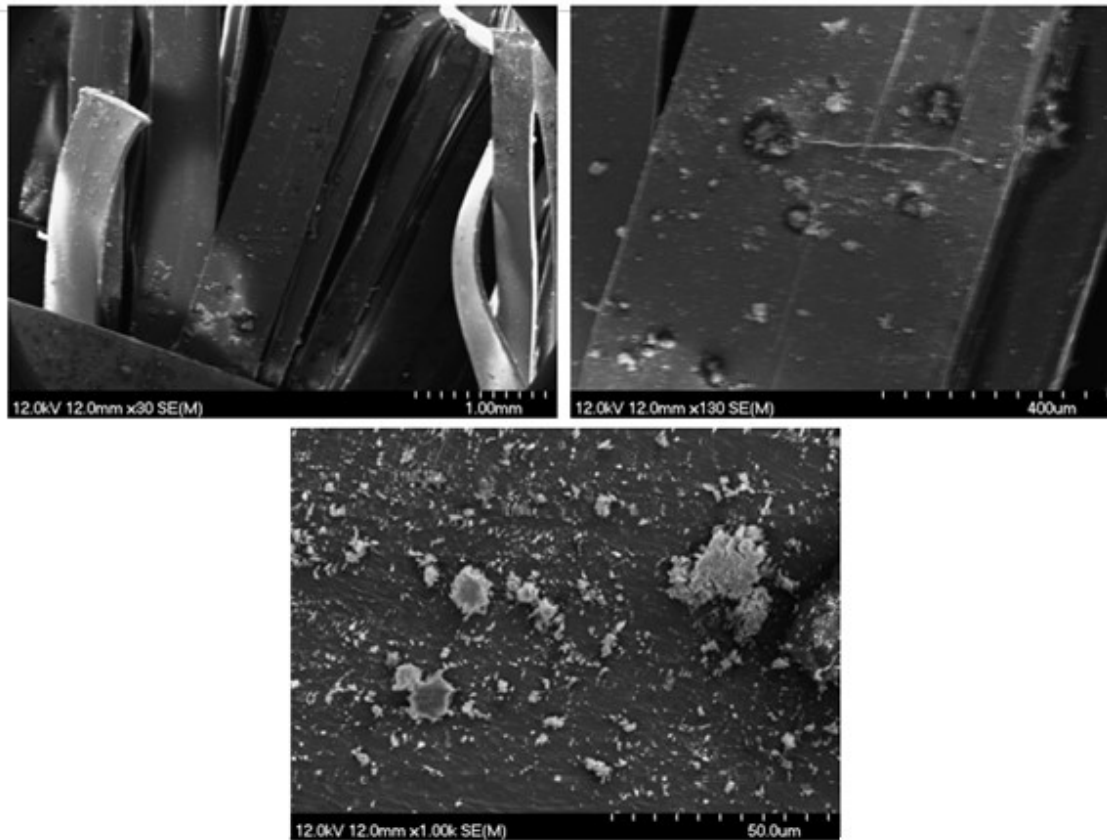| Adsorbents	Al K (Weight %)
Fe_3O_4 (1g)	0.10
CaO (1g)	0.10
MgO (1 g)	0.52
MgO (5 g)	1.61
CaO & Fe_3O_4 (1 g)	0.36
CaO & Fe_3O_4 (5 g)	2.00

Figure 4-26   SEM Analysis of CaO & Fe_3O_4 (5 g) Adsorbent

4.4 Evaluation of Findings in the Context of Water Treatment

This study has shown that SEM analysis on the flocs showed the presence of Al which agreed well with the removal of Al observed in the experiments.

The Zeta potential measurements of FBWW illustrated the zero point of charge at varied pH conditions for various categories of adsorbents. The FBWW was characterized by the overall surface net charge of approximately +33mV at pH 7.5 without any coagulant dosage. However, the addition of adsorbents (MgO, CaO and combination of CaO and Fe_3O_4) shifted the zeta potential to more negative values for pH value>6.0. At this pH level, charge neutralization occurs as the results showed that the zero point of charge was measured at pH 6.0 and at higher pH>6.0, adsorption process was likely to occur due to the increased adsorbent dosage. The zeta potential measurements were found more positive at PH 6.2~6.7, in the case of Fe_3O_4 dosage. At this pH level, particles reached at the stable condition and further increasing levels of adsorbents increased the cationic affinity of the surface charge. It appears that charge neutralization mechanism is occuring due to sweep floc coagulation mechanism and amorphous metal hydroxide precipitates as similar studies have found (e.g. Jiang and Graham, 1998). At pH range 6.2~11.3, floc particles grew in larger size and settled due to the gravitational force as an amorphous precipitated which probably helped in aluminium particle removal. As noted by Duan and Grogory (2003), higher removal efficiencies were likely to occur at higher pH and higher adsorbent dosage as similar results were found from the experiments. At this higher pH level, flocs were found larger in size at higher adsorbent dosage (i.e 5 g/L) due to the amorphous hydroxide precipitate.

The average size of the particles was increased with successive dosage of adsorbent at higher pH range during coagulation and flocculation process and hence aluminium flocs

were removed as similar studies were investigated by (Spicer and Pratsinis 1996). However, in that circumstances, flocs grew in larger size at higher pH through sweep floc mechanism and settled as amorphous precipitate. The results revealed that using the combination of metal oxides (CaO and Fe_3O_4), the flocs were found to be detected as in a higher range (>495 µm). Sun, S., Weber-Shirk, M. and Lion L. W. (2015). suggested that flocs in larger size (>120 µm) range are expected to contribute to the 100% removal efficiency due to the larger terminal velocity compared with capture velocity of tube settler. Hence, the experiments from this combination investigated that the maximum of 97% aluminium removal efficiency was present at higher adsorbent dosage. The probable Findings in this dissertation are shown in Table 4-5 in a summarized form below.

Table 4-5   Probable Mechanism Involved and Pathways

Cases	MgO	CaO	Fe₃O₄	CaO & Fe₃O₄
Observation (i.e 1 g/L Adsorbent dosage for each categories)	**1 g/L:** pH: 8.9 ZP: -11.4 Particle Size: 215 µm % Al Removal: 58% TSS: 20 mg/L	**1 g/L:** pH: 7.5 ZP: -12.5 Particle Size: 215 µm % Al Removal: 60% TSS: 308 mg/L	**1 g/L:** pH: 6.3 ZP: +34 Particle Size: 124 µm % Al Removal: 75% TSS: 252 mg/L	**1 g/L:** pH: 10.5 ZP: -7.9 Particle Size: 91µm % Al Removal: 93% TSS: 4 mg/L
Probable Mechanism Involved	Sweep Coagulation Charge Neutralization Adsorption Precipitation	Sweep Coagulation Charge Neutralization Adsorption Precipitation	Sweep Coagulation Charge Neutralization Precipitation	Sweep Coagulation Adsorption Precipitation
Probable Pathways				
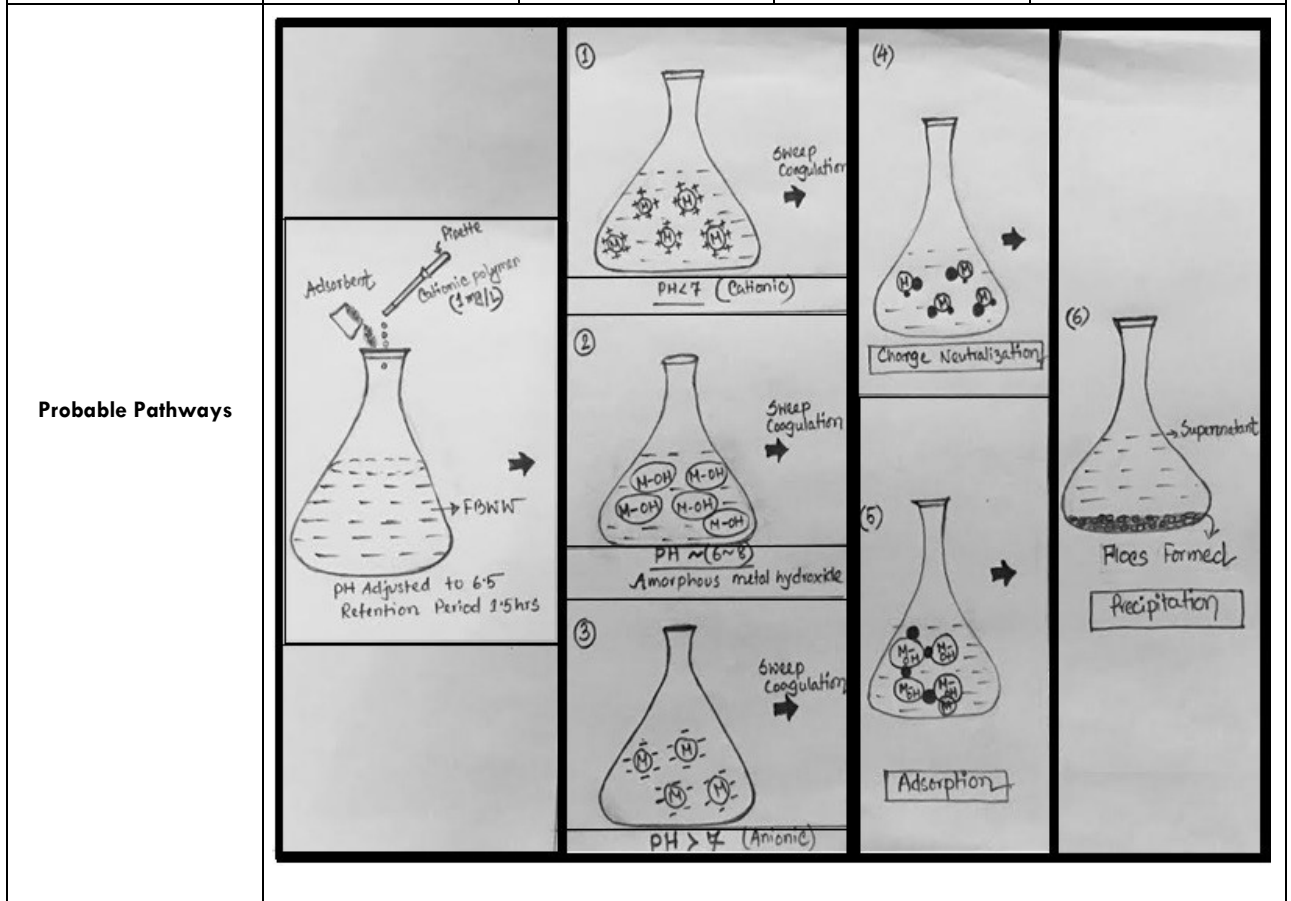
Chapter 5 Conclusions

5.1 General

The purpose of this chapter is to summarize the key findings of this research work and recommendations arising for future work. Overall, this thesis mainly focuses the need of adsorbent usage for the removal of aluminium from FBWW and the usage of GT500 Engineered geotextile for the removal of sludge in wastewater treatment strategies.

5.2 Conclusions

The conclusions which have been drawn from this dissertation are described as follows.

Total aluminium removal was the main parameter of interest of the overall experimental approach. Jar tests were performed considering a 1.5-hour retention period in order to get more flocs formed through the flocculation process to remove aluminium and maximum retention of solids on the geotubes. Suitable adsorbent dosage was chosen as 0.1 g/L, 1.0 g/L, 2.5 g/L and 5.0 g/L for each adsorbent dosage. The higher dosage of 5.0 g/L of CaO and MgO adsorbent worked well to remove aluminium from the FBWW. A combination of CaO and Fe_3O_4 adsorbent removed total Al conc. at the lower dosage of adsorbent at 1g/L.

The rapid dewatering method (RDT) was also incorporated with the jar test procedure to screen the performance of the Al removal capacity using GT500 geotextile filter media. The test results showed that the removal of aluminium was further accelerated using geotextile filter media in individual at higher adsorbent dosage and a combination of adsorbents at lower dosage. This removal met the JDKWTP site specific acceptable limit of 184 µg/L using higher adsorbent dosage of individual usage of CaO and MgO at 5 g/L and a combination of CaO and Fe_3O_4 at lower 1 g/L to higher dosage 5 g/L.

The second parameter that was highlighted throughout the experiments was TSS concentration. The results showed that the TSS concentration increased due to the higher adsorbent dosage may be the reason of new particles formed or excess adsorbents contributed to settle due to the gravitational forces and settled below the surface of the jars. Thus, these excess flocs contributed to increase the amount of TSS conc. after the jar test procedure. But after the geotube dewatering, the flocs of larger particles trapped on the top of the geotextile and that helped out to remove the TSS conc. which was expected to remove by geotubes.

In case of dissolved Al concentration Fe_3O_4 adsorbent dosage failed to decrease the Al concentration with increasing order of the adsorbent but the adsorbents i. e. CaO and MgO were able to decrease the dissolved Al concentration with an increasing order of the adsorbent dosage. Furthermore, the combination of adsorbents displayed the trend to decrease the dissolved Al concentration.

From the SEM analysis of the geotextile filter media, it was shown that the Al removal process was successfully accomplished using the above adsorbent dosage. Among them, the combination of adsorbents acted more satisfactorily at a lower dosage (1 mg/L) to remove Al. The detection of retained solids showed that there was aluminium present in the flocs at

the final stage. In addition, the particle size analysis and zeta potential analysis explained the same trends of results. The mechanism of aluminium removal that was discovered after the whole experimental work was detected as flocculation, rapid enmeshment, and adsorption and precipitation process.

Key Points of the Conclusion

- ❑ MgO and CaO adsorbent in individual dosages and also a combination of metal oxides (CaO & Fe_3O_4) adsorbents worked efficiently to remove total Al and dissolved Al.

- ❑ Combination of metal oxides (CaO & Fe_3O_4) as low as 1g/L dosage were found to be the most cost effective adsorbents at pH 10.5 in removing total Al about 93% from FBWW.

- ❑ GT500 Engineered Geotextile performed as an effective filter media in removing TSS as well as minimizing total Al conc. About 95% of total Al removed using above combination of metal oxide (as higher dosage of 5 g/L) adsorbents.

5.3 Recommendations for Future Research

In future research, a bench scale experimental set up might be introduced in order to study the experimental results to apply those combinations of adsorbents at lower dosage found from our study accompanied with lower polymer dosage for future application. This outcome may be beneficial for limiting Al to control according to provincial guideline standards as well as can be applied in the treatment plant prior to discharge of FBWW into the settling lagoons. The GT500 geotextile filter media may be altered with other kind of geotextiles

having small opening to modify the reduction rate of the TSS concentration as well as to accelerate Al removal. It may also be recommended to study a few more parameters i.e. TOC (Total organic carbon), DOC (Dissolved organic carbon) and turbidity of the FBWW and treated water samples for more and clear understanding of the samples and outcomes. In addition, experiments considering seasonal variations would have been recommended to observe the outcomes that might help more specifically to get clear ideas of temperature variations for future perspectives. Another focus might be given on solid sludge disposal depending on particle categories (i.e. hazardous material, lower pH water disposal) and also reuse of materials might be considered in future research endeavor. An approximate idea of the future bench scale set up has been outlined in the flow chart diagram below in Figure 5-1.
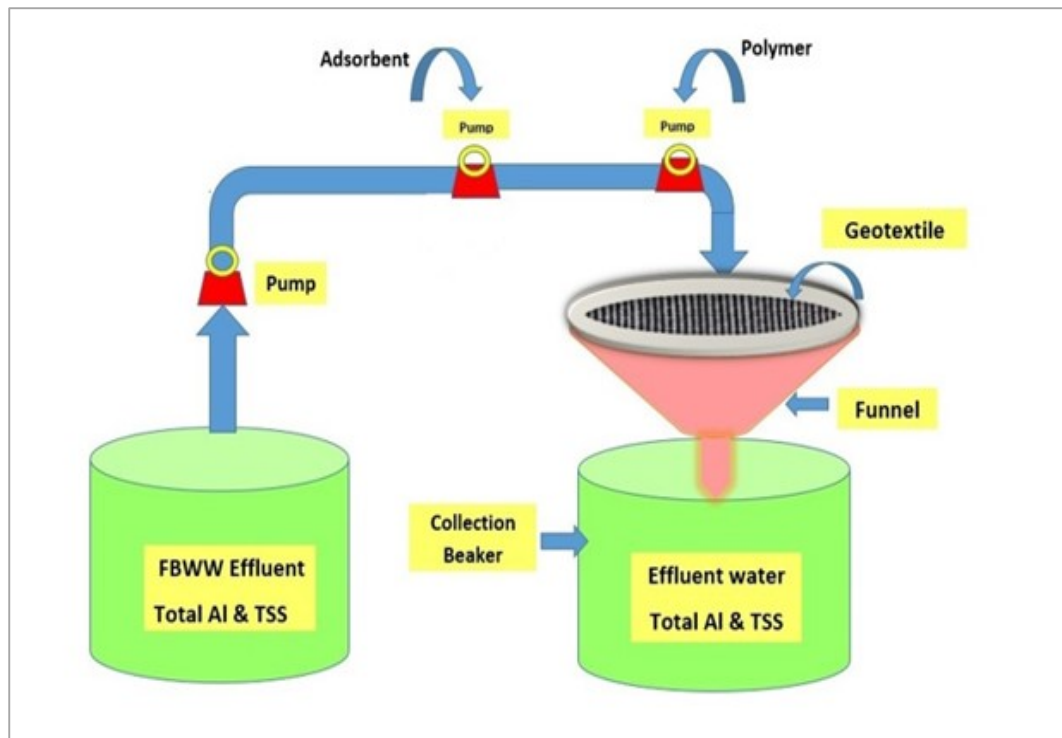

Figure 5-1   Flow Diagram of Proposed Future Laboratory Task

References

Alexandre, A., and Monica, R. (2012). Electrolytic Treatment of Wastewater in the Oil Industry, New Technologies in the Oil and Gas Industry, Dr. Jorge Salgado Gomes (Ed.), InTech, DOI: 10.5772/50712.

ASTM. (1992). *Standard Test Method for Measuring the Soil- Geotextile System Clogging Potential by the Gradient Ratio (D5101), in 1992 Annual Book of ASTM Standards, sect. 4, vol. 04.08. ASTM, Philadelphia, PA, pp. 1090-1196.*

Bishop Water Technologies Inc. (2013, 1 15). Retrieved from www.bishopwater.ca.

Canadian Council of Ministers of the Environment. (1999). CCME Canadian Water Quality Guidelines List of Chapters, (November 2008).

CCME. (1999). Canadian Water Quality Guidelines for the Protection of Aquatic Life. ISBN 1-896997-34-1.

CCME. (2004). Application and Testing of the Water Quality Index in Atlantic Canada Report Summary, 1–6.

Clark, W. W. (2010). Request for Qualifications. Sustainable Communities Design Handbook, (July), 313–366.

Dewatering Solution Inc. (DSI). (2007, 1 15). http://www.dewateringsolutions.net. Retrieved from http://www.dewateringsolutions.net/tech_data.htm.

Duan, J.M. and Gregory, J. (2003) Coagulation by hydrolysing metal salts. Advances in Colloid and Interface Science 100, 475-502.

Droste R. L. (1997). *Theory and practice of water and wastewater treatment*. New York: J. Wiley.

EPA, David A. Cornwell, John Tobiason, and Richard Brown (2010), *Innovative Applications of Treatment Processes for Spent Filter Backwash*, ISBN 978- 1-60573-084-4.

Exley, C., Chappell, J.S., and Birchall, J. D. (1991). *A mechanism for acute aluminium toxicity in fish*. Journal of Theoretical Biology, 151(3), 417–428.

Fanous, M. (2013). *Examining the use of geotubes for removing Aluminum in water treatment backwash water*, MENG Project Report. Halifax: Dalhousie University.

Fannin, R.J., Vaid, Y. P., Palmeria, E.M. and Shi, Y.C. (1996). *A modified gradient ratio test devic [J]*. Recent Developments in Geotextile Filters and Prefabricated Drainage GeoComposite. Philadelphia, PA : ASTM STP 1281, Shobha K Bhatia, L David Suits (Eds), American Society for Testing and Material.

Fowler, J. and Sprague, C.J. (1993). *Dredged Material Filled Geotextile Containers*. Proceedings from Coastal Zone (pp. 2415-2428.). ASCE, New Orleans.

Fowler, J., Duke, M., Schmidt, M.L., Crabtree, B., Bagby, R.M. and Trainer, E. (1996). *Dewatering sewage sludge and hazardous sludge with geotextile tubes*, Environmental Effects of Dredging Technical Notes, U.S. Army Engineer, Waterways Experiment Station, Vicksburg, MS.

Federal Emergency Management Agency (FEMA). (2008). *Geotextiles in Embankment Dams. Status Report on the Use of Geotextiles in Embankment Dam Construction and Rehabilitation*

Fischer, G. R., Mare, A. D., and Holtz, R. D. (1999). *"Influence of Procedural Variables on the Gradient Ratio Test,"* Geotechnical Testing Journal, Vol. 22, No. 1, pp. 22–31.

Frecker, M. F. (1991). "Dementia in Newfoundland: Identification of Geographical Isolate." Journal of Epidemiology and Community Health 45: 307–11.

Fowler, J., Bagby, R.M. and Trainer, E. (1995). Dewatering sewage sludge with geotextile tubes, Environmental Effects of Dredging Technical Notes, U.S. Army Engineer, Waterways Experiment Station, Vicksburg, MS.

Frank, W.B., W.E. Haupin, R.K. Dawless, D.A. Granger, M.W. Wei, K.J. Calhoun, and T.B. Bonney. (1985). Aluminum. In: Gerhartz, W., Y.S. Yamamoto, F.T. Campbell, R. Pfefferkorn, and J.F. Rounsaville. ed. Ullmann's encyclopedia of industrial chemistry - Volume A1: Abrasives to aluminum oxide, 5th rev. ed. pp. 459-480.

Gaffney, D. (2001). Geotextile tube dewatering. Geotechnical Fabrics Report, 19(7), 119-122. Geotechnical Fabrics Report, 19(7), 119-122. Retrieved from Gaffney, D.A. (2001). Geotextile tube dewatering. Geotechnical Fabrics Report, 19(7), 119-122.

Geremias, R., Laus, R., Macan, J. M., Pedrosa, R. C., Laranjeira, M. C. M., Silvano, J., & Fávere, F. V. (2008). Use of Coal Mining Waste for the Removal of Acidity and Metal Ions Al (Iii), Fe (Iii) and Mn (Ii) in Acid Mine Drainage. Environmental Technology, 29(8), 863–869.

GRANITE environmental. (2016). Geotextile and Sludge Tubes. Retrieved July 31, 2016, from http://www.erosionpollution.com/support-files/geotextile-tubes.pdf.

Gottfried, A., Shepard, A. D., Hardiman, K., & Walsh, M. E. (2008). Impact of recycling filter backwash water on organic removal in coagulation–sedimentation processes.

Halifax Media Co-op (HMC). (2009). *JD Kline Water Treatment Plant And Pockwock Watershed Tour.* Retrieved October 6, 2015, from (http://halifax.mediacoop.ca/fr/events/1572).

Hameiri, A. (2001). *On the design and commissioning of a cyclic Gradient Ratio test device.* ASTM Geotech. Testing , J. 25 (in press).

Hanan A. Fouad, Rehab M. El-Hefny and Mahetab Ali Mohamed, *Reuse of Spent Filter Backwash Water.* (2016). International Journal of Civil Engineering and Technology, 7(4), pp.176–187. http://www.iaeme.com/IJCIET/issues.asp?JType=IJCIET&VType=7&IType=4

Hawley, R. (2001). *Filtration performance of geotextiles in cyclic flow conditions: A laboratory study, MASc thesis.* Vancouver, Canada: The University of British Colombia.

Health Canada. (2007). *Aluminum and Human Health 2007.* Retrieved July 1, 2015, from http://www.hc-sc.gc.ca/ewh-semt/water-eau/drink-potab/aluminum-aluminium_e.html

Howells, G., Dalziel, T., Reader, J., and Solbe, J. (1990). *EIFAC water quality criteria for European freshwater fish. Report on Aluminium. Chemistry and Ecology, 4(3), 11–173.*

Hudson L.K., C. Misra, and K. Wefers. (1985). *Aluminum oxide. In: Gerhartz, W., Y.S. Yamamoto, F.T. Campbell, R. Pfefferkorn, and J.F. Rousaville. ed. Ullmann's encyclopedia of industrial chemistry - Volume A1: Abrasives to aluminum oxide, 5th rev. ed.* Weinheim, Verlag Chemie, pp. 557-594.

Humintech GmbH. (2014). *Humintech® | Agricultural & Humic Acids Based Products.* Retrieved October 1, 2014, from http://www.humintech.com/001/agriculture/information/general.html

Ikari et al. (1979). *United States Patent [19]. Japan.*

Jiang, J.Q. and Graham, N.J.D. (1998). *Pre-polymerised inorganic coagulants and phosphorus removal by coagulation - A review. Water Sa 24(3), 237-244.*

John C. Crittenden, R. Rhodes Trussell, David W. Hand, Kerry J. Howe, George Tchobanoglous (2005). *MWH's Water Treatment Principles and Design, 2nd Edition, ISBN 0-471-11018-3.*

Kadlec, R. H. and Wallace, S. D. (2009). *Treatment Wetlands. Boca Raton, FL: CRC Press.*

Kaggwa, R., Mulalelo, C., Denny, P. and Okurut, T. (2001). *"The Impact of Alum Discharges on a Natural Tropical Wetland in Uganda." Water Resources Management 35 (3): 795–807.*

Kuerbis, R. H. and Vaid, Y. P., (1988). *Sand Sample Preparation—the Slurry Deposition Method, Soils and Foundations, Vol. 28, No. 4, pp. 107-118.*

Kumari, A. A. and, & Ravindhranath, K. (2012). *Removal of aluminium (iii) ions from polluted waters using bio-sorbents derived from moryngea millingtonia and cygium arjunum plants. International Journal of ChemTech Research, 4(4), 1733–1745.*

Koerner, G.R. & Koerner, R.M. (2006). *Geotextile tube assessment using a hanging bag test. Geotextiles and Geomembranes 24 (2), 129–137.*

Lenntech B. V. (2015). *Aluminium - (Al) - Chemical properties, Health and Environmental effects. Retrieved April 22, 2015, from http://www.lenntech.com/periodic/elements/al.html*

Lawson, C.R. (2008). *"Geotextile containment for hydraulic and environmental engineering". Geosynthetics International, 15, No 6. pp 384- 427.*

Liao, K. (2008). *Dewatering of Natural Sediments Using Geotextile Tubes. New York, NY: Syracuse University.*

Lide, D.R. (1991). *CRC handbook of chemistry and physics: A ready reference book of chemical and physical data, 71st ed. Boca Raton, Florida, CRC Press pp. 4/3, 4/41-4/42.*

MacLeod, S., (2015). *Freshwater Aluminium Field Sampling.*

Mastin, B. J., Rapids, G., Lebster, G. E., & Rapids, G. (1999). *Use of geotube ® dewatering containers in environmental dredging.*

Moffat, R. (October 2002). *a labratory study of particle migration in cohesionless soil. British Colombia: The University of British Colombia.*

Moo-Young, H. M. (1999). *Contaminant Migration through Geo-containers used in dredging operations. Engineering Geology 53 (2), 167-176.*

Moo-Young, H. K., Gaffney, D. A., & Mo, X. (2002). *Testing procedures to assess the viability of dewatering with geotextile tubes. Geotextiles and Geomembranes, 20(5), 289–303.*

Nandhitha, S.M. & Ilamparuthi, K. (2010). *Performance of Geotextiles in Dewatering High WaterContent Sludges. Indian Geotechnical Conference, GEOtrendz.*

Palermo, M.R. and Wilson, J. (1997). *Dredging State of the Practice: Corps of Engineers Perspective. Proceedings, Geologan 97, The First National Conference of the Geo-Institute, Logan, Utah, July 15-19, 1997, American Society of Civil Engineers, New York, New York.*

Rowe, R. K. (2001). *Geotechnical and Geoenvironmental Engineering Handbook. First Edition. Massachusetts: Kluwer Academic Publishers.*

Segre, G. F. (2013). *A Physicochemical evaluation of the Compressibility and Dewatering Behavior of Dredged Sediments. Theses - ALL. Paper 6.*

Singh, T. S., & Parikh, B. (2006). *Investigation on the sorption of aluminium in drinking water by low-cost adsorbents. Water SA, 32(1), 49–54.*

Shi, Y. (1993). *Filtration behaviour of Non-Woven Geotextiles in the Gradient Ratio Test, MASC thesis,. Vancouver, Canada: The University of British Colombia.*

Smith, M. (2008). *Geotextile Tubes in Environmental Applications. Australia: Global Synthetics Pty Ltd.*

Spicer, P.T. and Pratsinis, S.E. (1996) *Shear-induced flocculation: The evolution of floc structure and the shape of the size distribution at steady state. Water Research 30(5), 1049-1056.*

Sun, S., Weber-Shirk, M. and Lion L. W. (2015). *Environmental Engineering Science. 33(1): 25-34. doi:10.1089/ees.2015.0311.*

Tencate. (2007). *Three New Tests Allow Accurate Assessment of Geotube Dewatering. Retrieved from TenCate Geosynthetics North America.*

Tencate Geotube (2006). *For Municipal Wastewater and Water Treatment, geotube®dewatering technology works.*

Tencate. (2011). *The Low Cost, High Volume Dewatering Solution. Industrial Fabrics Dewatering Systems, TenCate Geosynthetics North America. Retrieved from* http://www.tencate.com/amer/Images/BRO_Dewatering0207_tcm29-31796.pdf

Terms of Reference for System Assessment Reports for Municipal Drinking Water Systems. (2012), Nova Scotia Environment.

Tobiason, J., Edzwald, J., Levesque, B., Kaminski, G., Dunn, H., & Galant, P. (2003). FULL-SCALE ASSESSMENT of waste filter backwash recycle. *Journal (American Water Works Association), 95*(7), 80-93. Retrieved from http://www.jstor.org/stable/41311133.

US Fabrics Inc. (n.d.). *EcoTube™ Sludge Dewatering Tubes - US Fabrics.* Cincinnati, OH. Retrieved from http://www.usfabricsinc.com

Water Quality Association. (2013). *Aluminum fact sheet.* 4151 Naperville Road • Lisle, Illinois 60532. Retrieved from www.wqa.org.
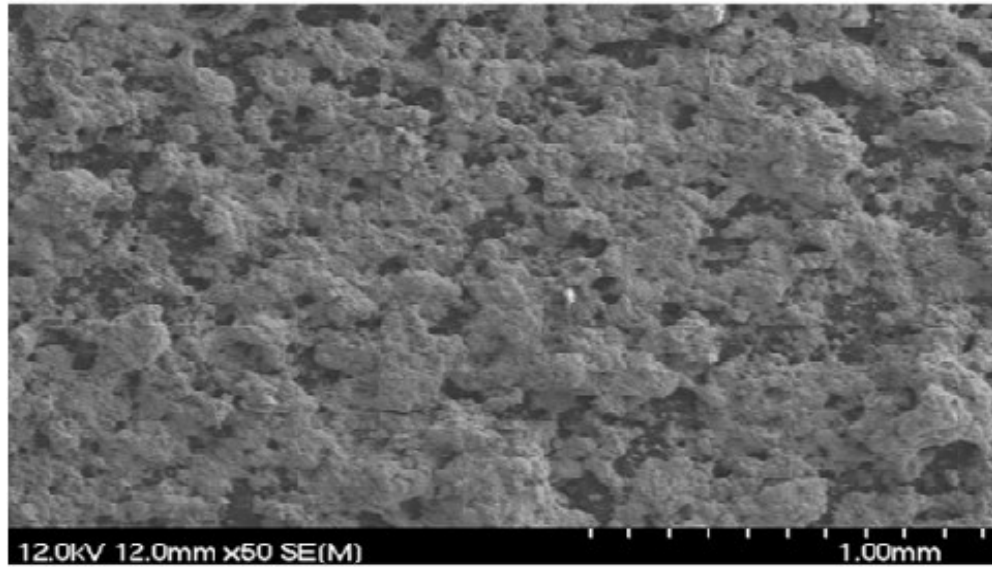
Wood (2014). *Removal of aluminum in filter backwash water: a treatment optimization case study.*

WHO (World Health Organization) (1997). *Environmental Health Criteria 194. Aluminum. International Programme on Chemical Safety (IPCS).* Geneva ISBN 92 4 157194 2.
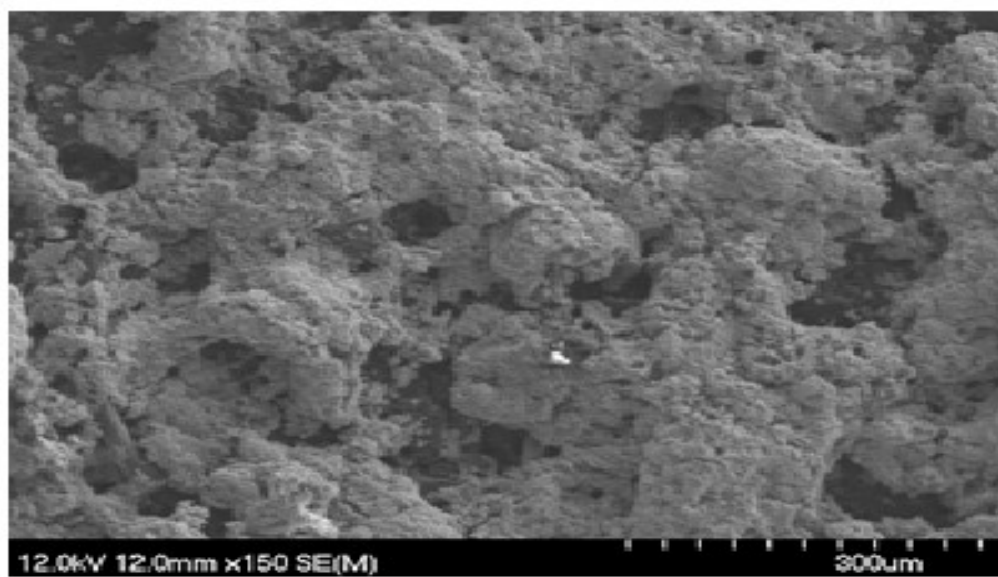
Appendix A

Figure A.1 SEM Analysis of CaO & Fe₃O₄ (1 gm) Adsorbent

500 Magnification

12.0kV 12.0mm x500 SE(M)　　　　　　　　　100um

Figure A.2 SEM Analysis using MgO (1gm) Adsorbent

50 Magnification

12.0kV 12.0mm x50 SE(M)　　　　　　　　　1.00mm

150 Magnification

10.0kV 12.0mm x150 SE(M)　　　　　　　　300um

500 Magnification

12.0kV 12.0mm x500 SE(M) 100um

Figure A.3   SEM Analysis of MgO (5 gm) Adsorbent

50 Magnification

12.0kV 12.0mm x50 SE(M) 1.00mm

150 Magnification

12.0kV 12.0mm ×150 SE(M)　　　　　300um

500 Magnification
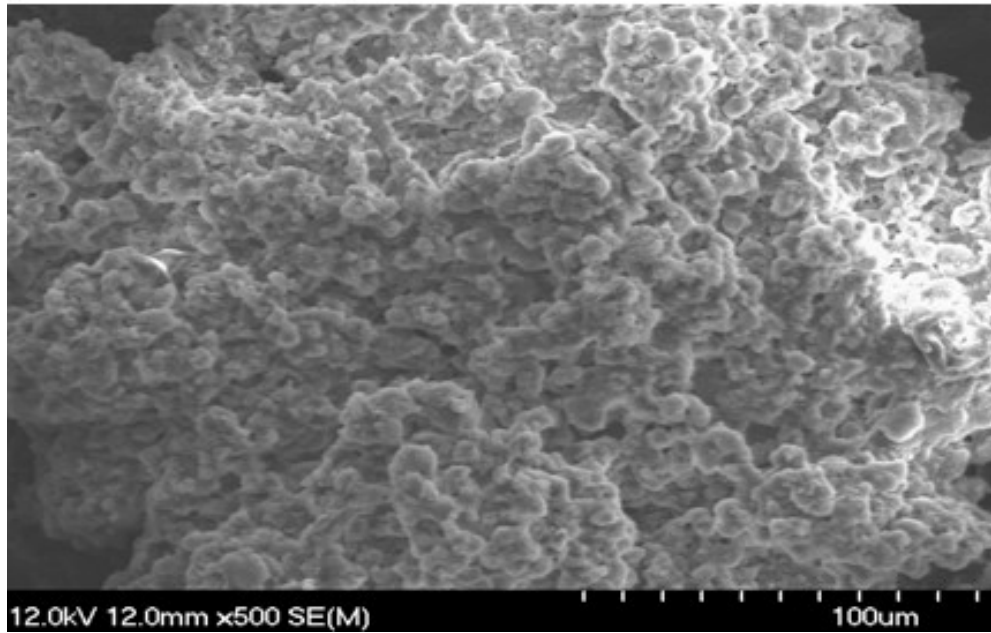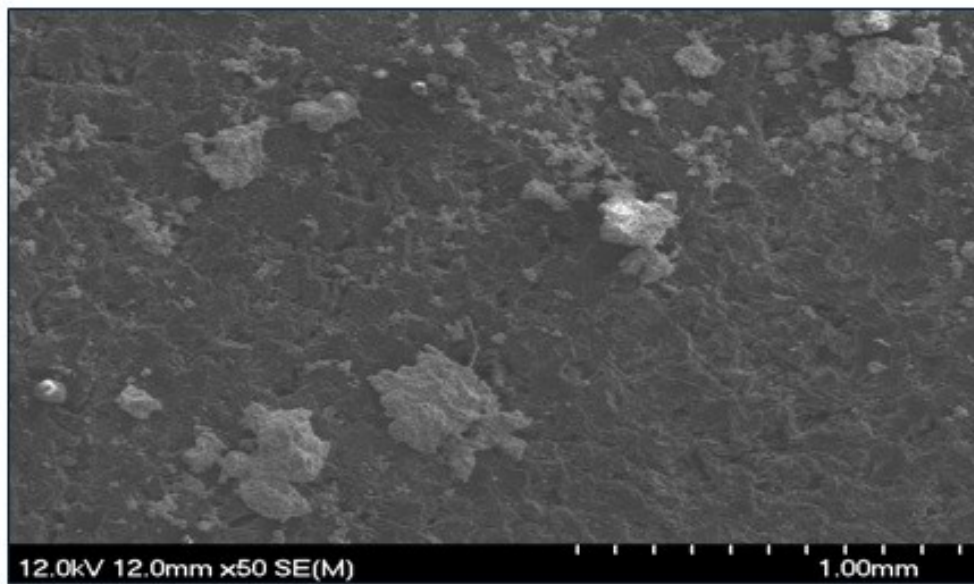

12.0kV 12.0mm ×500 SE(M)　　　　　100um

Figure A.4   SEM Analysis of Fe$_3$O$_4$ (5 gm)

50 Magnification
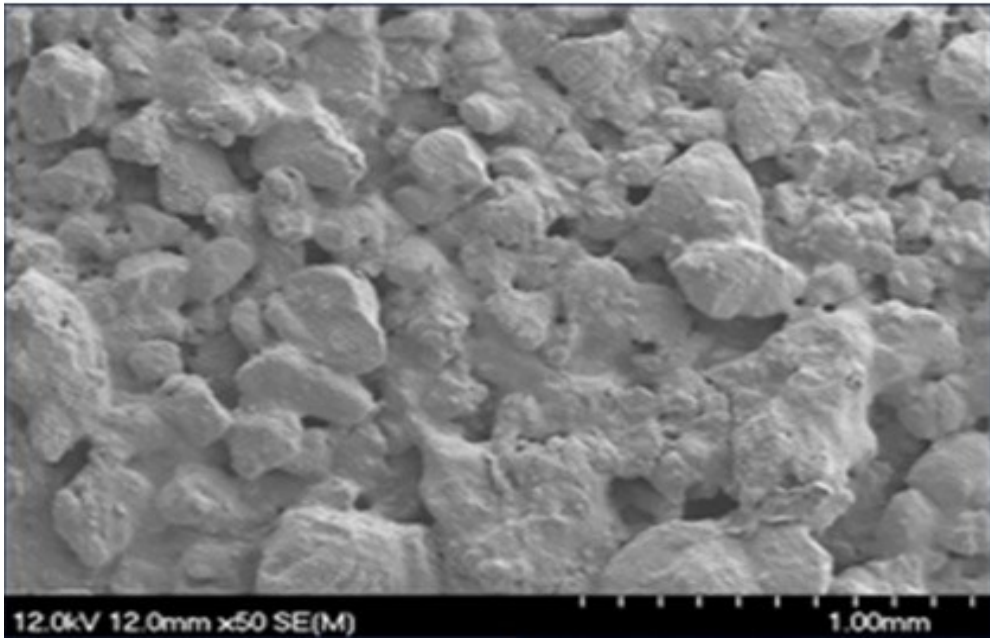
150 Magnification

500 Magnification

12.0kV 12.0mm x500 SE(M)   100um
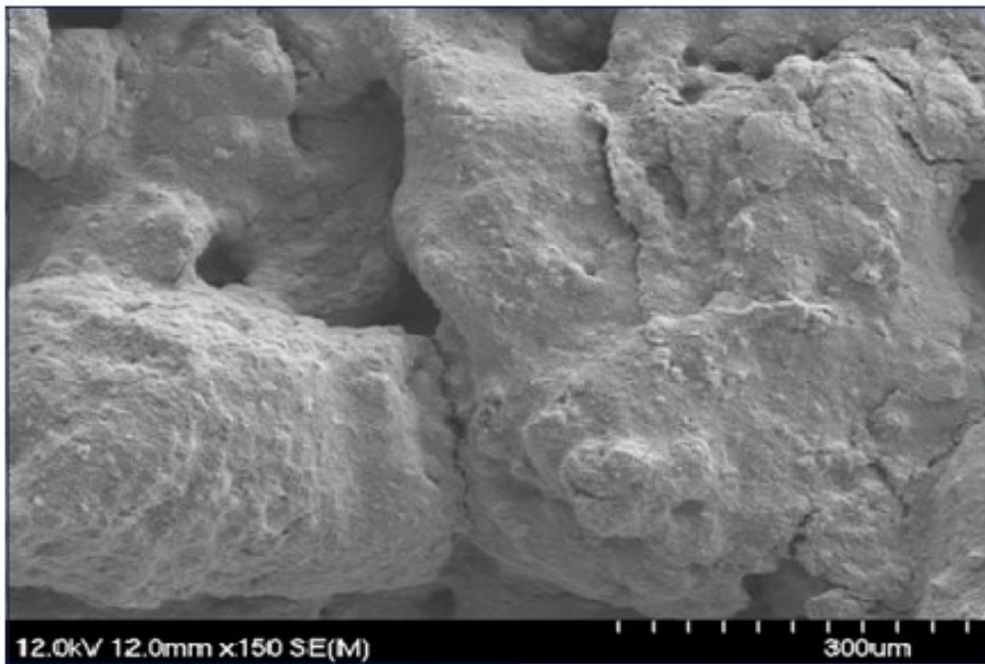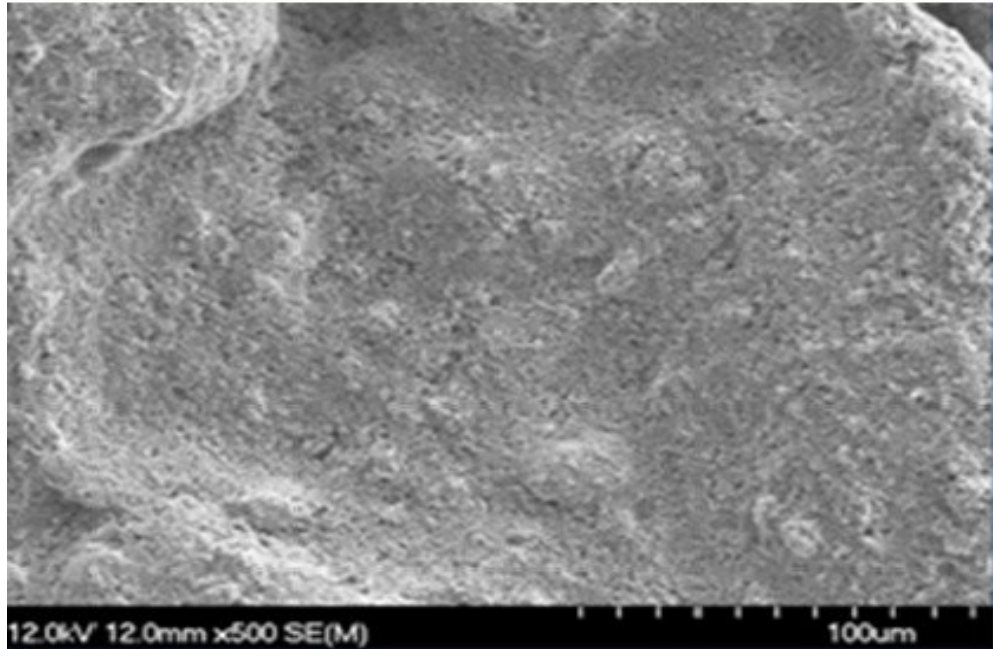
Figure A.5   SEM Analysis of CaO (1 gm) Adsorbent

50 Magnification

12.0kV 12.0mm x50 SE(M)   1.00mm

150 Magnification

12.0kV 12.0mm x150 SE(M)   300um

500 Magnification

12.0kV 12.0mm x500 SE(M)   100um
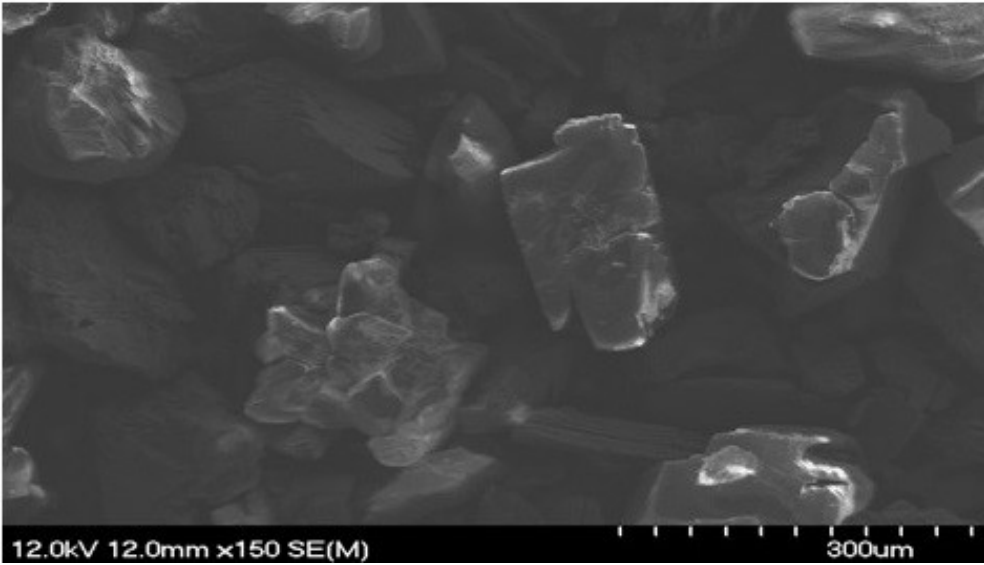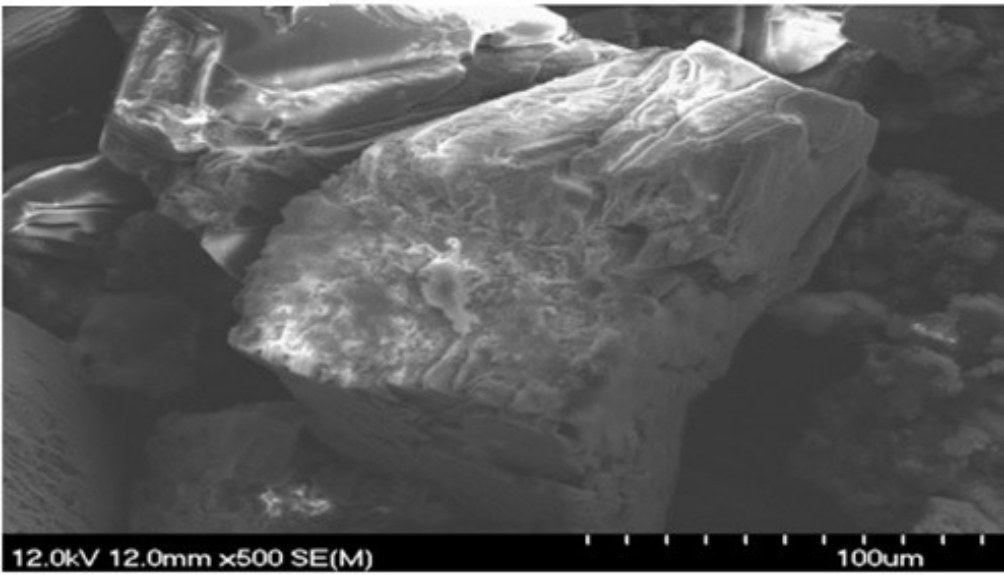
Figure A.6   SEM Analysis of CaO & Fe$_3$O$_4$ (1 gm) Adsorbent with Geotextile
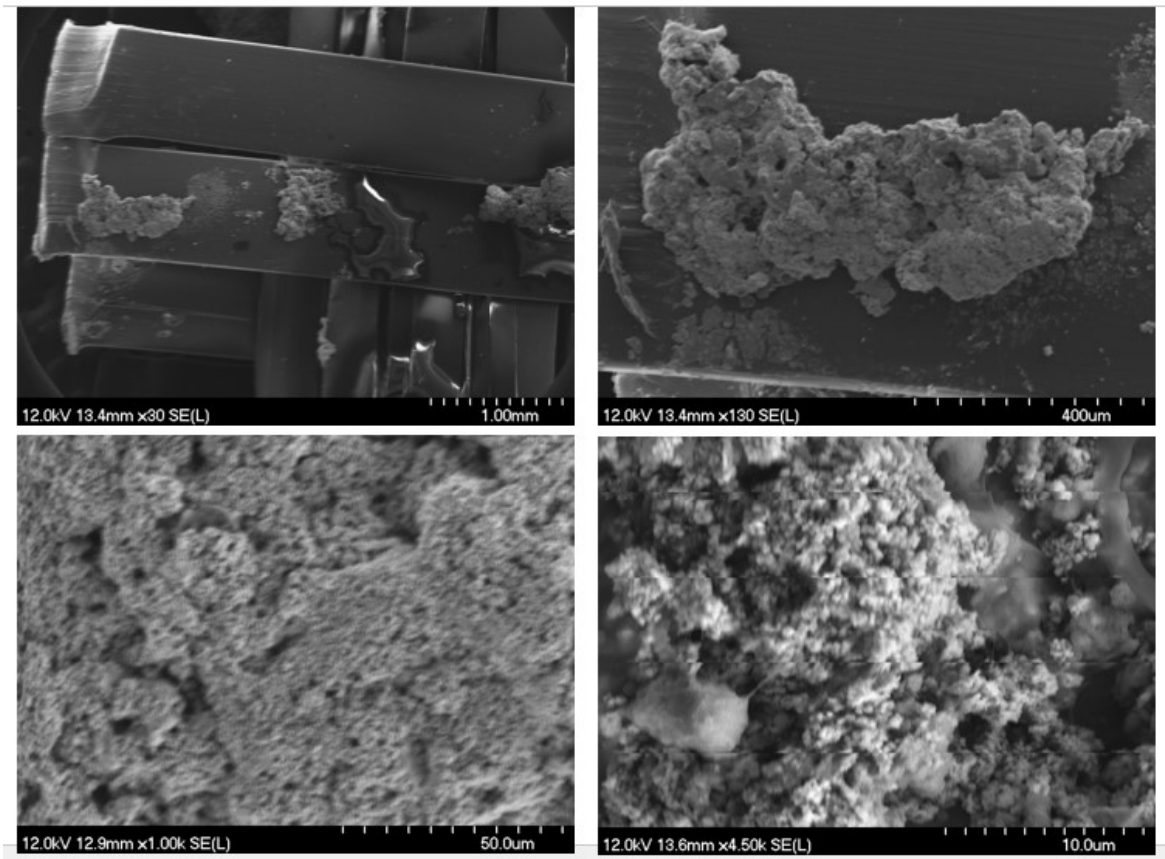
Figure A.7   SEM Analysis of CaO & Fe₃O₄ (5 gm) Adsorbent with Geotextile
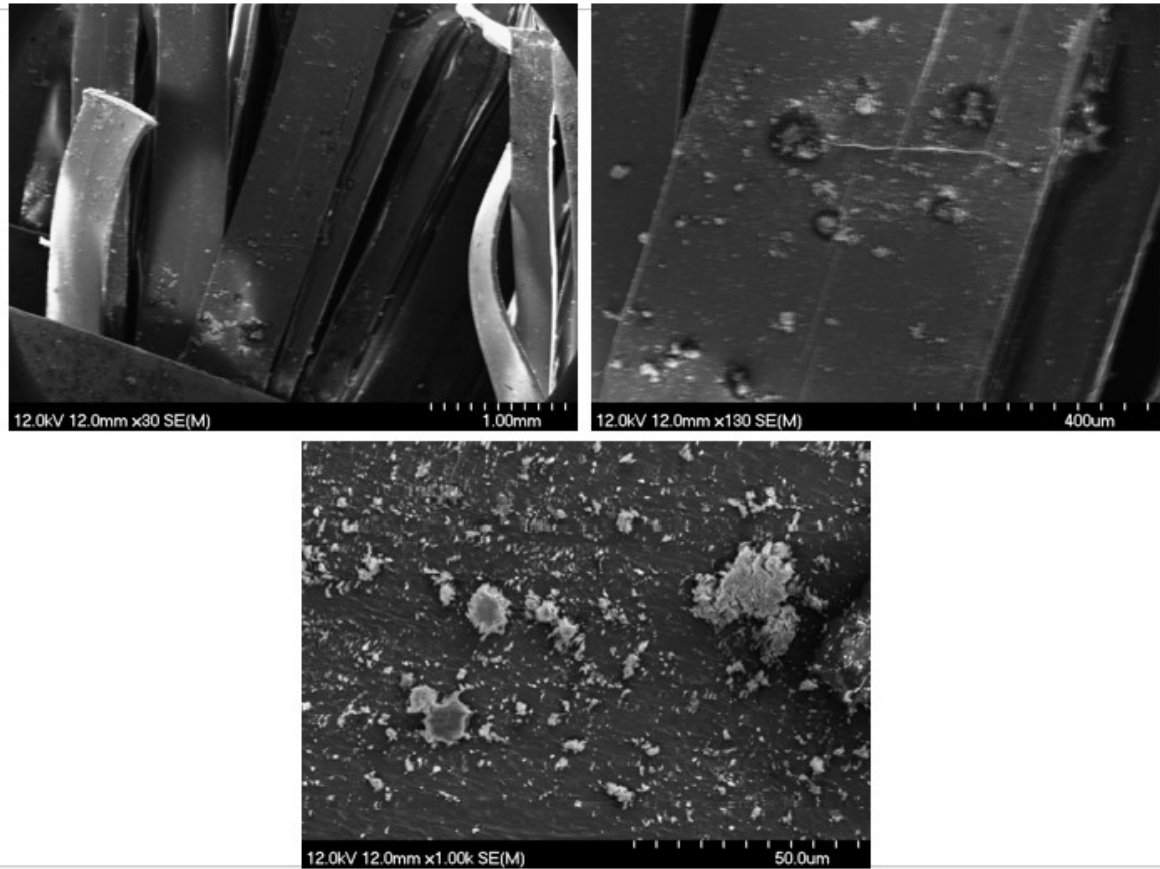
Figure A.8   SEM Analysis of Fe₃O₄ (1 gm) Adsorbent with Geotextile
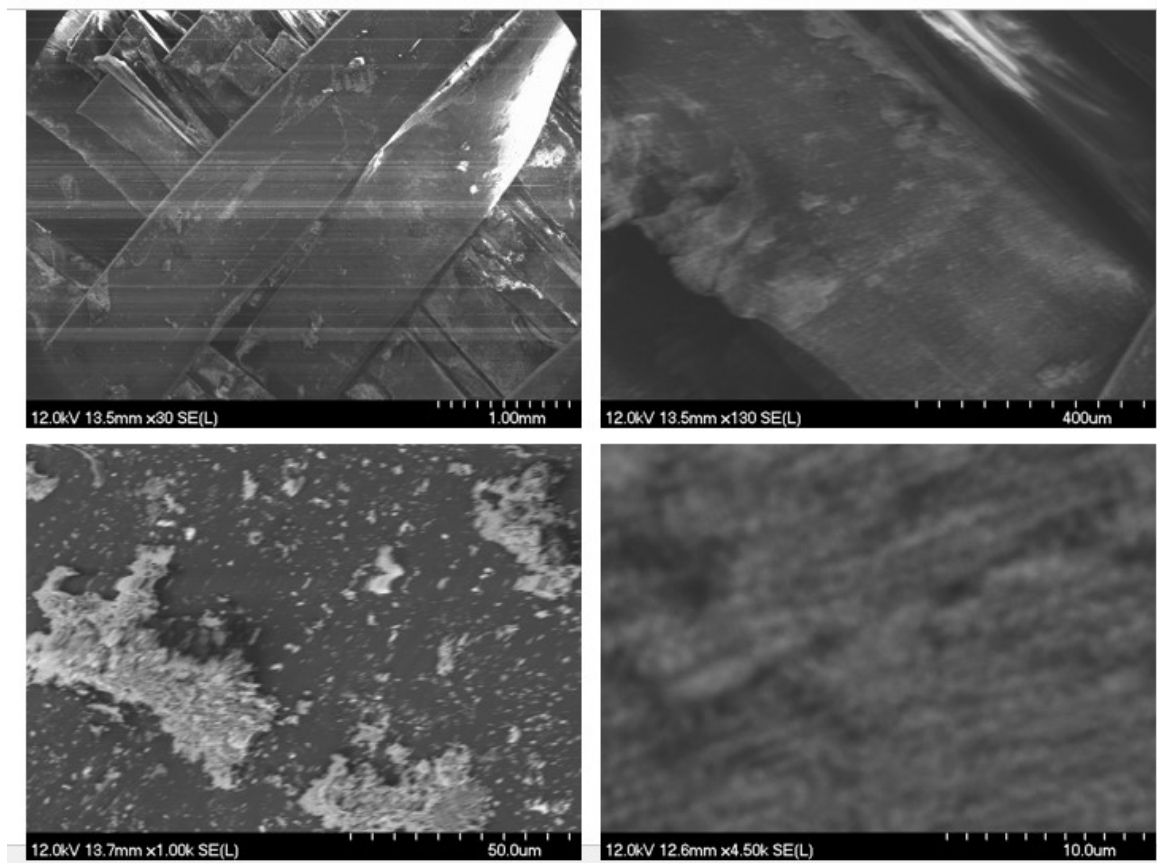
Figure A.9   SEM Analysis of CaO (1 gm) Adsorbent with Geotextile
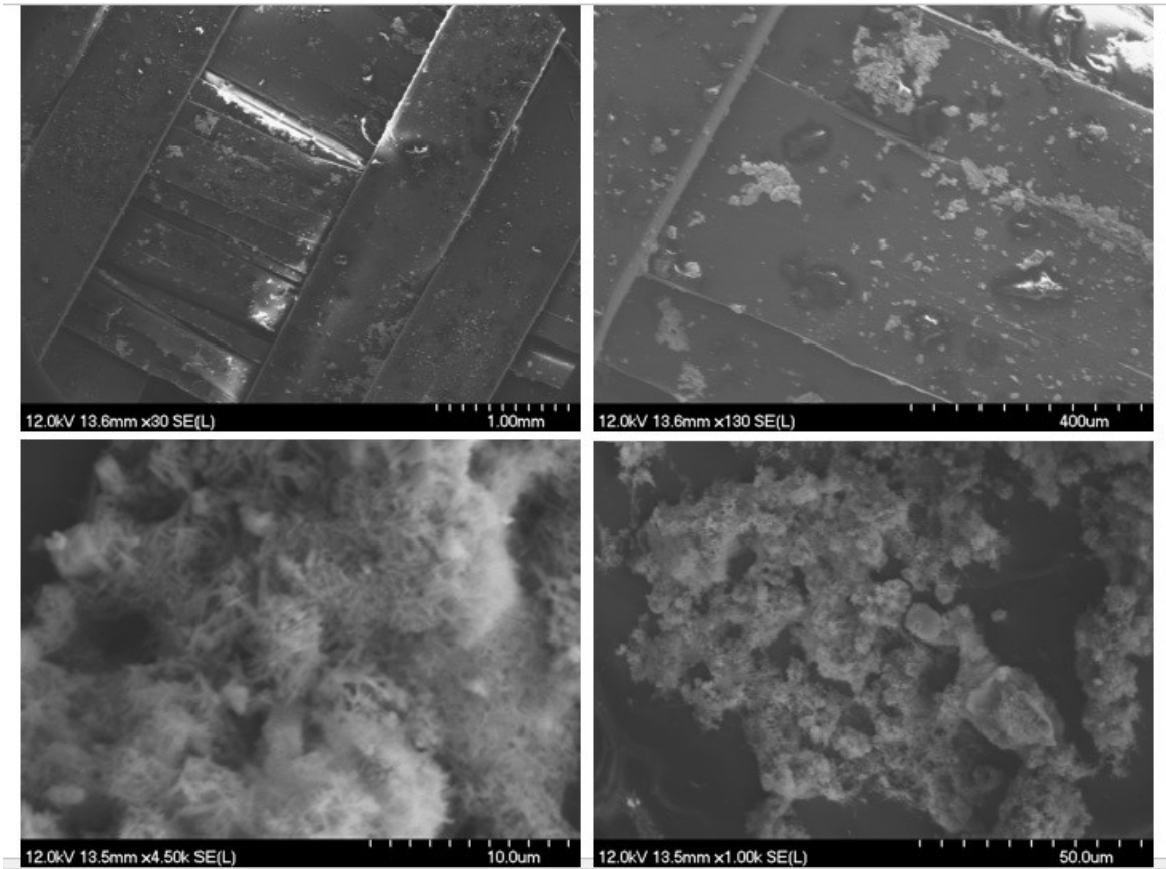
Figure A.10   ZP Analysis of FBWW

Results

		Mean (mV)	Area (%)	St Dev (mV)
Zeta Potential (mV): 33.4	Peak 1:	54.7	100.0	5.19
Zeta Deviation (mV): 79.2	Peak 2:	0.00	0.0	0.00
Conductivity (mS/cm): 0.161	Peak 3:	0.00	0.0	0.00
Result quality : Good				

Zeta Potential Distribution

Record 46: FBWW Avg
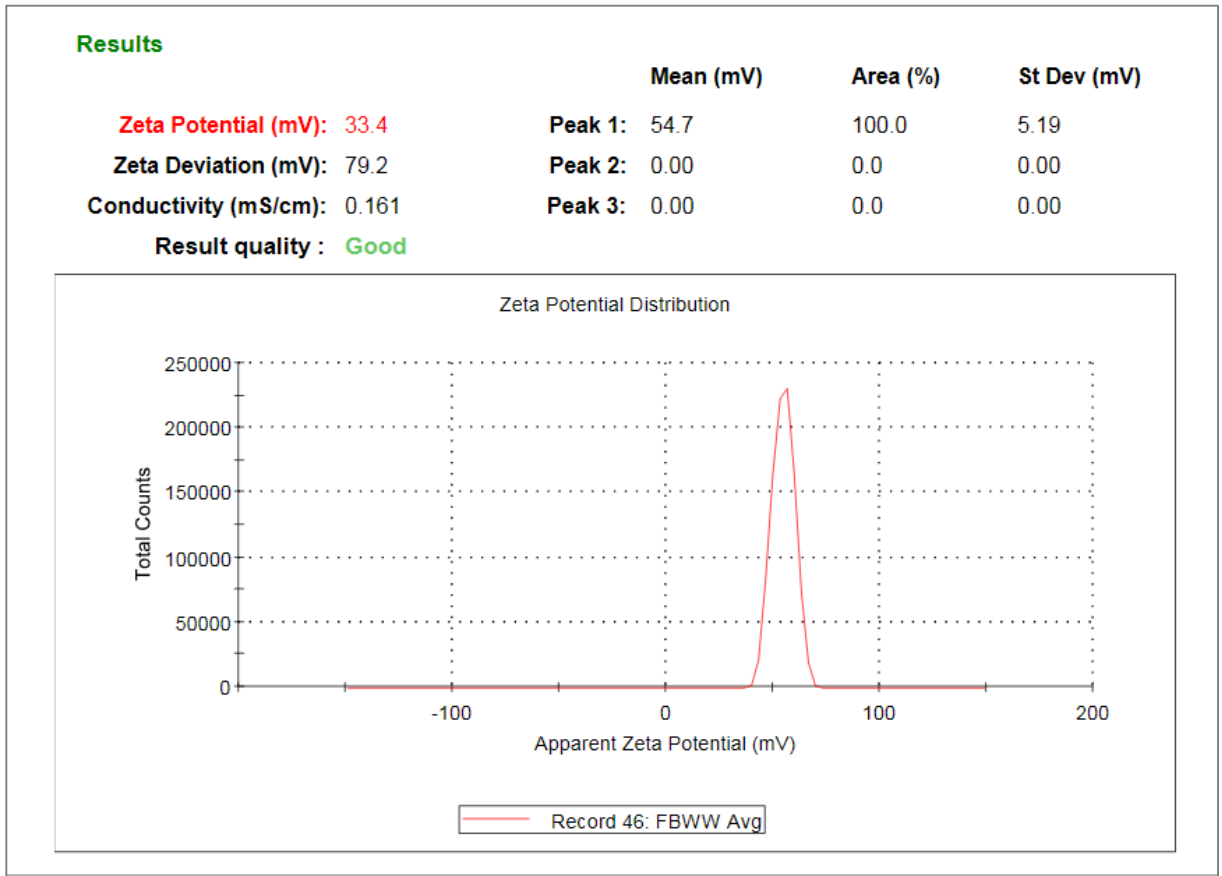
Figure A.11   ZP Analysis of CaO and Fe₃O₄ (1 gm) Adsorbent

Zeta Potential Distribution — Record 43: (CaO+FeO) Avg (1gm)

	Mean (mV)	Area (%)	St Dev (mV)
Results			
Zeta Potential (mV): -7.90	Peak 1: -7.92	100.0	3.79
Zeta Deviation (mV): 3.56	Peak 2: 0.00	0.0	0.00
Conductivity (mS/cm): 2.08	Peak 3: 0.00	0.0	0.00
Result quality : Good			
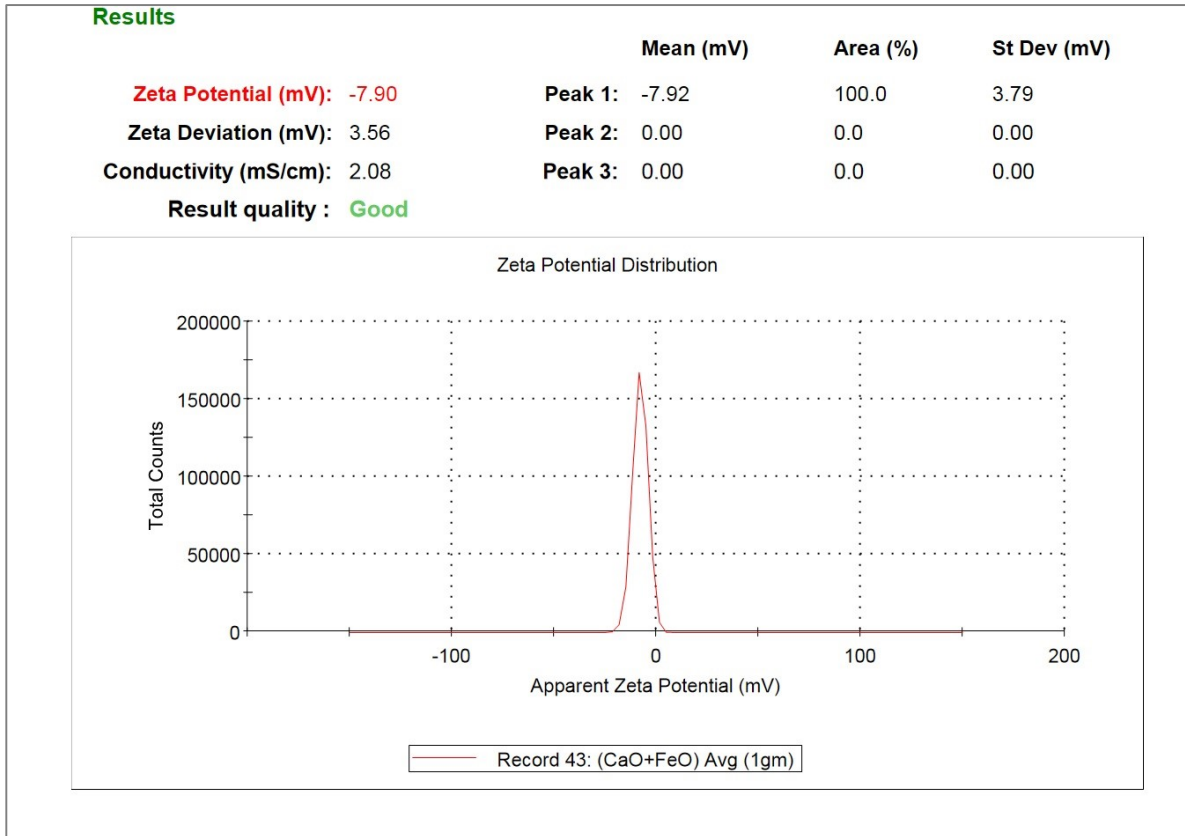
Figure A.12   ZP Analysis of CaO and Fe₃O₄ (2.5 gm) Adsorbent
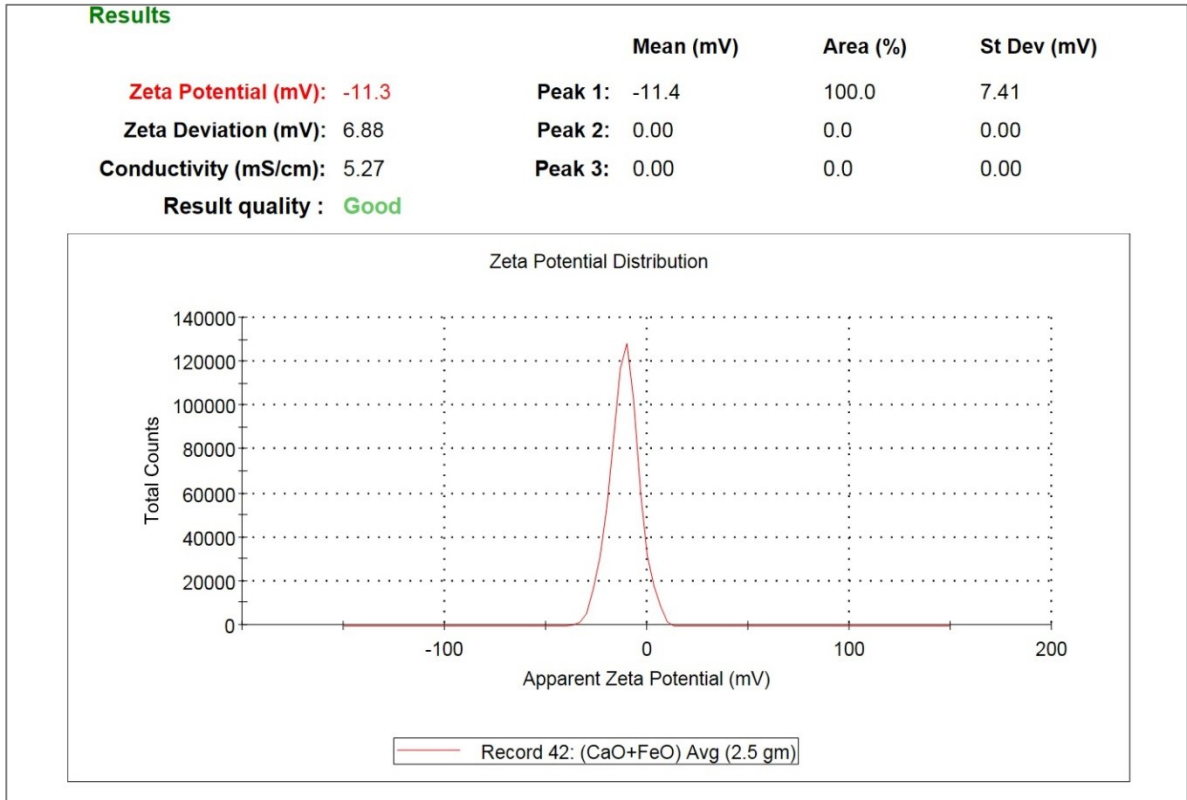
Figure A.13   ZP Analysis of MgO (0.1 gm) Adsorbent
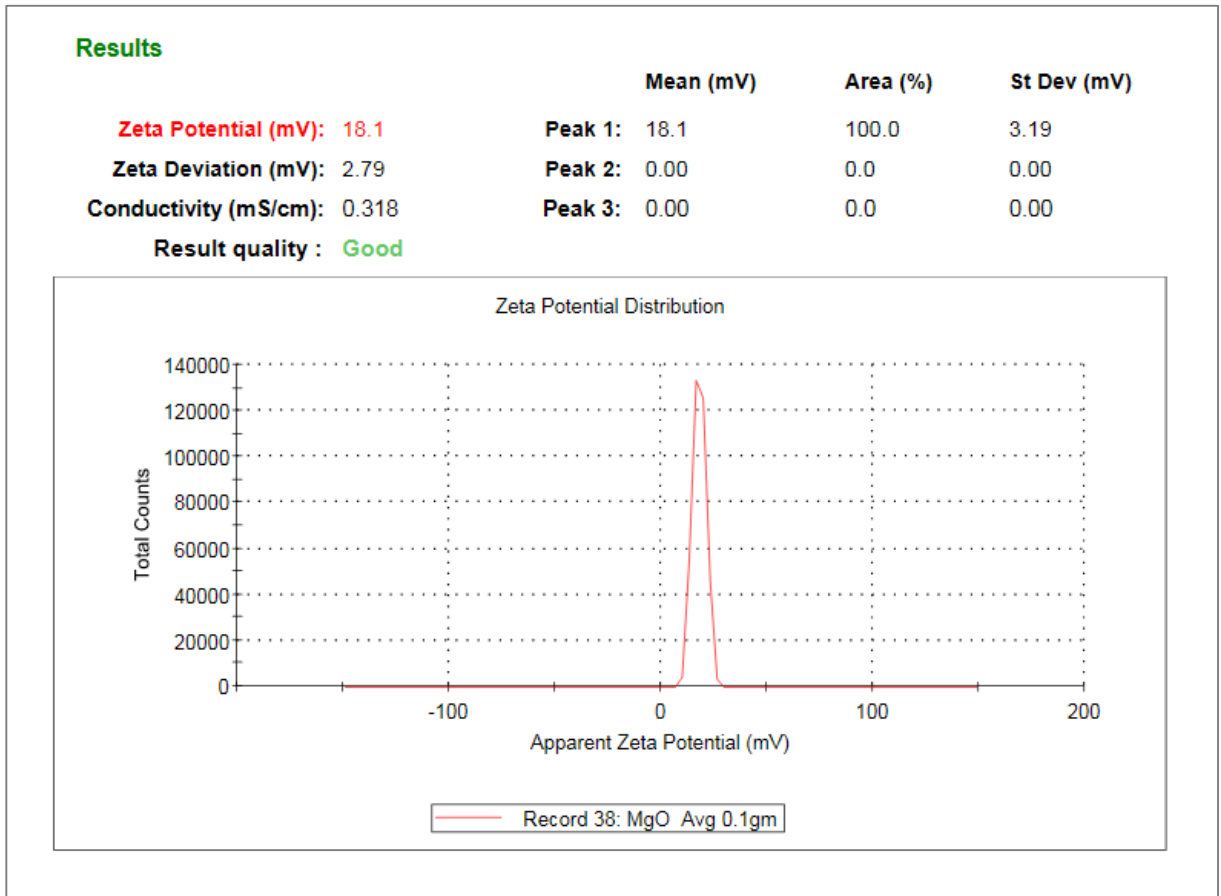
Figure A.14   ZP Analysis of MgO (1 gm) Adsorbent

Results		Mean (mV)	Area (%)	St Dev (mV)
Zeta Potential (mV): -11.4	Peak 1:	-6.46	59.6	2.19
Zeta Deviation (mV): 5.74	Peak 2:	-18.7	40.4	3.26
Conductivity (mS/cm): 1.11	Peak 3:	0.00	0.0	0.00
Result quality : Good				

Zeta Potential Distribution

Record 39: MgO Avg (1gm)
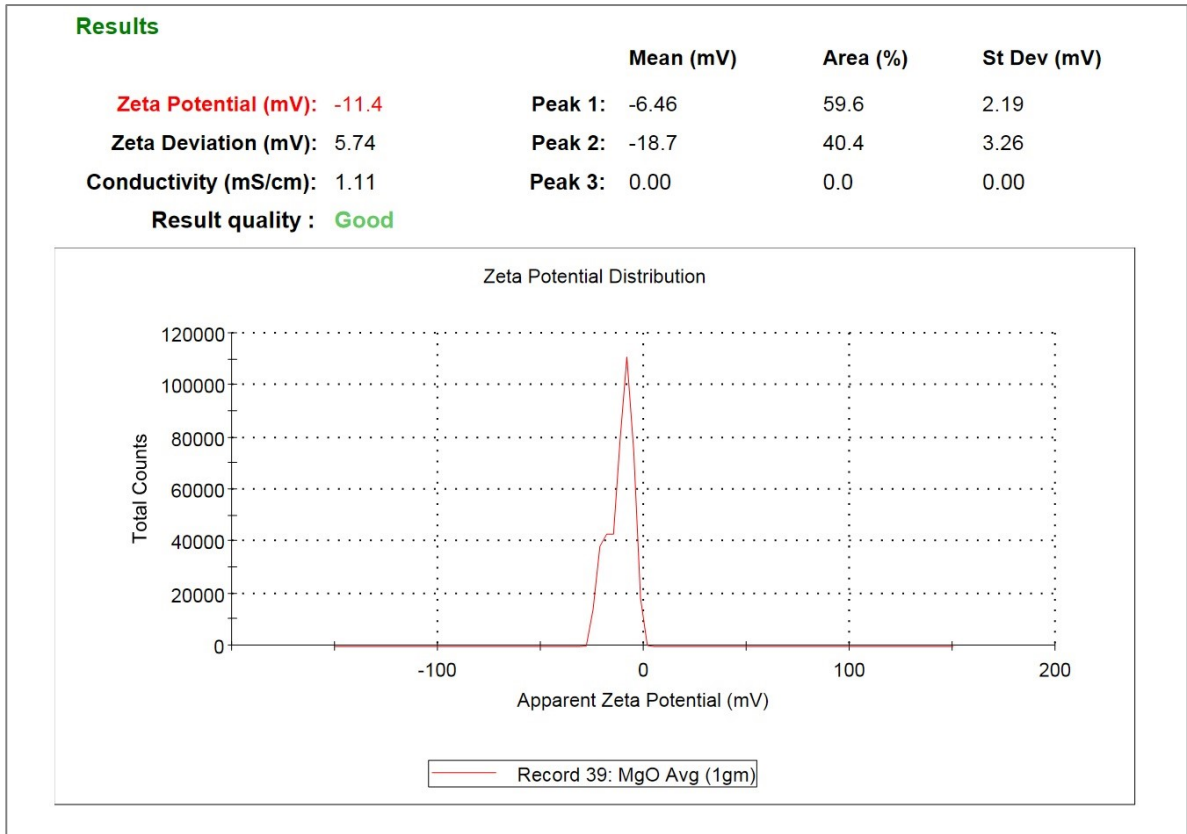
Figure A.15   ZP Analysis of MgO (2.5 gm) Adsorbent

Results

	Mean (mV)	Area (%)	St Dev (mV)
Zeta Potential (mV): -20.7	**Peak 1:** -20.7	100.0	3.84
Zeta Deviation (mV): 3.49	**Peak 2:** 0.00	0.0	0.00
Conductivity (mS/cm): 1.36	**Peak 3:** 0.00	0.0	0.00
Result quality : Good			

Zeta Potential Distribution

Record 40: MgO Avg (2.5 gm)
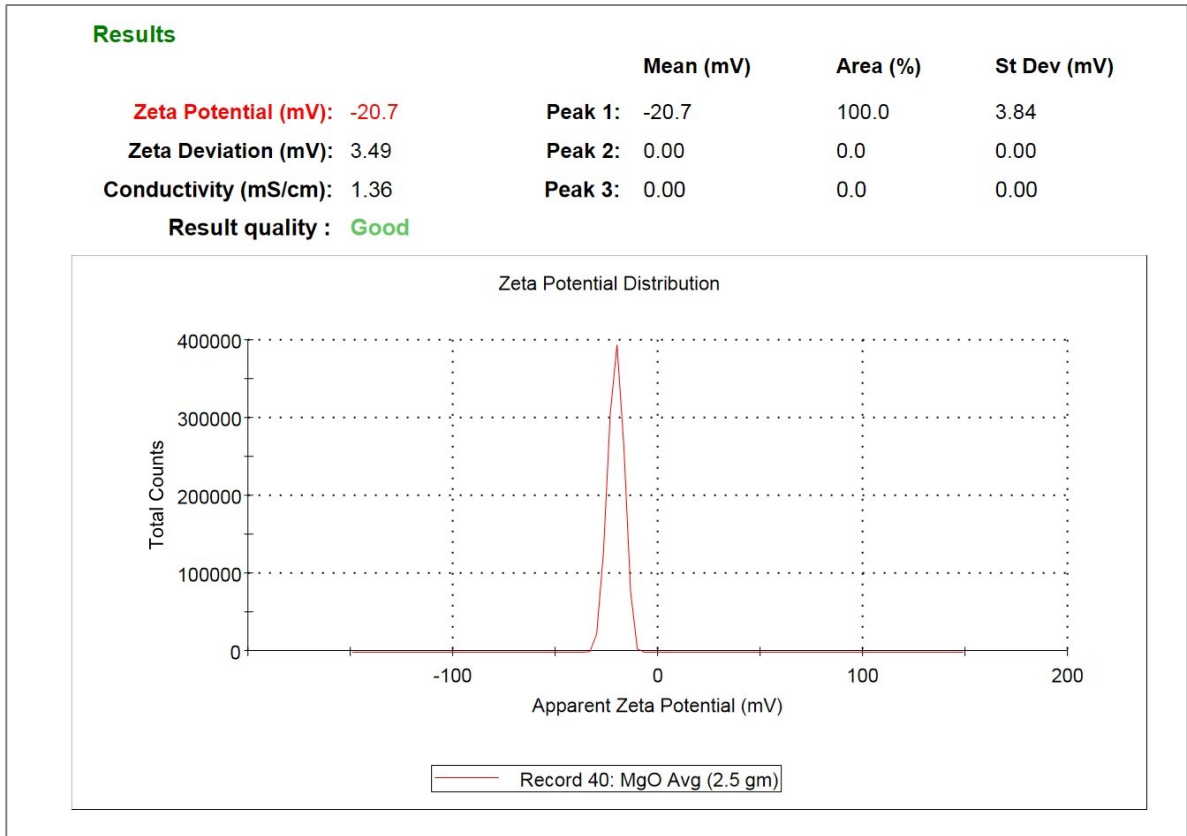
Figure A.16   ZP Analysis of MgO (5 gm) Adsorbent

Results			Mean (mV)	Area (%)	St Dev (mV)
Zeta Potential (mV):	-20.9	Peak 1:	-21.0	100.0	3.23
Zeta Deviation (mV):	2.76	Peak 2:	0.00	0.0	0.00
Conductivity (mS/cm):	0.896	Peak 3:	0.00	0.0	0.00
Result quality :	Good				

Zeta Potential Distribution

Record 41: MgO Avg (5 gm)
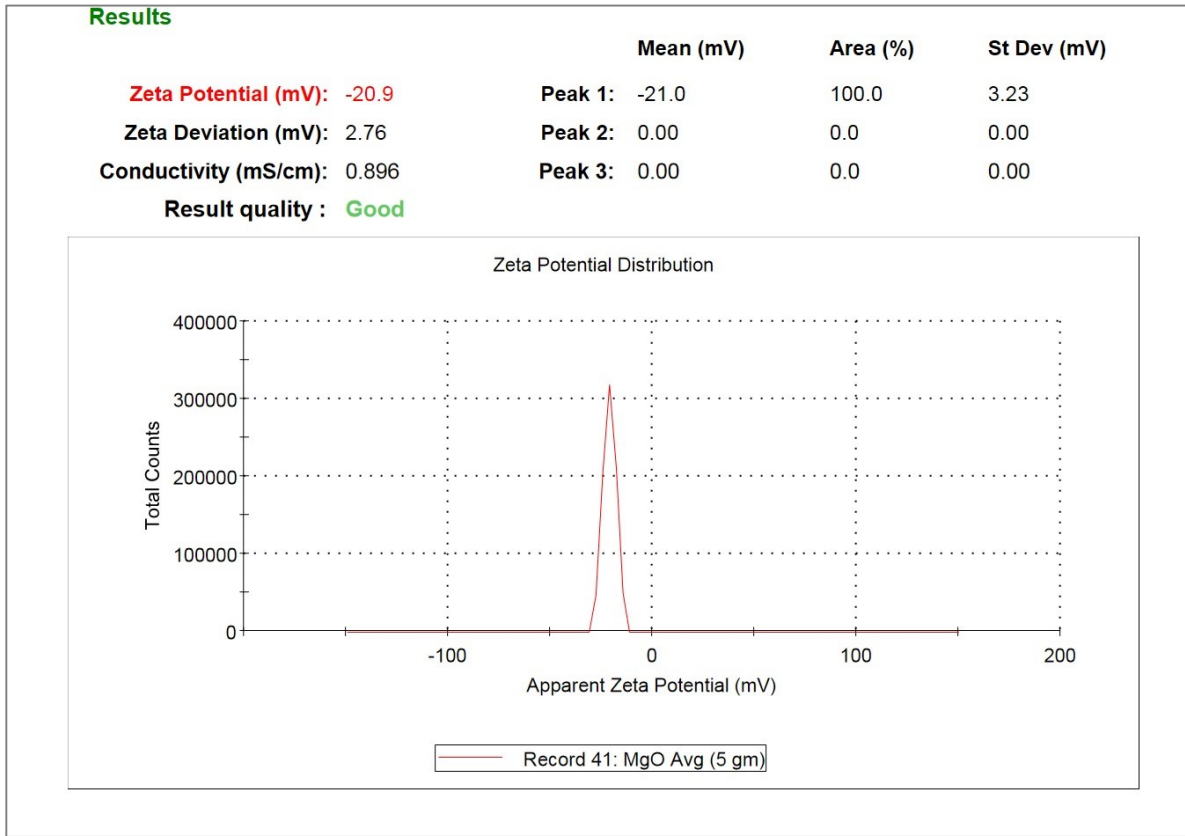
Figure A.17   ZP Analysis of Fe₃O₄ (0.1 gm) Adsorbent

Results

		Mean (mV)	Area (%)	St Dev (mV)
Zeta Potential (mV): 41.2	Peak 1:	63.4	100.0	4.60
Zeta Deviation (mV): 80.6	Peak 2:	0.00	0.0	0.00
Conductivity (mS/cm): 0.163	Peak 3:	0.00	0.0	0.00
Result quality : Good				

Zeta Potential Distribution

Record 50: Ferric ion Avg 0.1 gm/L
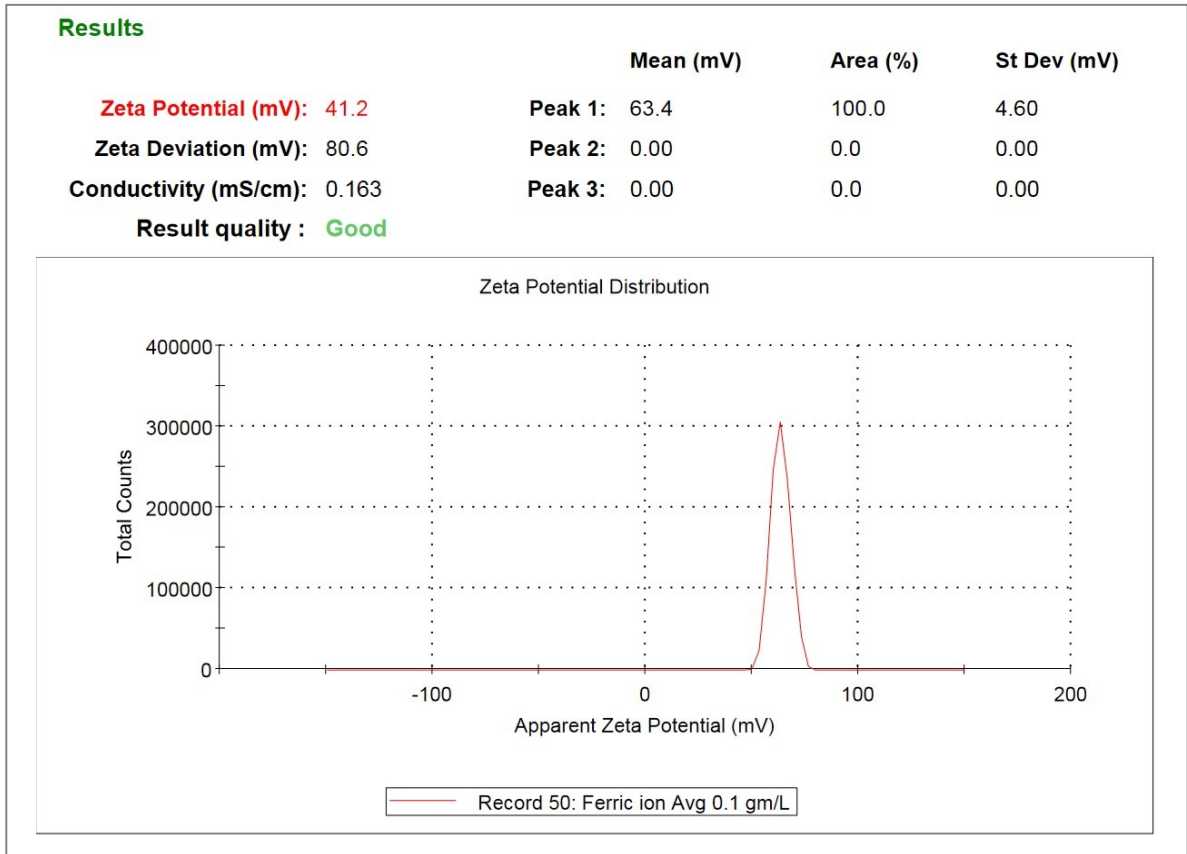
Figure A.18   ZP Analysis of Fe₃O₄ (1 gm) Adsorbent
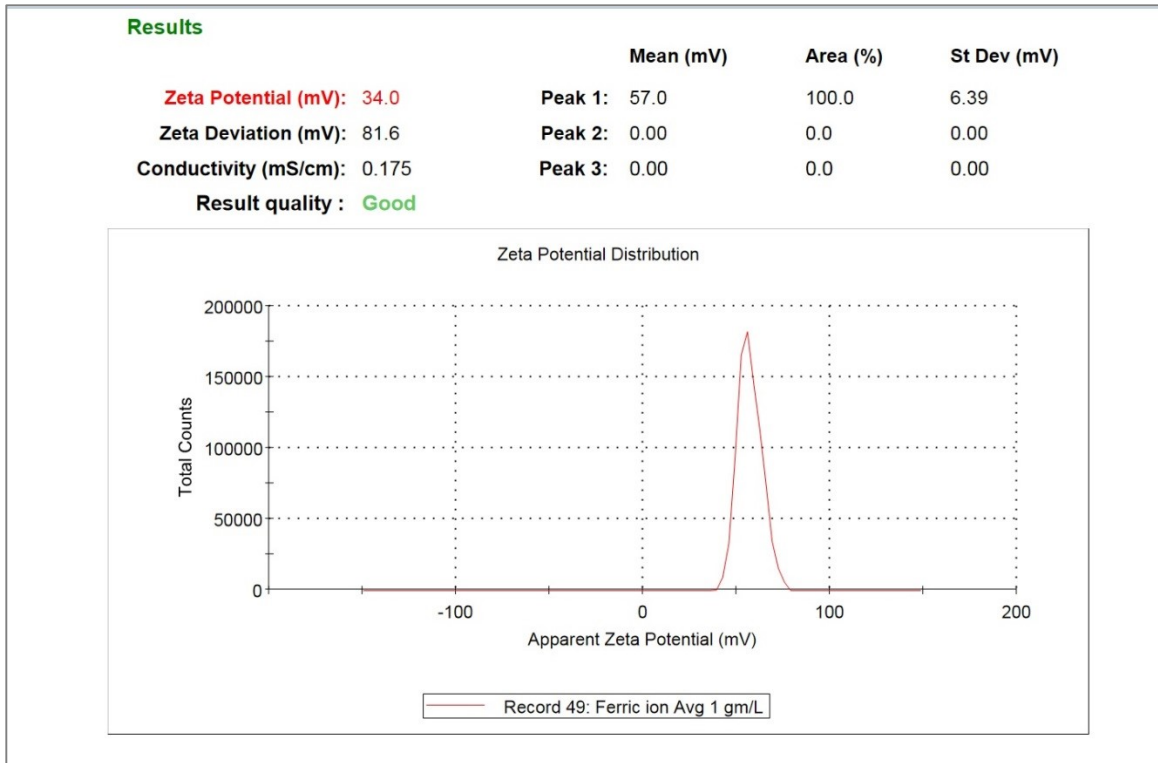
Figure A.19   ZP Analysis of Fe$_3$O$_4$ (2.5 gm) Adsorbent

		Mean (mV)	Area (%)	St Dev (mV)
Results				
Zeta Potential (mV): 38.0	**Peak 1:**	60.5	100.0	5.35
Zeta Deviation (mV): 80.7	**Peak 2:**	0.00	0.0	0.00
Conductivity (mS/cm): 0.182	**Peak 3:**	0.00	0.0	0.00
Result quality : Good				

Zeta Potential Distribution

Record 48: Ferric ion Avg 2.5 gm/L
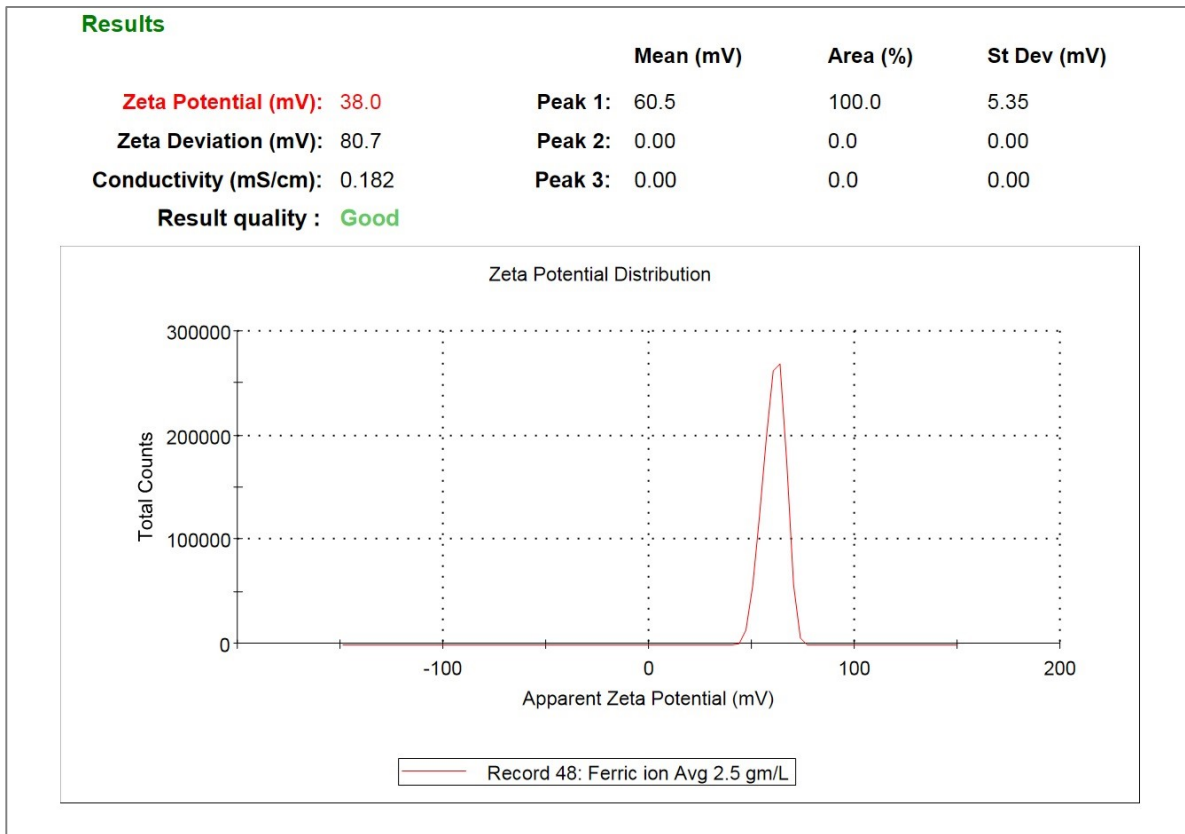
Figure A.20   ZP Analysis of Fe₃O₄ (5 gm) Adsorbent

Results		Mean (mV)	Area (%)	St Dev (mV)
Zeta Potential (mV): 40.5	**Peak 1:** 61.9		100.0	5.19
Zeta Deviation (mV): 80.1	**Peak 2:** 0.00		0.0	0.00
Conductivity (mS/cm): 0.262	**Peak 3:** 0.00		0.0	0.00
Result quality : Good				

Zeta Potential Distribution

Record 47: Ferric ion Avg 5 gm/L
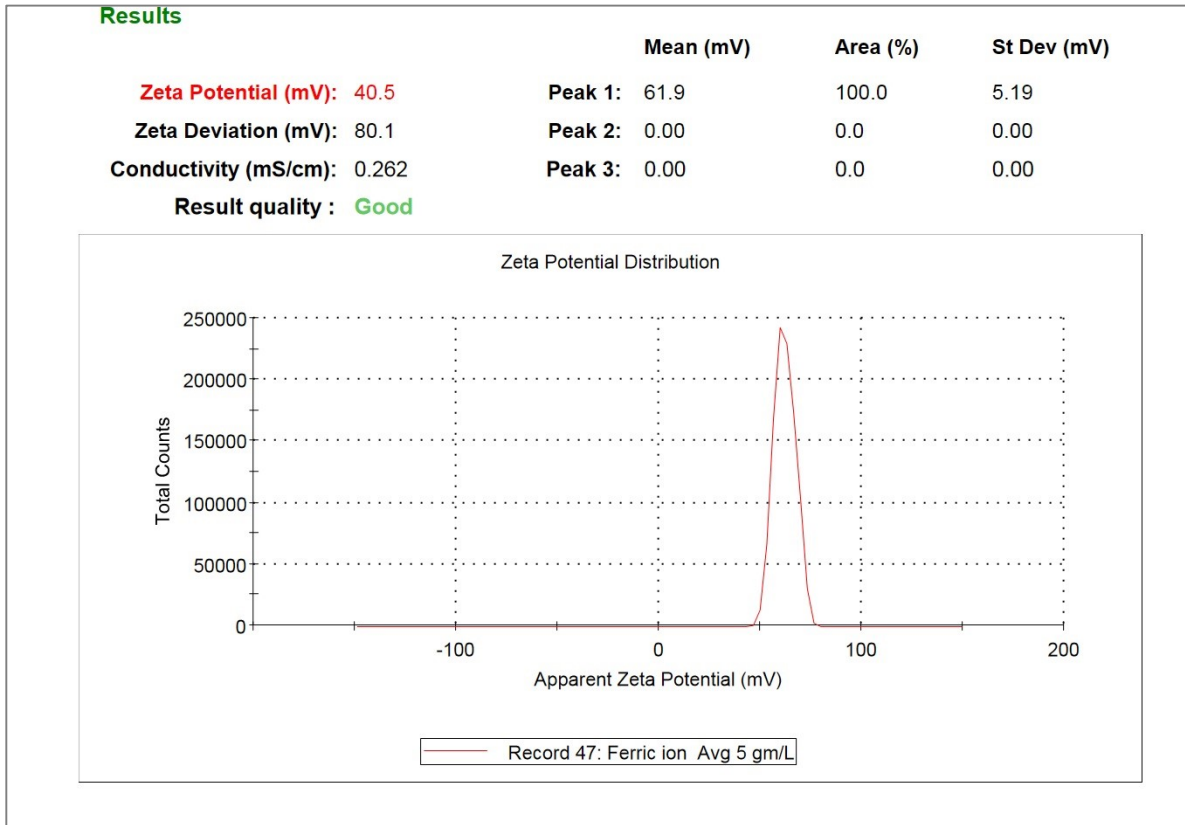
Figure A.21   ZP Analysis of CaO (0.1 gm) Adsorbent

Results

		Mean (mV)	Area (%)	St Dev (mV)
Zeta Potential (mV): -9.54	**Peak 1:**	-9.63	100.0	4.12
Zeta Deviation (mV): 3.94	**Peak 2:**	0.00	0.0	0.00
Conductivity (mS/cm): 0.608	**Peak 3:**	0.00	0.0	0.00
Result quality : Good				

Zeta Potential Distribution

Record 52: CaO Avg 0.1gm
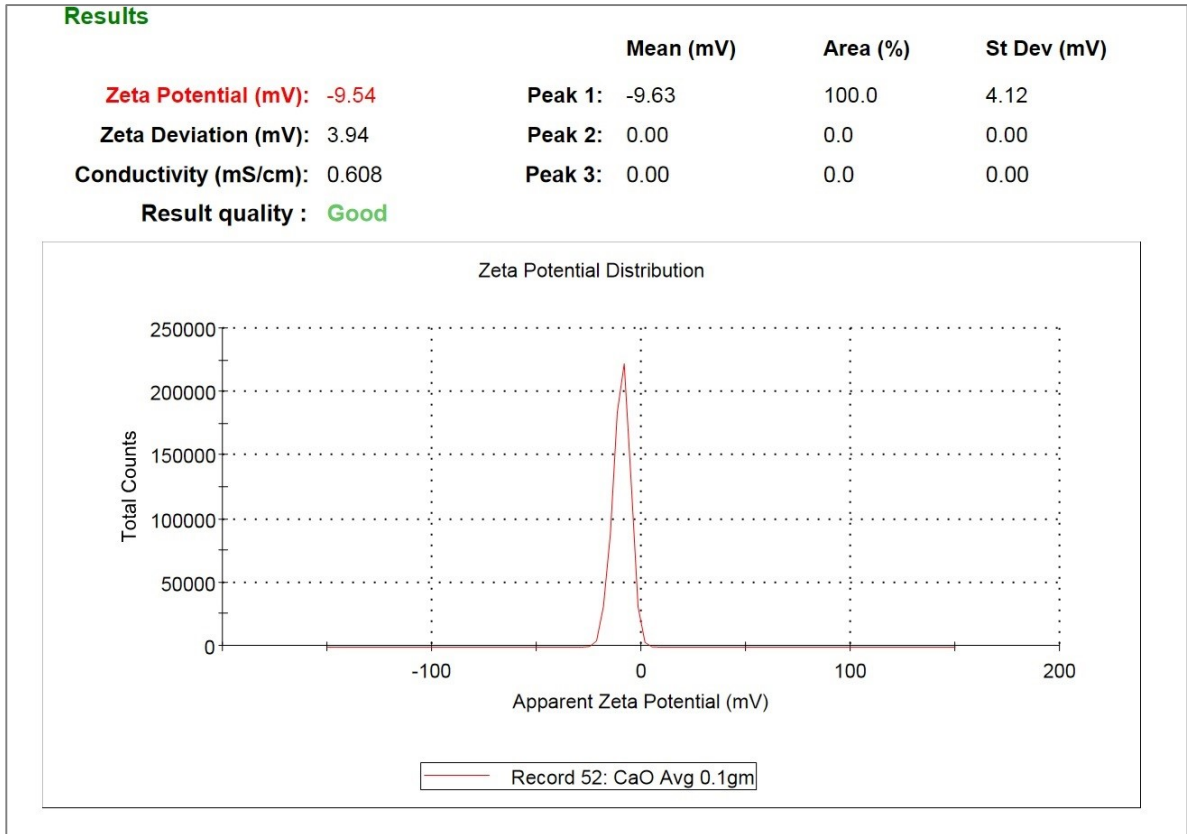
Figure A.22   ZP Analysis of CaO (1 gm) Adsorbent
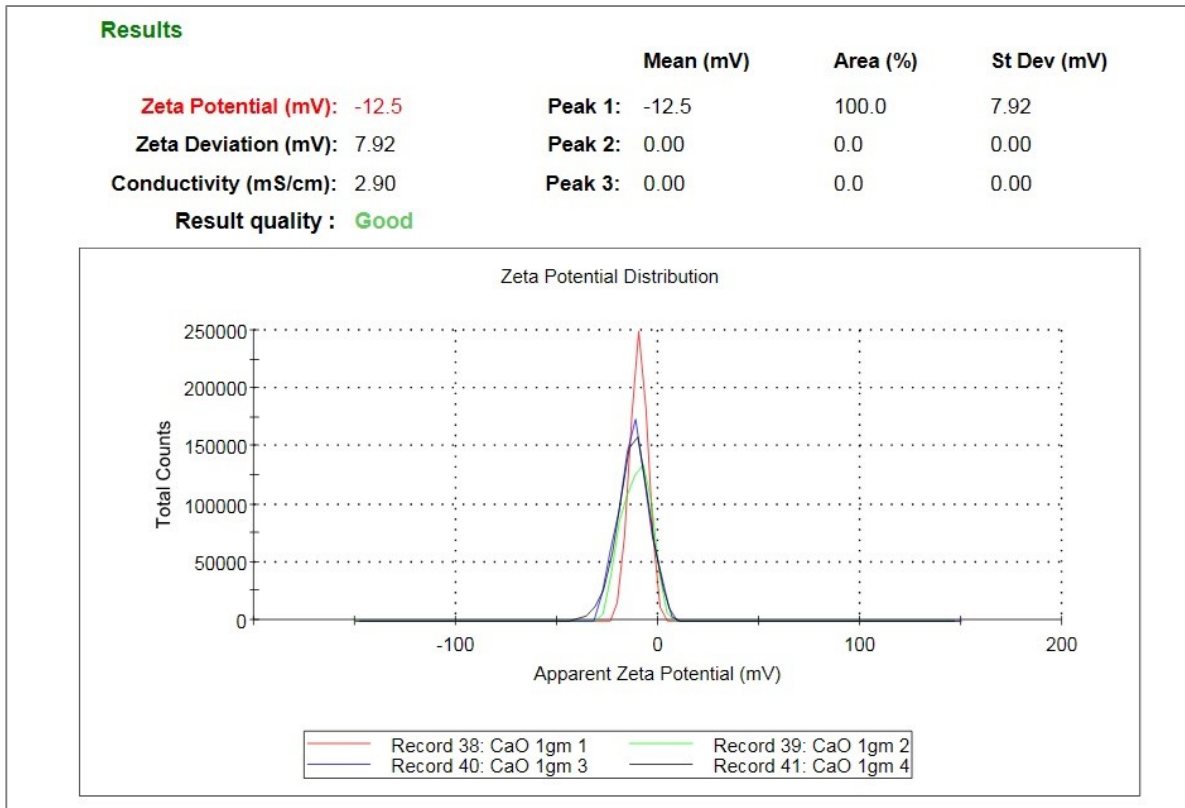
Figure A.23   ZP Analysis of CaO (2.5 gm) Adsorbent

Results		Mean (mV)	Area (%)	St Dev (mV)
Zeta Potential (mV): -9.78	Peak 1:	-9.87	100.0	7.69
Zeta Deviation (mV): 7.13	Peak 2:	0.00	0.0	0.00
Conductivity (mS/cm): 4.91	Peak 3:	0.00	0.0	0.00
Result quality : Good				

Zeta Potential Distribution

Record 53: CaO Avg 2.5 gm
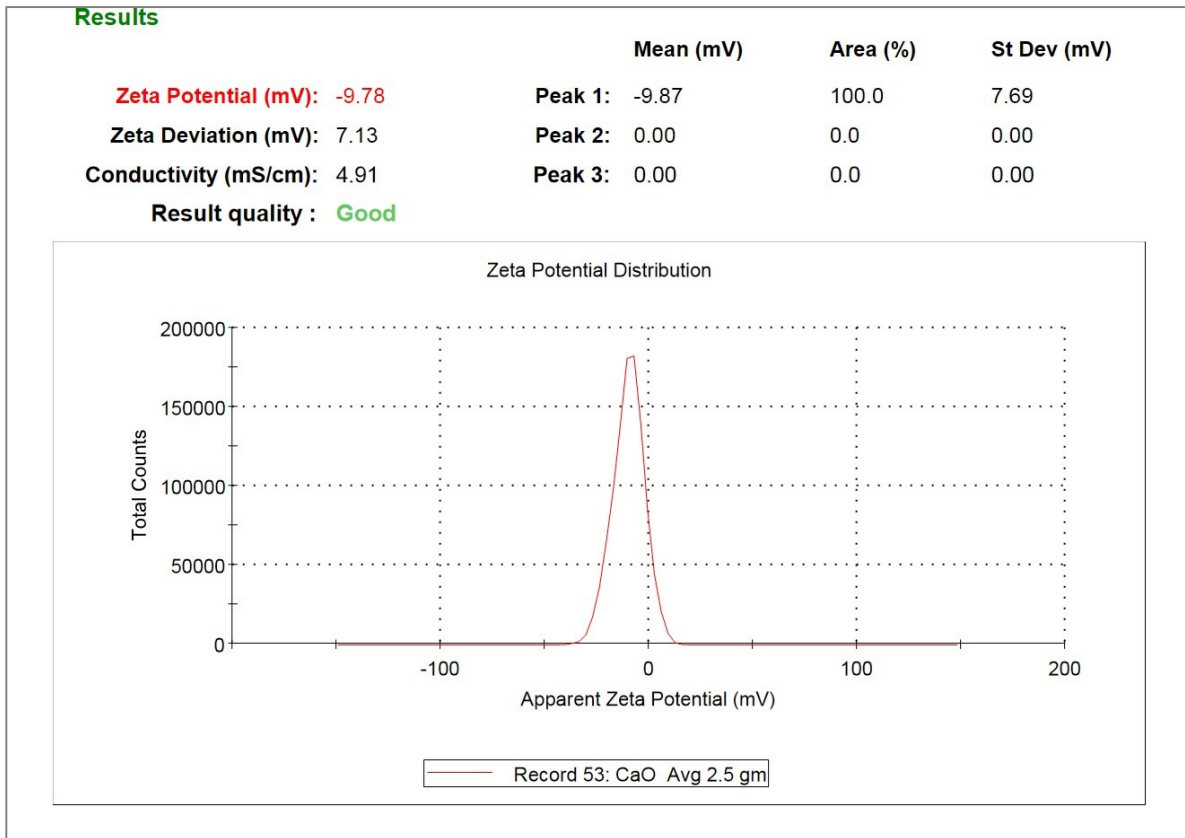
Figure A.24   ZP Analysis of CaO (5 gm) Adsorbent

Results

	Mean (mV)	Area (%)	St Dev (mV)
Zeta Potential (mV): -8.10	**Peak 1:** -8.10	100.0	8.92
Zeta Deviation (mV): 8.57	**Peak 2:** -26.3	12.7	2.98
Conductivity (mS/cm): 5.17	**Peak 3:** 0.00	0.0	0.00
Result quality : Good			

Zeta Potential Distribution

Record 51: CaO Avg 5gm

Figure A.25   Size Analysis of FBWW

Figure A.26   Size Analysis of CaO & Fe₃O₄ (1 gm) Adsorbent

Figure A.27   Size Analysis of CaO & Fe₃O₄ (2.5 gm) Adsorbent

Figure A.28   Size Analysis of CaO & Fe₃O₄ (5 gm) Adsorbent
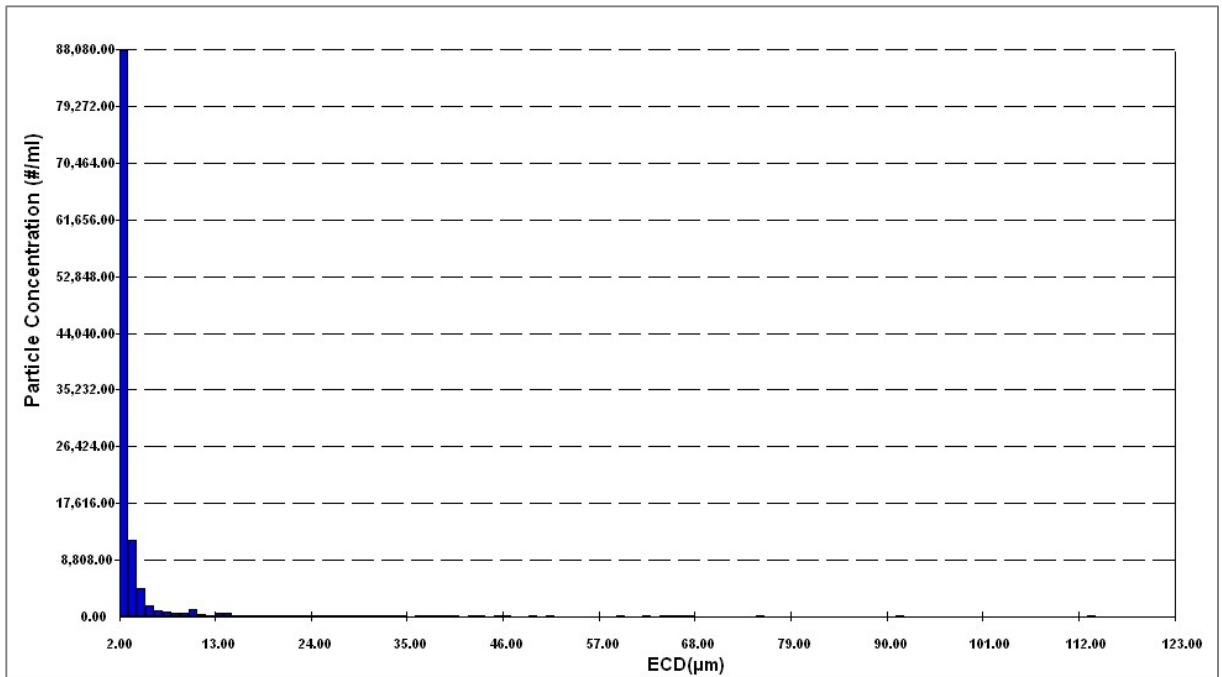
Figure A.29   Size Analysis of MgO (0.1 gm) Adsorbent
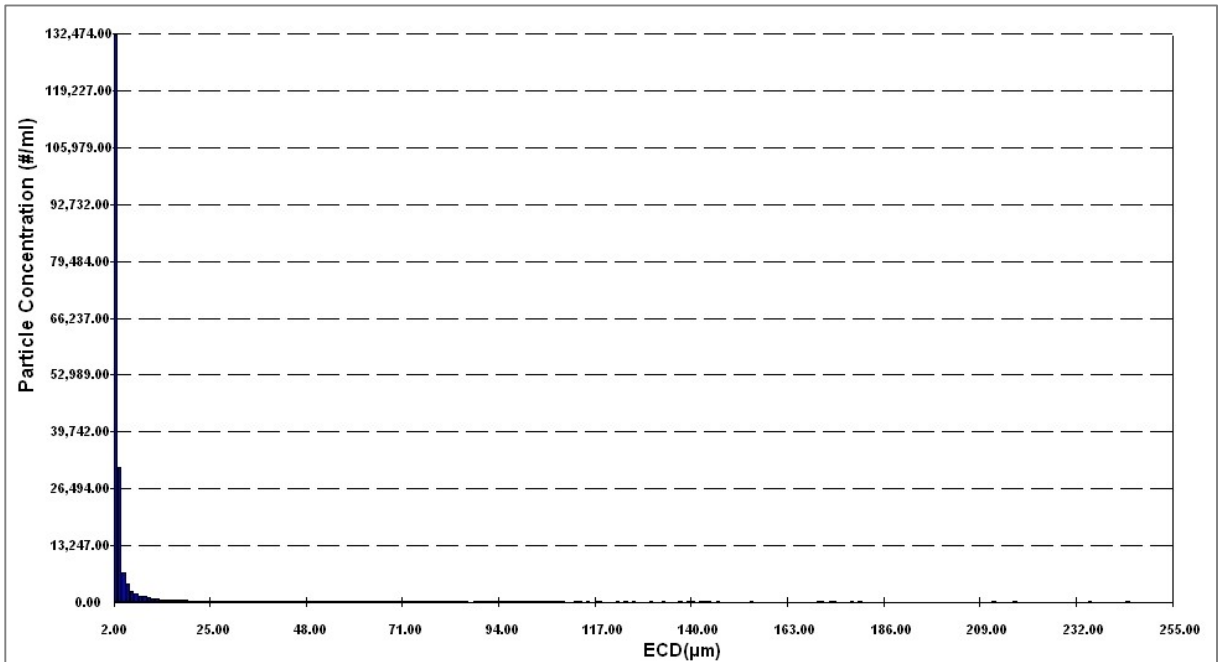
Figure A.30   Size Analysis of MgO (1 gm) Adsorbent
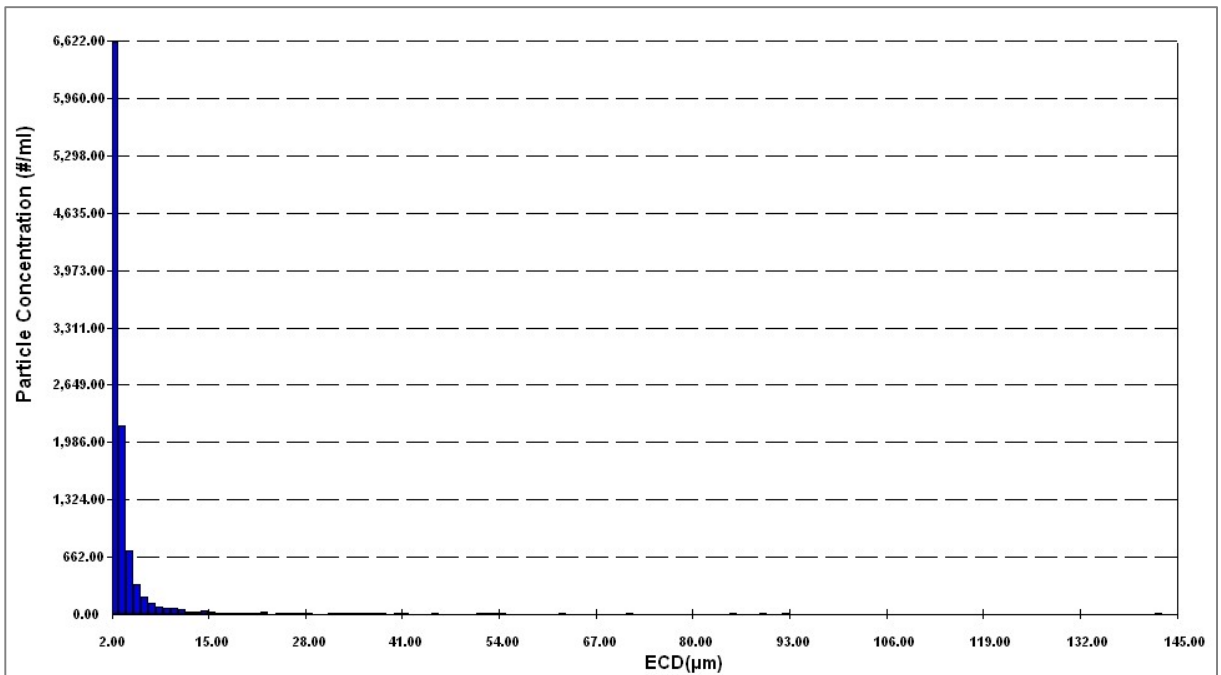
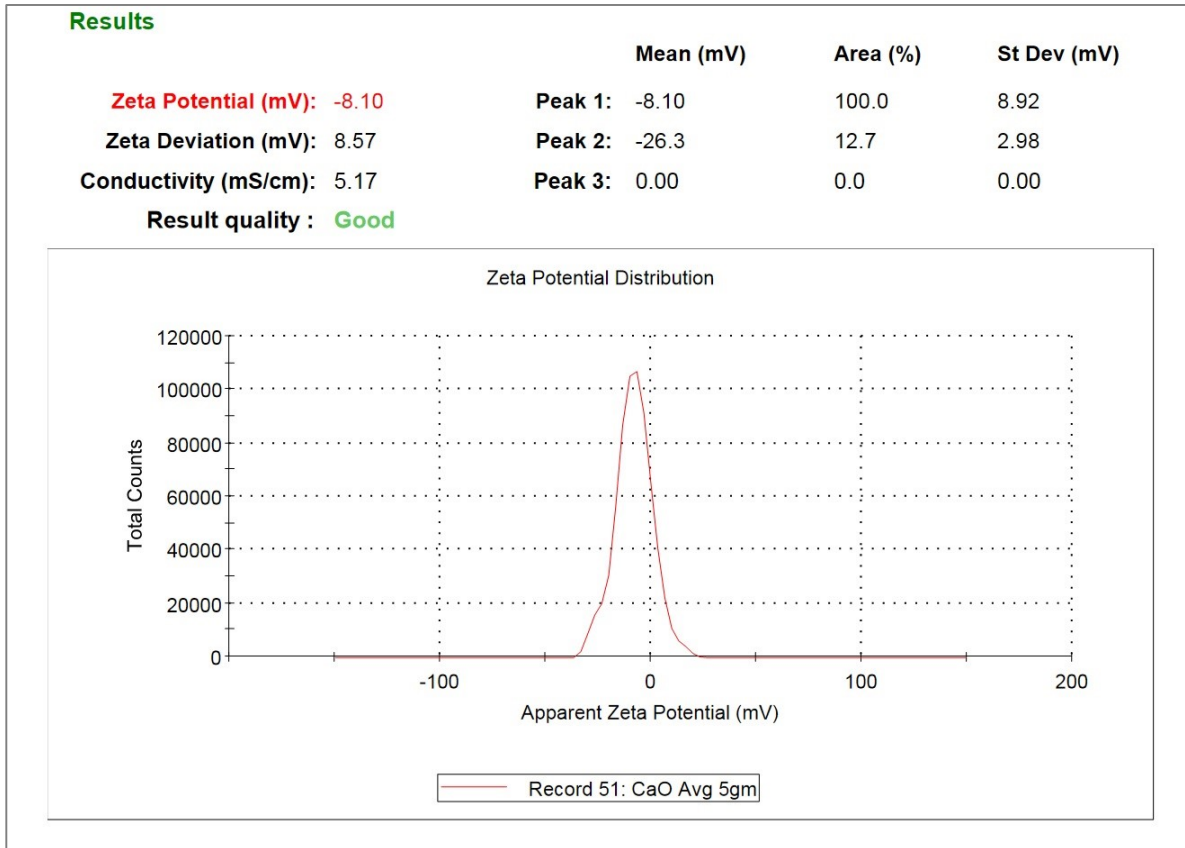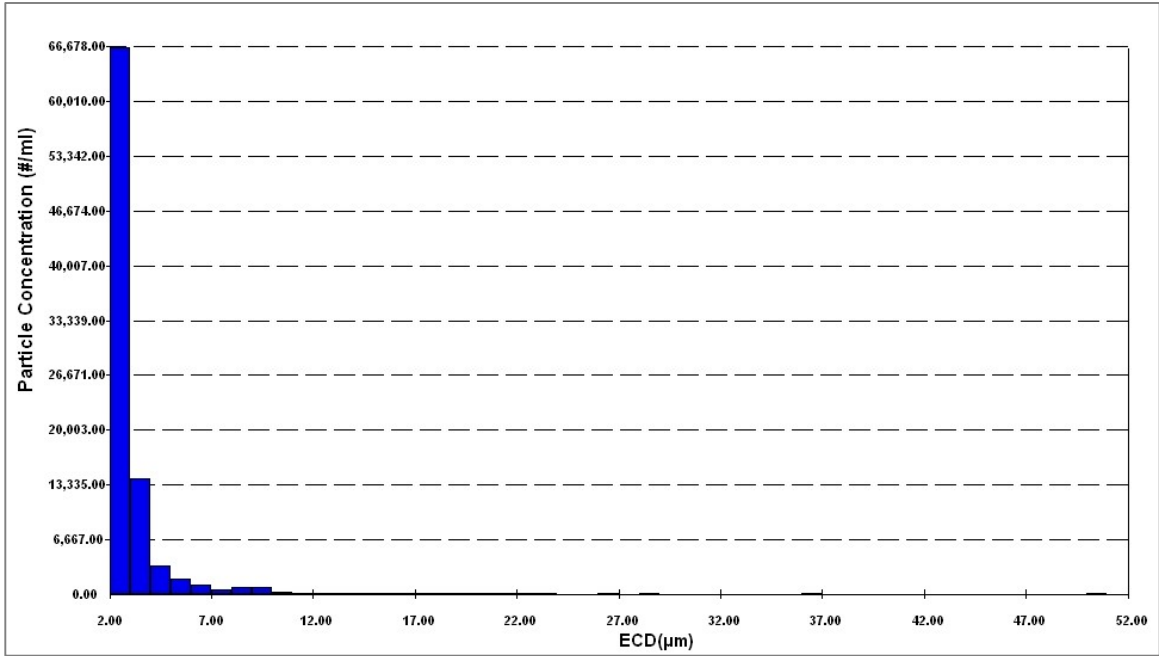**Figure A.31   Size Analysis of MgO (2.5 gm) Adsorbent**
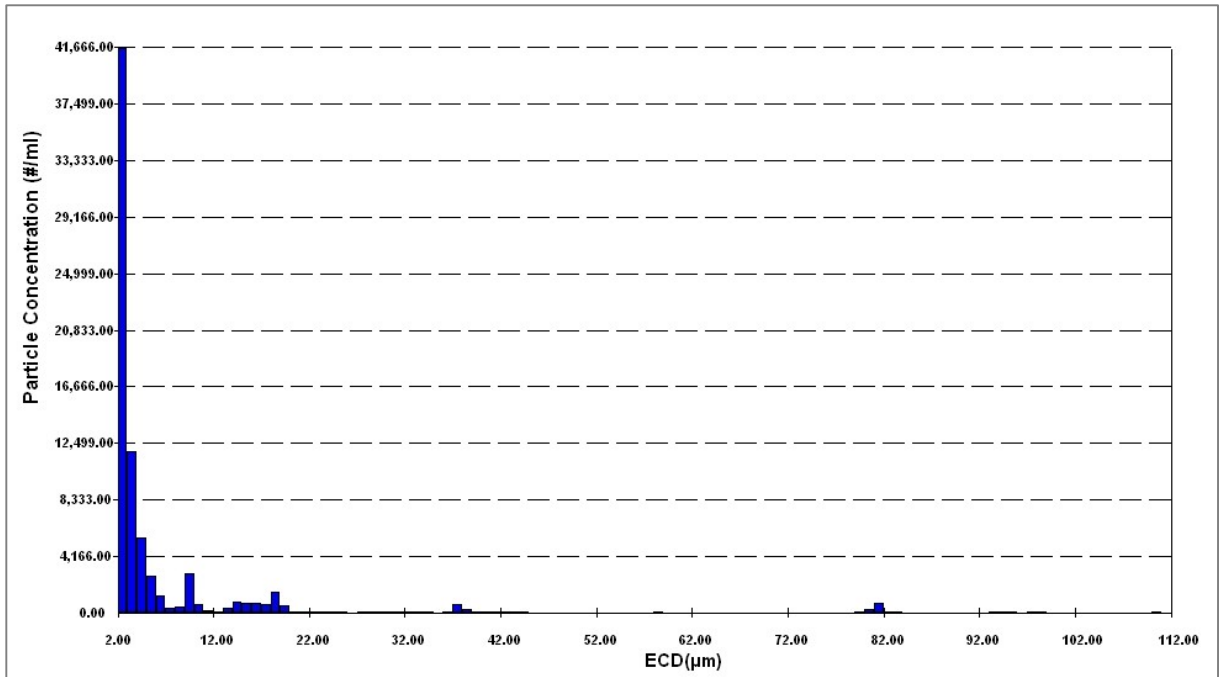
Figure A.32   Size Analysis of MgO (5 gm) Adsorbent
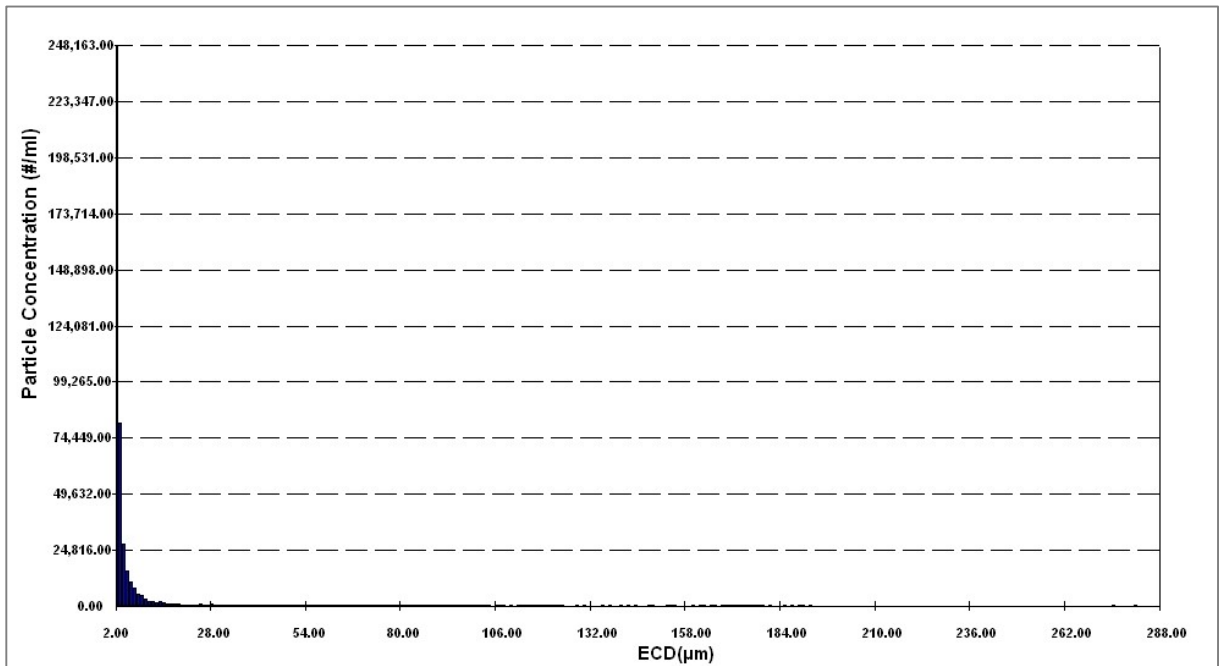
Figure A.33   Size Analysis of CaO (0.1 gm) Adsorbent

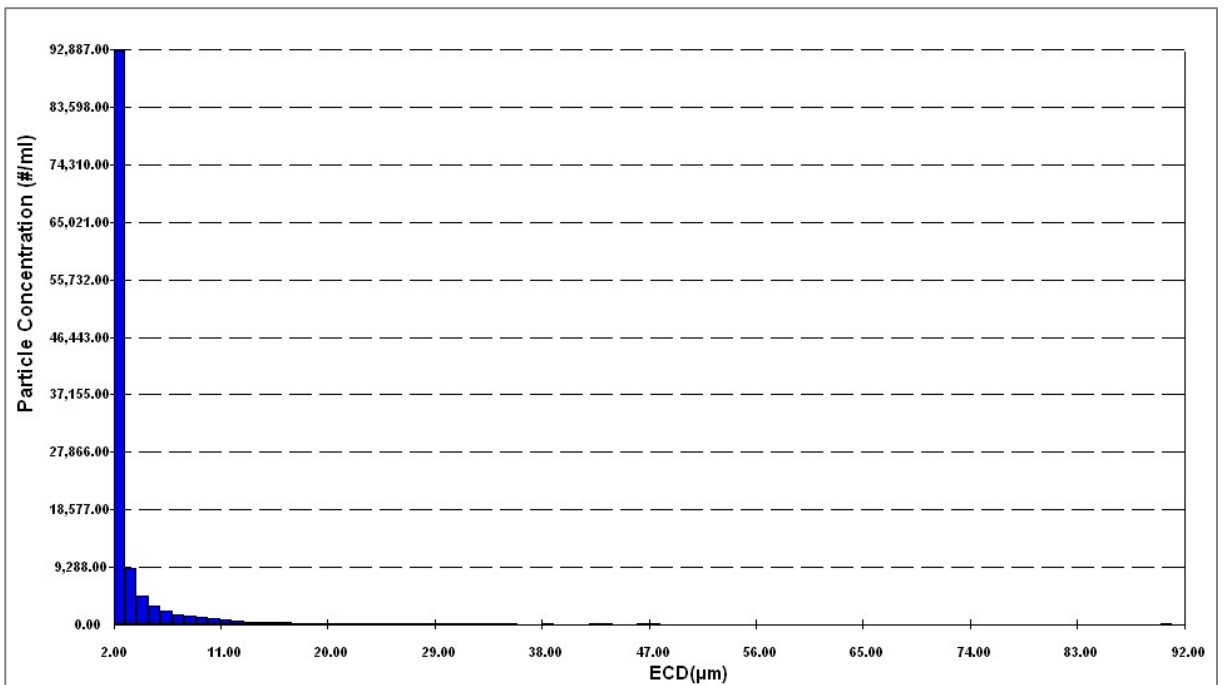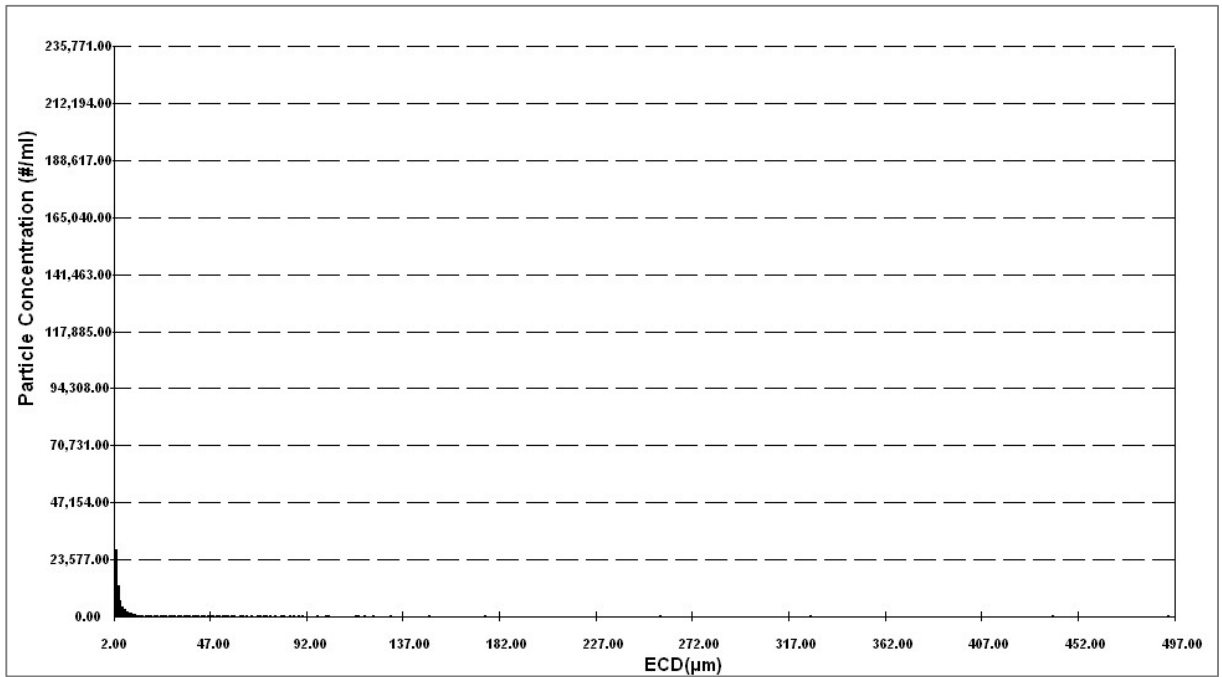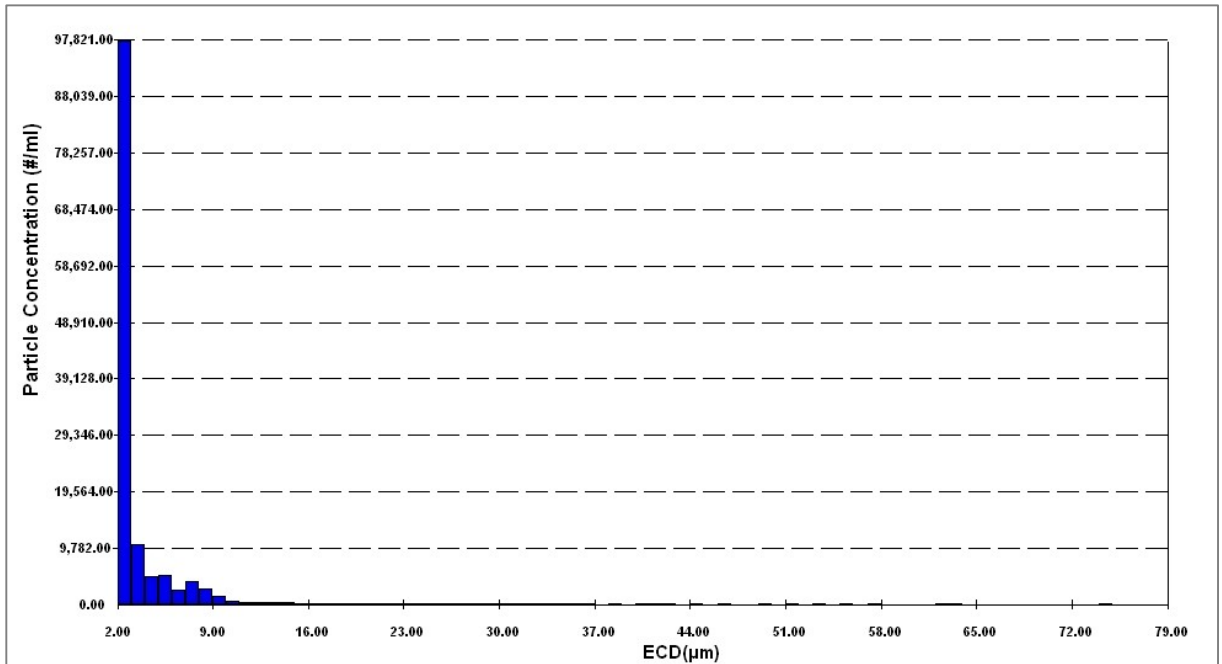**Figure A.34   Size Analysis of CaO (1 gm) Adsorbent**
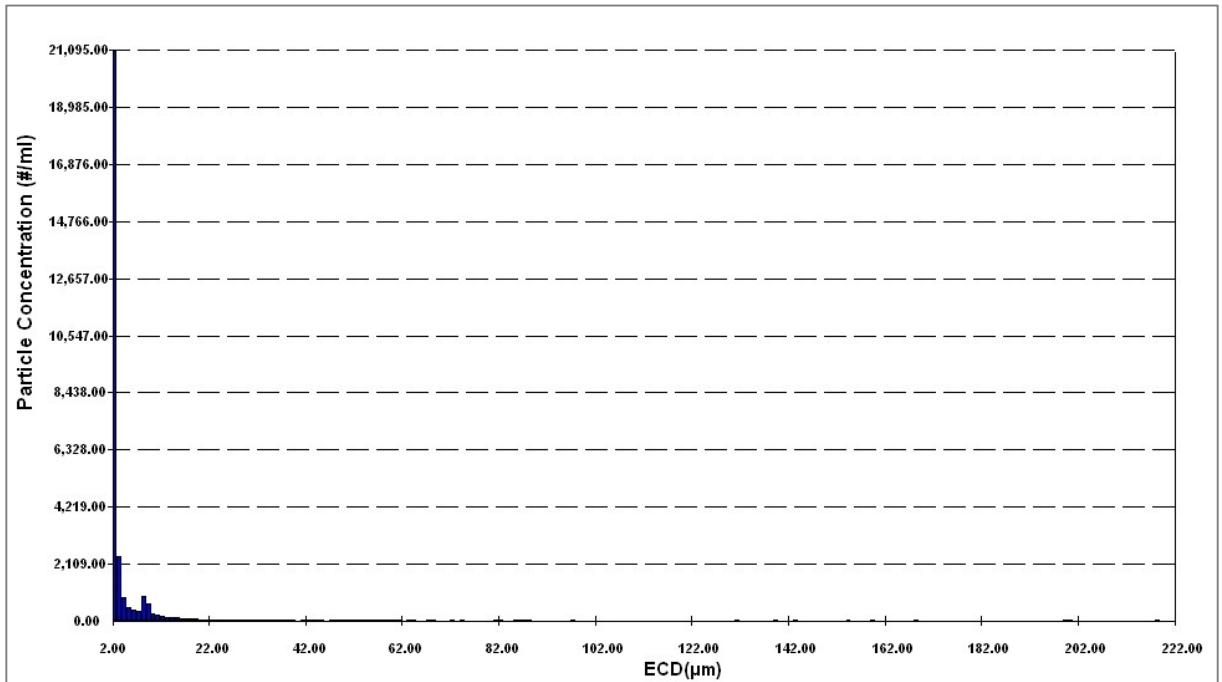
Figure A.35   Size Analysis of CaO (2.5 gm) Adsorbent
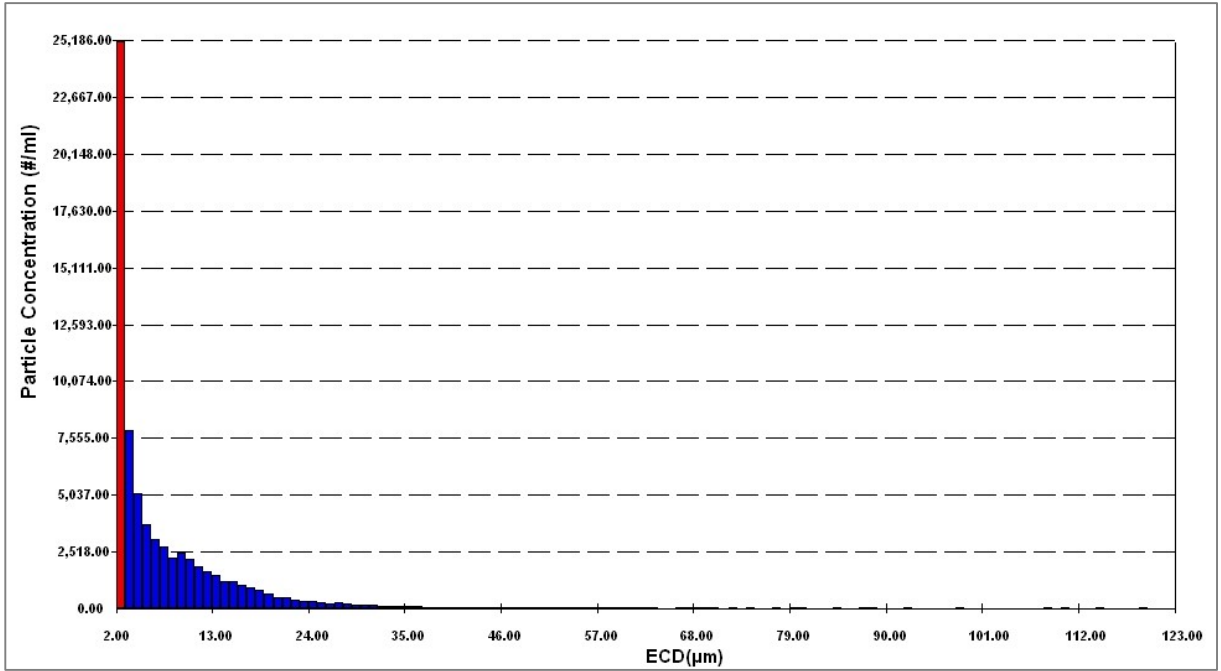
Figure A.36   Size Analysis of CaO (5 gm) Adsorbent
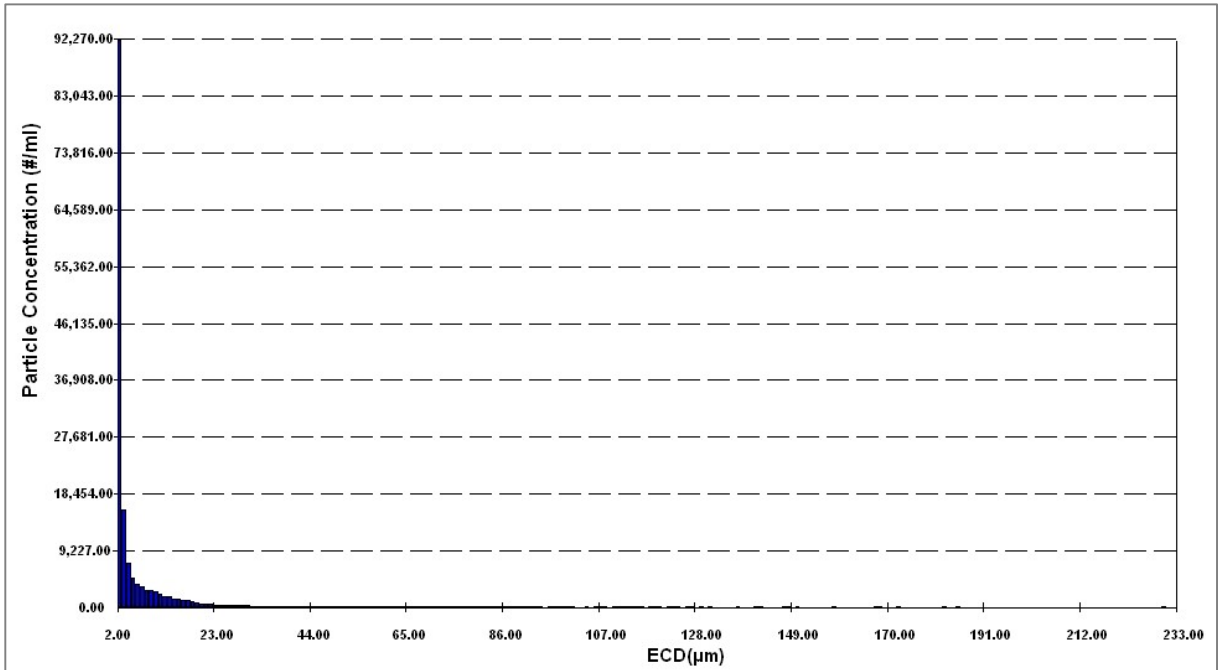
Figure A.37   Size Analysis of Fe$_3$O$_4$ (0.1 gm) Adsorbent
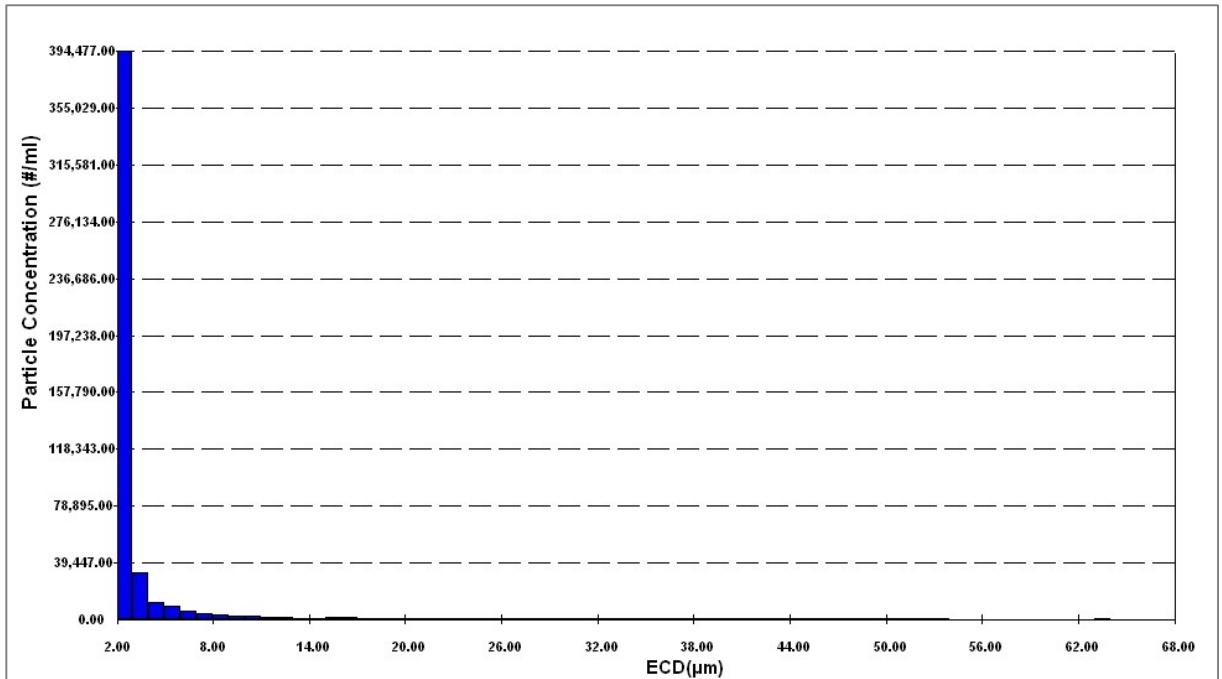
Figure A.38   Size Analysis of Fe$_3$O$_4$ (1 gm) Adsorbent
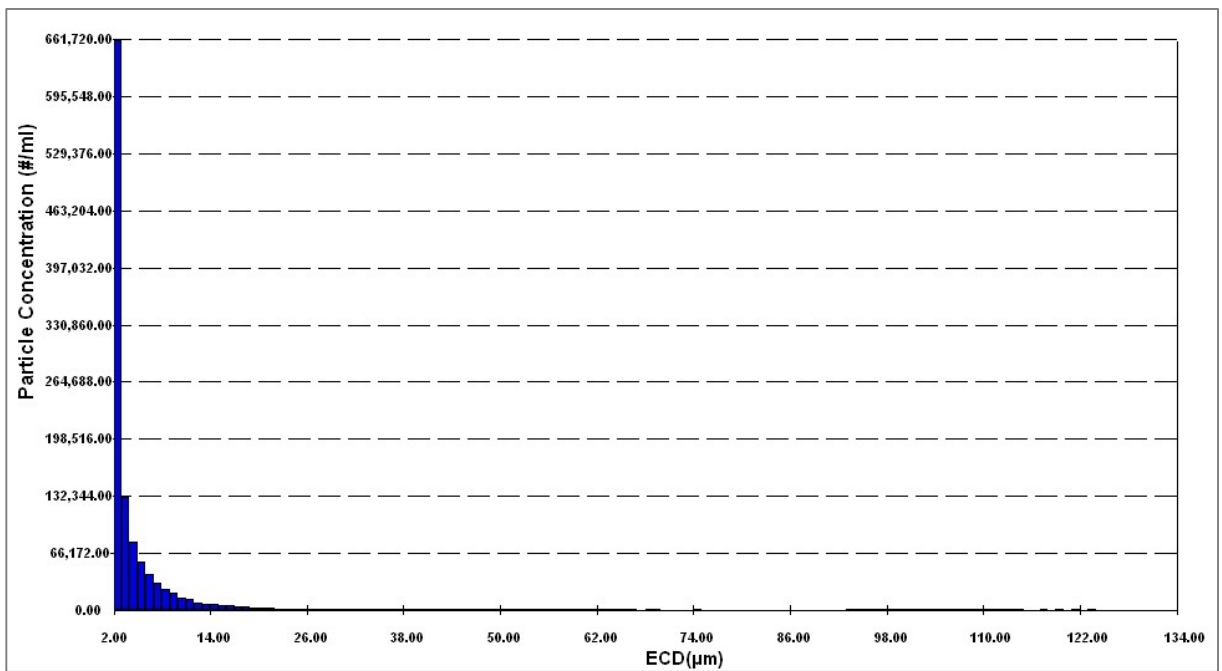
Figure A.39   Size Analysis of Fe$_3$O$_4$ (2.5 gm) Adsorbent
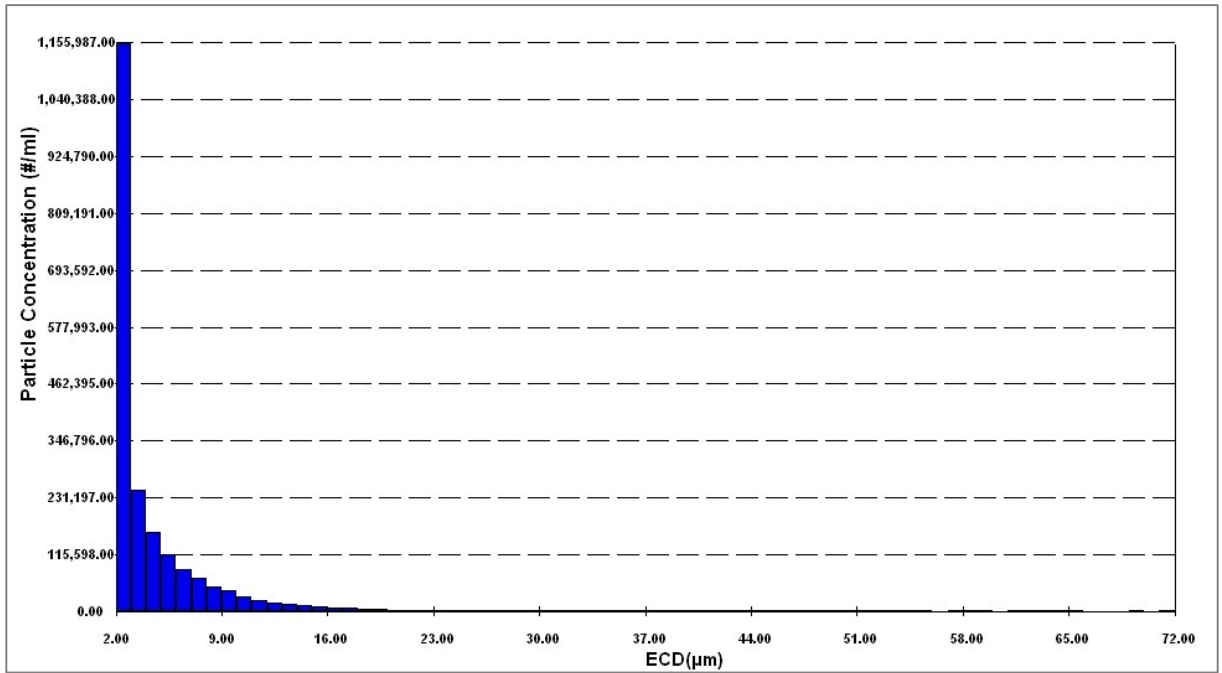
Figure A.40   Size Analysis of Fe$_3$O$_4$ (5 gm) Adsorbent
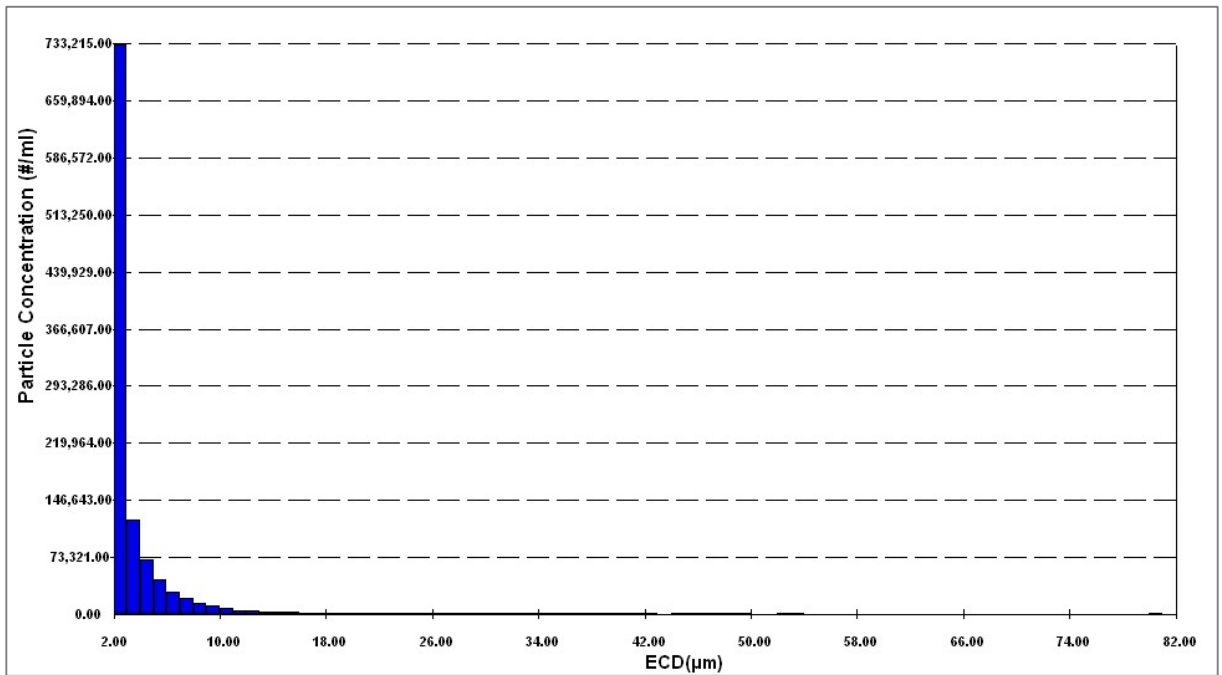
Appendix B

Table A-1   Elemental Composition of Flocs (by weight)

Adsorbents used	Element	Weight%	Atomic%
CaO & Fe_3O_4 (1 gm)	Al K	0.36	0.42
CaO & Fe_3O_4 (5 gm)	Al K	2.00	1.82
MgO (5 gm)	Al K	1.61	1.09
MgO (1 gm)	Al K	0.52	0.35
CaO (1 gm)	Al K	0.10	0.07
Fe_3O_4 (1 gm)	Al K	0.10	0.12

Table A-2   Characteristics of FBWW

Parameters	3 Trials	Avg Value
Total Aluminium, µg/L (Fall Season)	3032	3104
	3153	
	3127	
Total Aluminium, µg/L (Winter Season)	2250	2250
	2250	
	2250	
PH	7.7	7.5
	7.5	
	7.4	
Dissolved Aluminium µg/L	146.9	140
	136.0	
	136.9	
ZP (mV)	32.4	33
	33.6	
	34.6	
Size Analysis, µm (ECD range)	2-23	2-39
	2-51	(by 100 times dilution)
	2-44	
TSS (mg/L)	0.99	1.02
	1.1	
	0.98	

Table A-3   Total Aluminium Conc. Measurement without pH Adjustment Condition

Adsorbent Used	Polymer Dosage (mg/L)	Adsorbent dosage (g/L)	Total Aluminium (Trials) (μg/L)	Total Aluminium (Avg Value) (μg/L)	pH Measurement (after 1.5 hrs Without pH adjustment)
CaO (10 times dilution)	1	0.1 g/L	2192	2229	9.0
			2251		
			2243		
	1	1.0 g/L	2116	2145	11.3
			2159		
			2160		
	1	2.5 g/L	2203	2242	12.2
			2260		
			2261		
	1	5.0 g/L	722.6	688	12.7
			668.9		
			671.7		
MgO (10 times dilution)	1	0.1 g/L	1624	1654	9.1
			1669		
			1670		
	1	1.0 g/L	974.6	940	10.3
			1002		
			844.5		
	1	2.5 g/L	375.8	383	10.4
			387.5		
			384.5		
	1	5.0 g/L	139.3	142	10.4
			143.3		
			142.7		
	1	0.1 g/L	2382	2306	6.2
			2265		

			2271		
Fe₃O₄ (10 times dilution)	1	1.0 g/L	2812	2697	6.3
			2627		
			2652		
	1	2.5 g/L	2957	2825	6.4
			2777		
			2741		
	1	5.0 g/L	1378	1301	6.7
			1264		
			1262		

Table A-4   Total Aluminium Conc. Measurement with pH Adjustment Condition

Adsorbent Used	Polymer Dosage (mg/L)	Adsorbent dosage (g/L)	Total Aluminium (Trials) (μg/L)	Total Aluminium (Avg Value) (μg/L)	pH Measurement (after 1.5 hrs Without pH adjustment)
CaO (10 times dilution)	1	0.1 g/L	1337	1400	6.5
			1450		
			1413		
	1	1.0 g/L	906	900	7.5
			891		
			903		
	1	2.5 g/L	511	520	7.5
			488		
			561		
	1	5.0 g/L	52	70	6.9
			87		
			71		
MgO (10 times dilution)	1	0.1 g/L	1624	1630	8.7
			1597		
			1669		
	1	1.0 g/L	990	940	8.9
			910		
			920		
	1	2.5 g/L	620	670	9.4
			680		
			710		
	1	5.0 g/L	40	50	8.6
			60		
			50		
	1	0.1 g/L	620	630	6.2
			580		

			690		
Fe₃O₄ (10 times dilution)	1	1.0 g/L	590	570	6.3
			550		
			570		
	1	2.5 g/L	420	380	6.4
			321		
			399		
	1	5.0 g/L	189	240	6.7
			219		
			312		
CaO and Fe₃O₄ (10 times dilution)	1	1.0 g/L	141	151	10.5
			147		
			165		
	1	2.5 g/L	93	102	11.2
			110		
			103		
	1	5.0 g/L	68	61	11.3
			50		
			65		

Table A-5   Dissolved Aluminium Conc. Measurement with pH Adjustment Condition

Adsorbent Used	Polymer Dosage (mg/L)	Adsorbent dosage (g/L)	Dissolved Aluminium (Trials) ($\mu g/L$)	Dissolved Aluminium (Avg Value) ($\mu g/L$)	pH Measurement (after 1.5 hrs Without pH adjustment)
CaO (10 times dilution)	1	0.1 g/L	290	300	6.5
			315		
			295		
	1	1.0 g/L	199	200	7.5
			185		
			216		
	1	2.5 g/L	89	80	7.5
			96		
			55		
	1	5.0 g/L	43	50	6.9
			50		
			57		
MgO (10 times dilution)	1	0.1 g/L	74	80	8.7
			97		
			69		
	1	1.0 g/L	123	110	8.9
			115		
			92		
	1	2.5 g/L	301	300	9.4
			305		
			294		
	1	5.0 g/L	57	30	8.6
			13		
			20		
Fe_3O_4	1	0.1 g/L	9	10	6.2
			9		
			12		

(10 times dilution)	1	1.0 g/L	9	10	6.3
			8		
			13		
	1	2.5 g/L	55	60	6.4
			57		
			68		
	1	5.0 g/L	96	115	6.7
			94		
			155		
CaO & Fe$_3$O$_4$ (10 times dilution)	1	1.0 g/L	76	102	10.5
			89		
			141		
	1	2.5 g/L	37	38.5	11.2
			32		
			46.5		
	1	5.0 g/L	34	37	11.3
			53		
			24		

Table A-6   TSS Measurement of Influent and Effluent water with pH Adjustment

Adsorbent Used	Adsorbent dosage (g/L)	TSS for Influent water (Trials) (mg/L)	TSS (Avg Value) (mg/L)	TSS for Effluent water (Trials) (mg/L)	TSS (Avg Value) (mg/L)
CaO (10 times dilution)	0.1 g/L	53	50	44	48
		49		49	
		48		51	
	1.0 g/L	311	308	25.3	27
		306		26.5	
		307		29.2	
	2.5 g/L	55	60	75.8	77
		59		75.7	
		66		79.4	
	5.0 g/L	140	144	93	90
		146		89	
		147		87	
MgO (10 times dilution)	0.1 g/L	10	10	1.56	1.9
		10		1.98	
		10		2.16	
	1.0 g/L	19	20	16.7	18
		19.5		16.9	
		21.5		20.7	
	2.5 g/L	38.4	40	1.99	2
		41.8		1.99	
		39.2		1.98	
	5.0 g/L	139.2	140	1.94	1.5
		140.5		1.21	
		140.3		1.45	
		22.5	25	9.8	

Adsorbent Used	Adsorbent dosage (g/L)	TSS for Influent water (Trials) (mg/L)	TSS (Avg Value) (mg/L)	TSS for Effluent water (Trials) (mg/L)	TSS (Avg Value) (mg/L)
Fe$_3$O$_4$ (10 times dilution)	0.1 g/L	23.4		9.7	10
		29.1		10.5	
Fe$_3$O$_4$ (10 times dilution)	1.0 g/L	249	252	241.6	242
		248		239.7	
		259		244.7	
	2.5 g/L	259	260	55	58
		262		61	
		259		59	
	5.0 g/L	597	608	70.4	71
		620		72.6	
		608		70.0	
CaO & Fe$_3$O$_4$ (10 times dilution)	1.0 g/L	4.2	4	1.98	2
		4.0		1.97	
		3.9		2.02	
	2.5 g/L	14.5	16	16.9	16
		15.9		15.1	
		17.6		16.0	
	5.0 g/L	33.5	34	29	30
		32.9		28	
		35.6		33	